

University of Southampton

Faculty of Developmental Cell Biology

School of Biological Sciences

**The Transcriptional Regulation of
Nramp1 Promoter**

By

Irene Yue Ling Yeung (Hons)

**A thesis submitted in fulfilment of the requirements for
the Degree of Master of Philosophy**

September 2005

Acknowledgement

I would like to express my sincere thanks to my supervisors Dr. C.H. Barton and Prof. D.A. Mann for their valuable discussion, comments, advice and support throughout my M.Phil. research. Thank You! The financial support from the Golden Jubilee scholarship from the University of Southampton should be acknowledged. Thanks are due to my lab mates who provided me useful information, technical support for this study. I am indebted to Junlong, Chun lee, Mr. and Mrs. Barrie, for their kind support on my report. I would like to thank my brothers and sisters in Christ for your love, care, prayers and encouragement throughout my years in Southampton.

Last, but not the least, I am indebted to my parents and my sister, for their love, encouragement, continues support in both emotionally and financially during this research. I can never stop giving thanks for how you have impacted my life!

To my Mum, Dad and Francesca

In the beginning God created the heavens and the earth. Genesis 1:1

Summary

Murine *Nramp1* (Natural Resistance-Associated Macrophage Protein 1) encodes a bivalent-metal/Fe²⁺ transporter at the phagolysosome membrane and functions to control pathogen growth. *Nramp1* is known to be upregulated by lipopolysaccharide + Interferon-Gamma (LPS+IFN- γ), iron loading and redox stress; however, the direction of iron transported by *Nramp1* is not known. The purpose of this study is to increase knowledge of the regulation of the TATA-less *Nramp1* promoter by initiator element binding transcription factors, to identify the role of LPS+IFN- γ , and oxidant stress (OS) and examine the effect of host-cell *Nramp1* genotype on these responses.

Transient transfection of *Nramp1* promoter-reporter constructs demonstrated upregulation of *Nramp1* by upstream stimulatory protein 1 (USF1) in synergy with transcription factor II-I (TFII-I), but not with c-Myc interacting zinc finger protein-1 (Miz-1). Ying yang 1 (YY1) prevented c-Myc mediated repression of *Nramp1* promoter function. Mutation of the specificity protein 1 (Sp1) binding site within the proximal *Nramp1* promoter attenuated *Nramp1* transcriptional responses. Oxidant stress (OS) activated *Nramp1* and Sp1-dependent transcriptional responses in macrophage cells.

Nramp1 allele *G169* increased tolerance to iron- or butathione sulphoximine-induced oxidant stress compared with cells expressing the *D169* allele. Higher basal *Nramp1* transcription was observed following transient transfection into *D169* allele cells which was reduced with iron chelation. Furthermore, the transfected *Nramp1* promoter construct was more responsive to LPS+IFN- γ activation in *G169* allele cells.

In conclusion, results showed that *Nramp1* carried a classical Inr element that functions in tandem with a consensus Sp1 binding site. A role for Sp1 was proposed for the activation of *Nramp1* promoter under oxidative stress. It is proposed that *Nramp1* in depleting iron from the cytosol caused a low OS response, providing an environment to facilitate a strong inflammatory response to LPS+IFN- γ signalling pathways activation.

Content

Acknowledgement.....	2
Summary.....	4
Content.....	5
Figure List	8
Abbreviations	10
1. Chapter 1	12
1.1. General Introduction.....	12
1.1.1. The Discovery of <i>Nramp1</i> Gene.....	12
1.1.2. The Nramp Family.....	12
1.1.3. The <i>Nramp1</i> Protein.....	13
1.1.4. Role of Murine <i>Nramp1</i>	14
1.1.5. The <i>Nramp1</i> Promoter	14
1.1.6. Regulation of <i>Nramp1</i> by LPS and IFN- γ	16
1.1.7. Regulation of <i>Nramp1</i> by Iron and Redox Stress	16
1.1.8. The Controversy of <i>Nramp1</i> Function.....	17
1.2. General Aim	20
2. Chapter 2	21
Materials and Methods.....	21
2.1. Cell Culture.....	21
2.2. Construction of <i>Nramp1</i> Promoter Reporter Plasmids	21
2.3. Transformation using the Competent <i>E. coli</i> JM109 cells.....	22
2.4. Extraction of Plasmid DNA from the Recombinant <i>E. coli</i> cells	23
2.5. Extraction of Sterile DNA for Cell Transfection.....	24
2.6. Extraction of Transcription Factor Expression Plasmids	24
2.7. Cell Transient Transfection	25
2.8. Firefly Luciferase Reporter Assay.....	26
2.9. CAT Reporter Gene Assay	27
2.9.1. CAT Protein Assay	28
2.10. Stable Transfectant Macrophage Cell lines	29
2.11. SDS – Polyacrylamide Gel Electrophoresis and Immunoblotting.....	30
2.12. Cell Proliferation Assay.....	32
3. Chapter 3	33
Role of the Initiator Binding Factors - USF1, YY1, c-Myc, Miz-1, TFII-I on the Regulation of <i>Nramp1</i> Promoter Activity.....	33
3.1. Introduction.....	34
3.1.1. c-Myc	34
3.1.2. USF1	35
3.1.3. Miz-1.....	35
3.1.4. TFII-I	36
3.1.5. YY1.....	37

3.2. Specific Aims	38
3.3. Results.....	39
3.3.1. 5' Deletion Analysis of the <i>Nramp1</i> Promoter Activity	39
3.3.2. USF1 Activated the <i>Nramp1</i> Promoter.....	39
3.3.3. Functional Redundancy of <i>Nramp1</i> promoter Inr Elements.....	39
3.3.4. USF1 Activated the <i>Nramp1</i> Promoter was Dependent upon the Inr.....	39
3.3.5. YY1 Blocked the c-Myc Mediated Repression on the <i>Nramp1</i> Promoter	40
3.3.6. Synergistic Effect of TFII-I + USF1 on the <i>Nramp1</i> Promoter	40
3.3.7. Miz-1 and USF1 did not Functionally Interact at the <i>Nramp1</i> Promoter	40
3.4. Discussion + Future Experiments.....	49
3.4.1. USF1 Positively Regulated the Murine <i>Nramp1</i> Promoter Transcription at the Inr.....	49
3.4.2. TFII-I and USF1 Synergistically Activated the <i>Nramp1</i> Promoter	50
3.4.3. USF1 and Miz-1 do not Functionally Interact with each other at the <i>Nramp1</i> Promoter.....	51
3.4.4. YY1 Blocked the c-Myc Mediated Negative Regulation of the <i>Nramp1</i> Promoter.....	51
4. Chapter 4	53
The Importance of the Sp1 Binding Site on the Regulation of <i>Nramp1</i> by LPS+IFN-γ, L-Glutamine and Oxidative Stress.....	53
4.1. Introduction.....	54
4.1.1. The Transcription Factor Sp1	54
4.1.2. Sp1 is Regulated and Function as a Regulator	54
4.1.3. Regulatory Role of Sp1 on the Promoter Regulation by L-Gln	55
4.1.4. Role of Sp1 on the Promoter Regulation with LPS	55
4.1.5. Regulatory Role of Sp1 under Oxidative Stress	56
4.1.6. Reason for Studying the Transcriptional Regulation of the <i>Nramp1</i> Promoter via Sp1	56
4.2. Specific Aims	58
4.3. Results	59
4.3.1. The Consensus Sp1 Binding Site was Necessary for the Upregulation of <i>Nramp1</i> Promoter Activity by LPS+IFN- γ	59
4.3.2. L-Gln Induced the <i>Nramp1</i> Promoter Activity.....	59
4.3.3. Induction of the <i>Nramp1</i> Promoter Activity by L-Gln is Sp1 Dependent.....	59
4.3.4. BSO Activated the <i>Nramp1</i> Promoter Activity	59
4.3.5. BSO-Induced OS Upregulated the Sp1-Dependent Promoter Transcription in Macrophage Cells	60
4.4. Discussions + Future Experiments	66
4.4.1. Sp1 Binding Site was Necessary for the Basal Transcriptional Regulation of <i>Nramp1</i> Promoter	66
4.4.2. Sp1 Binding Site was Necessary for the Activation of <i>Nramp1</i> Promoter by LPS+IFN- γ	66
4.4.3. Sp1 was Necessary for the Upregulation of <i>Nramp1</i> Promoter by L-Gln.....	67
4.4.4. Regulation of Promoter Transcription in Macrophages under OS is Sp1-Dependent	68

5. Chapter 5	69
The Role of <i>Nramp1</i>-mediated Iron Transport in the Regulation of Oxidative Stress Status and the <i>Nramp1</i> Promoter Responsiveness to LPS+IFN-γ Activation in Macrophages	69
5.1. Introduction	70
5.1.1. What is Oxidative Stress?	70
5.1.2. Depletion of Glutathione Induce Oxidative Stress	72
5.1.3. Oxidative Stress is Provoked by Excess Redox Active Free Iron	73
5.1.4. Role of Iron in the Regulation of Bacterial Infection, Immune Responses and the Pleiotropic Effect of <i>Nramp1</i>	73
5.2. Specific Aims	74
5.3. Results	75
5.3.1. Expression of <i>Nramp1 G169</i> Increased Cell Viability against BSO-Induced OS	75
5.3.2. Expression of <i>Nramp1 G169</i> Induced Cell Viability against BSO- and Iron-Induced OS	75
5.3.3. Basal <i>Nramp1</i> Transcription was Greater in Cells which Lacked the Functional <i>Nramp1</i>	75
5.3.4. Iron Chelation Caused a Reduction of Basal <i>Nramp1</i> Transcription in Cells which Lacked the Functional <i>Nramp1</i>	76
5.3.5. Function of <i>Nramp1</i> Was Necessary for the Activation of <i>Nramp1</i> Transcription in Response to LPS+IFN- γ Signalling	76
5.4. Discussions + Future Experiments	82
5.4.1. <i>Nramp1</i> Reduced the Iron Content in the cells.....	82
5.4.2. <i>Nramp1</i> Protects the <i>Nramp1</i> Stable Transfectant Cells against OS caused by GSH Depletion.....	82
5.4.3. Potential Role of <i>Nramp1</i> in the Protection of Cells from Oxidative Stress, via Iron Transport	83
5.4.4. Role of <i>Nramp1</i> which determined the Stimulatory or Attenuated Effect of LPS+IFN- γ on <i>Nramp1</i> Transcription	84
6. Chapter 6	86
Final Conclusion	86
6.1. <i>Nramp1</i> is a Classical Initiator Promoter.....	87
6.2. Consensus Sp1 Binding Site is Necessary for the Basal and Activated <i>Nramp1</i> Transcription.....	87
6.3. Potential Role of <i>Nramp1</i> to Protect Cells against Oxidative Stress via Iron Depletion.....	88
6.4. Role of <i>Nramp1</i> in the Regulation of the Pleiotropic Effects Associated with Iron / Iron generated Oxygen Radicals.....	89
References	92

Figure List

Chapter 1

Figure 1.1	14
The Schematic Representation of the Membrane Associated Arrangement of the Murine <i>Nramp1</i> Protein	
Figure 1.2	16
Sequence Alignment of the Inr Elements from Different Promoters	
Figure 1.3	17
Schematic Diagram of the Murine <i>Nramp1</i> Promoter Consensus Sequence Elements	
Figure 1.4	20
Two Proposed Opposing Models on the Function of Bivalent Cation Transporter <i>Nramp1</i>	

Chapter 2

Figure 2.1	33
Calculation of % Chloramphenicol Acetyl Transferase (CAT) conversion	

Chapter 3

Figure 3.1	36
A Schematic Diagram of the c-Myc Polypeptide Structure	
Figure 3.2	37
The Schematic Diagram of USF1 Polypeptide Structure	
Figure 3.3	38
A Schematic Diagram Representing the Miz-1 Protein Structural Domain	
Figure 3.4	38
Schematic Diagram of TFII-I	
Figure 3.5	39
Schematic Diagram of the Human YY1 Primary Protein Structure	
Figure 3.6A	43
5' Deletion Analysis of <i>Nramp1</i> Promoter Activity	
Figure 3.6B	44
Activation of <i>Nramp1</i> Promoter Activity by Co-transfecting USF1 plasmids	
Figure 3.7	45
Functional Redundancy of the 2 Putative Inr Elements on <i>Nramp1</i> Promoter	
Figure 3.8	46
Functional Redundancy of the Inr Elements on <i>Nramp1</i> Promoter	
Figure 3.9	47
Functional Redundancy of Inr Elements on the Activation of <i>Nramp1</i> by USF1	
Figure 3.10	48
YY1 Prevented the Inhibitory Role of c-Myc on <i>Nramp1</i> Promoter	
Figure 3.11	49
USF1 and TFII-I Activated <i>Nramp1</i> Promoter in a Synergistic Manner	
Figure 3.12	50
Miz-1 and USF1 Independently Activated <i>Nramp1</i> promoter but not in Synergy	
Figure 3.13	54
The Proposed Model on the role of Inr-binding Factors on the Regulation of Murine <i>Nramp1</i> Promoter	

Chapter 4

Figure 4.1	56
Schematic Diagram Represent the Sp1 Polypeptide Structure	
Figure 4.2	59
The Alignment Sequence of the Proximal <i>Nramp1</i> Promoters between Human, Mouse and Rat	
Figure 4.3	63
Sp1 Consensus Binding site was Necessary for the Basal and Activation of <i>Nramp1</i> Promoter by LPS+IFN- γ	
Figure 4.4A	64
Dose Dependent Increased of <i>Nramp1</i> Promoter by L-Gln	
Figure 4.4B	64
Western Immunoblotting Indicated the Increased Expression of Nramp1 Protein with L-Glutamine	
Figure 4.5	65
The Sp1 Consensus Binding Site was Necessary for the Upregulation of <i>Nramp1</i> Promoter with L-Glutamine	
Figure 4.6A	66
BSO-Induced Oxidative Stress Activated <i>Nramp1</i> Promoter	
Figure 4.6B	66
BSO-Induced Oxidative Stress Activated Nramp1 Protein Expression	
Figure 4.7	67
Sp1-dependent Promoter Transcription in Macrophage Cells was Responsive to OS	

Chapter 5

Figure 5.1	73
Metabolic Pathways of Reactive Oxygen Radicals Formation	
Figure 5.2	74
Mechanism of BSO Function	
Figure 5.3	79
Increased Cell Viability with Nramp1 Polypeptide Expression Under OS	
Figure 5.4	80
Increased Cell Viability with Nramp1 Expression Under BSO+FAS-Induced OS in the <i>Nramp1</i> Expressing Stable Transfectant Cells	
Figure 5.5A	81
The Absence of the <i>Nramp-1</i> Allele <i>G169</i> in Stable Transfectant R21 Cells Caused a Higher Basal <i>Nramp1</i> Transcription	
Figure 5.5B	82
Role of Nramp-1 Regulated Iron transport which Affected <i>Nramp1</i> Transcription	
Figure 5.6	83
The Presence of <i>Nramp1</i> Allele <i>G169</i> in Stable Transfectant Cells R37 Cells Regulated the <i>Nramp1</i> activation in response to LPS+IFN- γ	

Chapter 6

Figure. 6.1	92
Potential Role of the <i>Nramp1</i> – Mediated Bivalent Cation / Iron Transport	

Abbreviations

AdML- Adenovirus major late promoter
APS - Ammonium persulphate
BSA - Bovine serum albumin
BSO – Butathione Sulphoximine
BTB/POZ - Broad-complex, Tramtrack, and Bric-a-brac / poxvirus and zinc finger
C₂H₂ – Cystein and Histidine
CAT - Chloramphenicol Acetyl Transferase
CHIP – Chromatin Immunoprecipitation
c-Myc - Cellular Myelocytomatosis
CTD – Carboxy -terminal domain
Def – Deferroximine
DMEM - Dulbecco's modified Eagle's Medium
DNA – Deoxyribonucleic Acid
EMSA – Electrophoresis Mobility Shift Assay
FAS – Ferric Ammonium Sulphate
GSH – Glutathione / L- γ -glutamyl-L-cysteine-glycine
GP – Glutathione Peroxidase
H₂O₂ - Hydrogen Peroxide
HAT – Histone Acetylase
HDAC - Histone Deacetylases
IFN- γ - Interferon- γ
IL-1 β – Interleukin 1 β
iNOS - inducible Nitric oxidase
Inr – Initiator
IRE - Interferon regulatory elements
IRP - Iron regulatory proteins
KCL – Potassium chloride
L-Gln – L-Glutamine
LPS - Lipopolysaccharide
MAPK - Mitogen activating protein kinase
MgCl₂ – Magnesium chloride
MHC II - Cell-surface major histocompatibility class II
Miz-1 – c-Myc Interacting Zinc Finger Protein-1

NaCl – Sodium chloride
NF-IL6/CEBP β - Nuclear factor interleukin-6 / CCAAT/enhancer binding protein- β
Nramp1 – Natural Resistant Associated Macrophage Protein 1 / Solute carrier family member 11a
NTD - Amino-terminal domain
O₂[•] - Superoxide
OH[•]/OH⁻ - Hydroxyl radicals/anions
OS – Oxidative Stress
PKC – Protein Kinase C
PMA - Phorbol 12-myristate 13-acetate
PTM – Post Translational Modification
PTP – Protein tyrosine phosphatase
ROS – Reactive Oxygen Species
SDS - Sodium Dodecyl Sulfate
SHP-1 – Src Homology 2 (SH2) domain-containing protein tyrosine phosphatase
SOD – Superoxide Dismutase
Sp1 – Specificity Protein 1
TBE - Tris-Boric-EDTA
TBP – TATA box binding protein
TBS - Tris Buffered Saline
TF – Transcription Factor
TFII-I – Transcription factor II-I
TfR - Transferrin receptor
USF1 – Upstream stimulatory protein 1
VEGF - Vascular endothelial growth factor
YY1 – Ying Yang 1

1. Chapter 1

1.1. General Introduction

1.1.1. The Discovery of *Nramp1* Gene

Nramp1 is the positional gene candidate for that defined by the *Ity/Lsh/Bcg* phenotype ¹, originally described for its roles in regulating the resistance or susceptibility to *Salmonella typhimurium*, *Leishmania donovani*, and *Mycobacterium bovis* infection in mice ²⁻⁵. The *Ity/Lsh/Bcg* loci were individually mapped to proximal mouse chromosome 1 ⁶ and it was proposed that this single gene, termed *Nramp1*, was responsible for controlling all responses to these phylogenetically distinct organisms.

The mouse *Nramp1* gene is presented in two naturally occurring allelic forms ⁷. A non-conserved glycine (G) to aspartic acid (D) mutation at codon 169 of *Nramp1* makes the mice susceptible to *Leishmania donovani*, *Salmonella typhimurium* and *Mycobacterium bovis* infection ^{8,9}. The other *Nramp1* allele *G169* provides a phenotype in mice that restricts early pathogen growth (termed resistant) ⁷.

1.1.2. The Nramp Family

Human NRAMP1 is composed of 15 exons and spans 11.5 kb of genomic DNA encoding a 550-amino acid (90- to 100-kDa integral membrane protein) protein ¹⁰, showing 92% similarity with mouse *Nramp1* ¹¹. Human NRAMP1 is associated with multiple infectious and autoimmune diseases. The infectious diseases include viral (HIV), bacterial (tuberculosis, leprosy, meningococcal meningitis) and protozoan (visceral leishmaniasis) pathogens ¹²⁻¹⁹. The autoimmune diseases include rheumatoid arthritis, juvenile rheumatoid arthritis, diabetes, sarcoidosis and Crohn's disease ²⁰⁻²⁵. It has been concluded that hypermorphic alleles associate with resistance to infection and susceptibility to autoimmune/inflammatory diseases (alleles 3 and 7) and reciprocal responses were described for hypomorphic alleles (allele 2) ²⁶⁻²⁸.

Mouse *Nramp1* is paralogous (77% identity) to mouse *Nramp2* ^{29,30}. A non-conserved mutation G185R in mouse *Nramp2* is responsible for microcytic anaemia associated with abnormal TfR receptor/transferrin iron assimilation, reticulocyte iron uptake and gastrointestinal iron absorption ³¹.

1.1.3. The *Nramp1* Protein

Mouse *Nramp1* encodes a ~90-100kDa (548 amino acid) transmembrane protein^{1,32}. The protein is heavily N-linked glycosylated on the extracellular loop (close to 50% of its mass)^{1,33}. It contains a Ser- and Pro-rich N-terminal domain and a consensus transport signature³⁴. The intra-cytoplasmic loop between transmembrane 8-9 contains a conserved transport motif (CTM) known as the 'Binding-protein-dependent transport system inner membrane component signature', which is believed to participate in substrate translocation across the membrane¹ (Figure. 1.1).

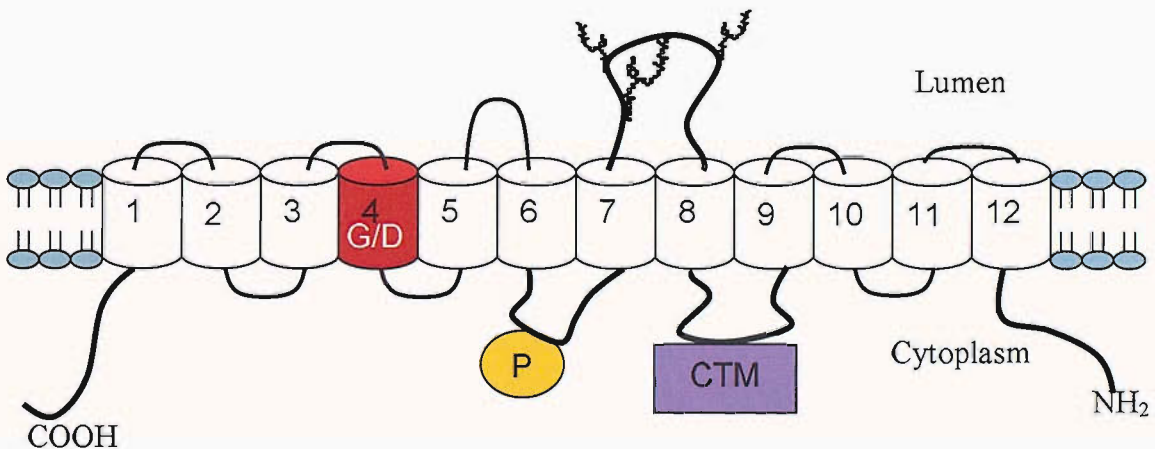


Figure 1.1. The Schematic Representation of the Membrane Associated Arrangement of the Murine *Nramp1* Protein. The amino (NH₂) and carboxyl terminal (COOH) of the protein are identified on the cytoplasmic side of the phagosomal membrane, and the individual predicted transmembrane domains (TMD) 1-12 are represented as open columns. The predicted TMD 4 (shown in red) carries a natural mutation in mice bearing the susceptible allele D169 of *Nramp1*. Possible phosphorylation (P) and glycosylation (luminal loop 4) sites are identified. The consensus transport motif (CTM) found in several bacterial and eukaryotes membrane transport protein is in the cytoplasmic loop 4¹.

The *Nramp1* protein is expressed exclusively in the late endosomal and lysosomal sub-cellular compartments of monocytes and macrophages in mice, but not in the early endosomes³⁵.

1.1.4. Role of Murine *Nramp1*

The *Nramp1* protein is implicated with direct divalent cation transport (Mn^{2+} , Fe^{2+} , Zn^{2+})³⁶. The intimate co-localisation of the *Nramp1* polypeptide with a phagocytosed pathogen has provided clues to its putative function in antimicrobial activity³⁷. Upon infections in mice, macrophages are activated by LPS, and release the pro-inflammatory cytokines such as IFN- γ then triggers the recruitment of *Nramp1* from endocytic vesicles to the phagosomal membrane where it alters the microenvironment of the vesicles and thereby control the replication of the pathogen³⁵. It was found that the macrophages that contained the resistant *Nramp1* *G169* allele has a greater capacity to control the proliferation of phagocytosed bacteria³⁸. In addition, the *M. bovis*³⁹ and *M. avium*⁴⁰ containing phagosomes are more acidic than those with the non-functional *Nramp1* or null *Nramp1* alleles. These studies support the hypothesis that *Nramp1* controls the replication of intracellular parasites by directly (or indirectly) altering the intravacuolar environment of the microbe-containing phagosome.

Apart from the direct role of transporting cations across the macrophage membrane, *Nramp1* exerts a wide range of other pleiotropic effects in IFN- γ and LPS-activated macrophages. They include the increased expression of the chemokines, IL- β , iNOS and MHC II^{26,41-45}. Macrophages carrying the resistant *Nramp1* allele also caused an increase in respiratory burst, the release of nitrates, L-arginine flux and PKC activity^{11,41,46,47}. *Nramp1* also stabilizes the mRNA of several IFN- γ inducible genes and TNF- α which provides the co-stimulus for NO production⁴⁸. This increase of NO production by *Nramp1* could be part of the protective function of *Nramp1* to control infections with Mycobacteria. However, macrophages carrying the mutated infection susceptible *Nramp1* allele *D169* have a defect in antigen processing and presentation which reduces the capacity to control bacteria proliferation⁴⁹.

1.1.5. The *Nramp1* Promoter

Murine *Nramp1* promoter does not contain a TATA box sequence but carries two putative consensus sequence motifs for the Inr element (Inr#1: CACT₊₁CGCT, Inr-like#2: TCCCCTACT₊₁CTT) located near to the start site of transcription⁵⁰ (Figure. 1.2) The first Inr conform to the consensus sequence for Inr elements; Py Py A₊₁ N^{T/A} Py Py, with a core motif of (CACT). The second sequence is an Inr-like sequence due to the difference in purine instead of the pyrimidine at the 3' end⁵¹ (Figure. 1.3).

Many known Inr-binding factors such as c-Myc⁵², USF1⁵³, YY1⁵⁴, TFII-I⁵⁵ and Miz-1^{56,57} interact at the Inr elements. Miz-1 is a zinc finger transcription factor that positively regulates *Nramp1* promoter^{56,57}. YY1 belongs to the zinc finger transcription factors family that functions as an Inr-binding protein⁵⁴, which either activates⁵⁸ or represses⁵⁹ transcription at the Inr. USF1 and TFII-I are transcription factors that bind to the Inr and also to the E-box site (CACGTG or CACATG)⁶⁰. While 2 Inr elements and 7 consensus E-box elements are found within the *Nramp1* promoter, little is known on the role of the above factors in regulating *Nramp1* promoter activity (for more details on Inr-binding factors, see chapter 3).

Additionally, the ubiquitous transcription factor Sp1 binding site or GC box (5'-GGGCG-3') is found at position -26/-21bp, which is necessary for Miz-1 to mediate the upregulation of *Nramp1* promoter⁵⁷. Alignment sequences of the *Nramp1* core promoter region has shown a 100% conservation of the Sp1 binding site between human, mouse and rat indicating the importance of the Sp1 binding site on *Nramp1* promoter regulation (Figure. 4.2) (for more details on Sp1, see chapter 4).

Gene	Inr element
Ad-MLP	T C A C T C T
C/EBP	T C A C C T T
MT-1	T C A C C A C
NCAM	T C A C T C A
LFA-1	T C A T T T T
HLA-A2	T C A G A T T
HLA-C	T C A G A T T
Cav-1	T C A G T T C
<i>Nramp1</i> #1	C C A C T C T
<i>Nramp1</i> #2	T C A C T C G
Consensus	Y Y A N ^T _A Y Y

Figure 1.2. Sequence Alignment of the Inr Elements from Different Promoters. Consensus Inr element alignment matches perfectly with the first *Nramp1* Inr element (*Nramp1* #1). The 2nd Inr-like element (*Nramp1* #2) which spans the transcription initiation site does not match with the Inr consensus sequence where the 3' end of the nucleotide is a purine and is not a pyrimidine.⁵².

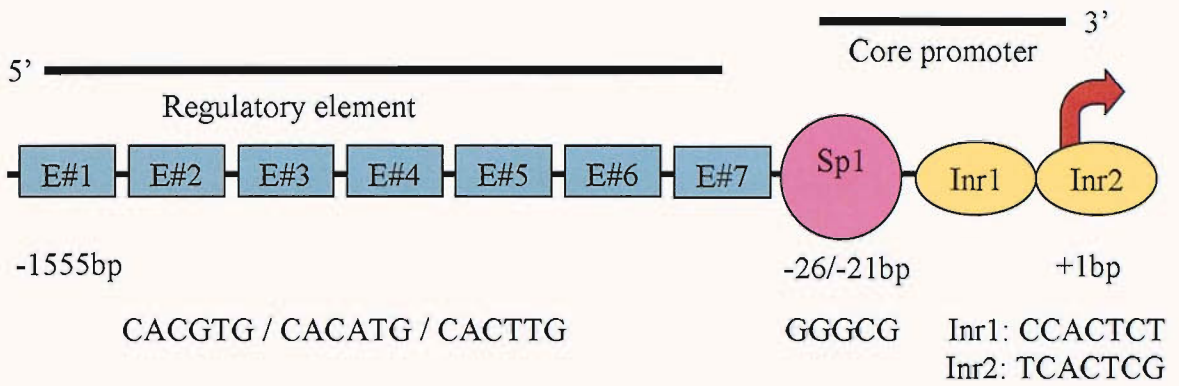


Figure 1.3. Schematic Diagram of the Murine *Nramp1* Promoter Consensus Sequence Elements. The *Nramp1* nucleotide sequences can be found in the EMBL data base (accession number AJ458183). The sequence is also available from the mouse genome data base (www.ensembl.org/Mus_musculus/). The 7 non-canonical E boxes (Myc/Max 1-7) (CACGTG or CACATG or CACTTG) are represented as blue squares E#1- E#7. The 2 pyrimidine rich Inr elements (Inr1: CCACTCT and Inr2: TCACTCG) are represented by yellow ovals with the transcription initiation start site represented by the red arrow above (CTC at +1bp). The single Sp1 binding site (GGGCG -21/-26bp) is represented by the pink circle. The diagram is modified and adapted from Govoni *et al.*, 1995⁵⁰ and Bowen *et al.*, 2002^{1,56}.

1.1.6. Regulation of *Nramp1* by LPS and IFN- γ

Upregulation of *Nramp1* mRNA by LPS+IFN- γ resulted in increased levels of the 90-100kDa mature Nramp1 protein in the resistant *Nramp1 G169* cells^{8,50,61,62}. There are cis-acting sequence motifs associated with macrophage expression or associated with differentiation specific to this cell lineage by LPS+IFN- γ in the region between -265bp to +127bp on *Nramp1* promoter which include the IRE (CWKKANNY, positions -183bp) and (TKNNGNAAK, positions -144 and -243bp) respectively⁵⁰. The mechanism of the upregulation of *Nramp1* promoter by LPS + IFN- γ has not yet been worked out although a recent report suggested that Miz-1 is implicated in the LPS + IFN- γ induction of *Nramp1*⁶³ (More details on transcription factor Miz-1 in chapter 3).

1.1.7. Regulation of *Nramp1* by Iron and Redox Stress

Nramp1's own transport substrate, iron and iron loading-induced redox stress enhanced *Nramp1* polypeptide and mRNA accumulation, as efficiently as the inflammatory

cytokines^{62,64}. *Nramp1* regulates iron metabolism as demonstrated by modulating the IRP2 binding activity^{62,65}. Studies have reported that cells with the resistant *Nramp1* allele *G169* have a low labile iron pool and iron treatment induced *Nramp1* expression, therefore, the transport of iron by *Nramp1* from the cytoplasm was suggested to serve as a negative autoregulatory link between *Nramp1*'s function and expression⁶².

Iron is involved with a lot of physiological responses such as cell growth as well as combating infection. Dysregulation of iron increase bacteria growth and cause the excess formation of ROS via Fenton/Harber-Weiss reaction⁶⁶. Excessive ROS overcomes the anti-oxidant defences which provokes OS, leading to the destruction of cellular components including lipids, protein, and DNA⁶⁶ (for more details on OS, see chapter 5). While *Nramp1* regulates the divalent cation/iron transport, little is known on the role of *Nramp1* in mediating iron induced-OS in macrophage.

1.1.8. The Controversy of *Nramp1* Function

There is controversy regarding the mechanism of *Nramp1* on the direction iron transport activity has on bacterial growth. Some data suggest that iron depletion from the phagosome to the cytoplasm by *Nramp1* results in a bacterial-static mechanism⁶⁷⁻⁶⁹. However, others suggest that the transport of divalent cation, Fe^{2+} into the phagosome, (where iron catalyses the Fenton chemistry) mediates the bacterial-cidal killing within the phagosome^{36,70} (Figure. 1.4).

Some studies have indicated the depletion of iron from the cytoplasm. Barton and Atkinson⁶⁵ showed that *Nramp1* does not increase iron uptake in Cos-1 cells that express *Nramp1*, and the *Nramp1* expression was associated with reduced cellular iron load. A lower cytoplasmic iron is also found in *Nramp1* expressing cells, compared with the non-*Nramp1* expressing cells^{71,72}, and greater flux of iron in *Nramp1*-expressing cells from the cytoplasm has been found⁷³. Cell growth rates are also reduced in macrophage cell lines expressing *Nramp1*, suggesting a decrease in iron availability together with the decrease of the iron storage protein ferritin expression^{62,74}. The mutant *Nramp1* allele *D169* transfected macrophage cells is found to contain more iron than the wild-type-transfected cells³⁹. The increased cytosolic iron is shown to attenuate NF-IL6 activity and *iNos* expression, contributing to the susceptibility of bacterial infection⁷⁵⁻⁷⁷. These results provide support for the notion that *Nramp1* depletes cation/iron levels within the cytosol.

In contrast to the results shown above, others have shown that the addition of excess iron increased the growth of *Mycobacterium avium*, hypothesising that *Nramp1* carries out

anti-microbial action by transporting iron out of the *M. avium* phagosome ⁶⁷. In addition, Gomes ⁶⁷ and Jabado ⁶⁸ proposed the transport of cations into the cytosol. Thus, the function of *Nramp1*-mediated iron transport is still unclear.

Despite the controversy of *Nramp1* function, little is known about the transcriptional regulation of *Nramp1*. A negative autoregulatory link was proposed between the *Nramp1* function and *Nramp1* promoter activity in the macrophage (i.e. the increase of *Nramp1* expression by iron functions to deplete the cytosolic iron which reduces the expression of *Nramp1*). However, no model of mechanism has been described that could mediate regulation by iron or OS. Wu ⁷⁸ showed that c-Myc induced *IRP2* transcription and inhibit ferritin expression which co-ordinately enhanced the cytosolic iron pool for cell growth. Recent experiments have shown that c-Myc represses *Nramp1* transcription, which provides support for the notion that *Nramp1* deplete cation/iron levels within the cytosol ⁶². Hence, the study of the regulation of *Nramp1* promoter activity will provide information concerning the direction of divalent cation transport by *Nramp1*.

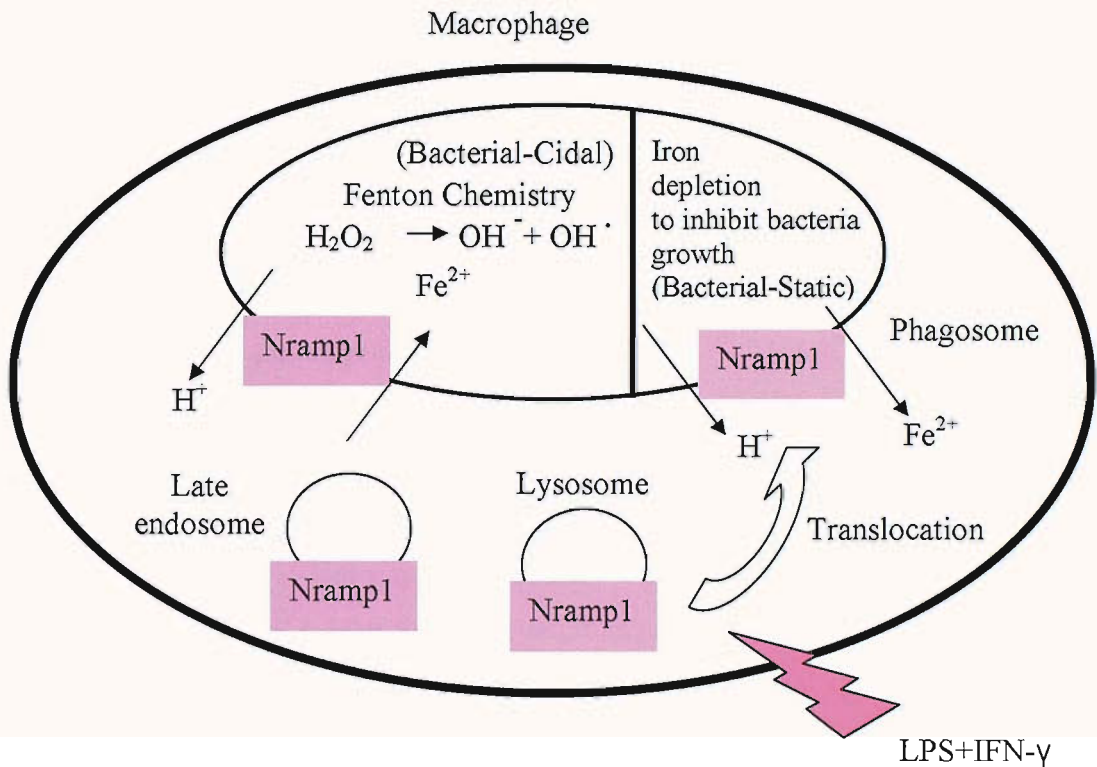


Figure 1.4. Two Proposed Opposing Models on the Function of Bivalent Cation Transporter Nramp1. Nramp1 (represented by pink rectangle) is expressed in the late endosome/lysosomes. Upon LPS+IFN- γ stimulation, Nramp1 is recruited to the phagosome membrane which regulates the pathogen growth by direct iron (Fe^{2+}) transport. Iron, which is essential for pathogen growth is either depleted or it is being transported into the phagosome vesicle to catalysis the Fenton/Haber Weiss reaction to generate hydroxyl radicals in killing the pathogens.

1.2. General Aim

The *Nramp1* gene sequence is known. However, little is known about the transcriptional regulation of *Nramp1*. The purpose of this study is to investigate the transcriptional regulation of the proximal *Nramp1* promoter; to gain insights into the molecular mechanisms underlying the regulation of *Nramp1* promoter activity by LPS+IFN- γ , iron and oxidative stress and its direct cation/iron transport function in mediating those responses in macrophages.

Nramp1 is a TATA-less promoter, but contains the Inr element(s) and a single consensus Sp1-binding site close to the initiation start site⁵⁰. Hence, *Nramp1* is a suitable model for the study of many macrophage-expressed genes and for Inr promoters in general.

The Inr-binding factor Miz-1 upregulated the *Nramp1* promoter⁷¹; however, no results have been published on the potential role of other Inr-binding factors that may function cooperatively with Miz-1. The aim is to examine the role of these other factors such as USF1, YY1, TFII-I, Miz-1, c-Myc for their role, if any, on the regulation of *Nramp1*.

Studies have shown that transcription factor Sp1 is responsive to LPS stimulation in macrophages^{79,80}. The Sp1 binding site was found to be necessary for the upregulation of *Nramp1* by Miz-1^{56,57} where Miz-1 was involved with the upregulation of *Nramp1* promoter by LPS+IFN- γ ⁶³. Furthermore, Sp1 was suggested to play a regulatory role in response to L-Gln and OS. Therefore, we hypothesised that the Sp1 binding site is necessary for the regulation of *Nramp1* promoter by LPS+IFN- γ , L-Gln and OS where Sp1 may play a regulatory role on *Nramp1* transcription under different stimulus.

Previously, the *Nramp1* promoter was found to be positively regulated by redox stress/iron loading which proposed that the direct mediation of iron activity by *Nramp1* may control its own expression and supports the notion of cytosolic iron depletion⁶². Hence, *Nramp1* which transports iron could modulate oxidant stress responses. Therefore, by investigating the regulation of *Nramp1* promoter in function/non-functional *Nramp1* cells, this may provide insights into the role of *Nramp1* in the regulation of OS status in macrophages and the possible evidence to support the controversies of *Nramp1* function.

2. Chapter 2

Materials and Methods

2.1. Cell Culture

The macrophage Raw 264.7 cell lines and Cos-1 Monkey fibroblast cell lines were cultured in the low-endotoxin complete Dulbecco's Modified Eagle's Medium (DMEM) (Sigma-Aldrich), supplemented with 100 U/ml penicillin, 100 µg/ml streptomycin, 2 mM L-glutamine, and 10% FBS (Life sciences Gibco). Raw 264.7 and Cos-1 cells were grown to confluent on a Nunc 75cm² flask and maintained at 37°C at an atmosphere of 5% CO₂.

2.2. Construction of *Nramp1* Promoter Reporter Plasmids

Nramp1 constructs pHB4, pHB4Sp1M, pHB20, pHB22, pHB23 were generated by the previous PhD. student Holly Bowen⁵⁶.

Nramp1 construct pCAT24 (with the first mutation on 1st Inr) was generated by Abi Lapham corresponding to the 5' restriction endonuclease cleavage sites *Sal I* (with TC fill in) and *BamHI* site of pBLCAT₃ plasmid. Oligonucleotides (sense, 5'-GATTCCCACTCTTACTCACggGGACC-3' and antisense, 5'-CTGGTCCcGTGAGTAAGAGTGGGAA-3' was annealed and ligated with annealed oligonucleotides 5'-AGCACCCACAGAAGGGGACAGATTGAG-3' and 5'-GATCCTCAATCTGTCCCCTTCTGTGGGTG - 3').

Nramp1 construct and pCAT25 (second Inr mutation) was generated in the same way as pCAT24 but with different oligonucleotides (sense 5'-GATGCCACggGTACTCACTCGGACC-3' and 5'-CTGGTCCGAGTGAGTAcccGTGGGCA-3'). The underline DNA sequence was the natural Inr sequence and the small letters represents the mutation of the Inr sequence).

Nramp1 luciferase reporter plasmids pL4, pL4Sp1M, pL4Sp1MGal4 were generated by Emma Philips^{57,81}. Briefly, a restriction fragment of the *XbaI* site at -1555bp and a synthetic *BamHI* site from the *Nramp1* CAT reporter construct pHB4⁵⁶, pHB4Sp1M⁵⁶ was subcloned into the pGL3-basic luciferase vector, generating *Nramp1* luciferase construct named pL4 and pL4Sp1M.

The Gal4-Sp1 site substitution mutant *Nramp1* construct (pL4Sp1MGal4) was prepared from a Sp1 site mutant in pBLCAT3 (pHB4Sp1M). Briefly, a double stranded oligonucleotide pair incorporating a Gal4 DNA binding site were cloned into pL4, for use in transfection reporter gene studies via *Xba*I and *Bam*HI sites on the insert and *Nhe*I and *Bgl*III sites on the vector; sense 5'-tttCGGGTGACAGCCCTCCGA-3', anti-sense 3'-aGCCCACTGTCGGGAGGCTt-5', the lower case letters represent bases introduced to facilitate cloning into the *Eco*RI site. Recombinant clones were selected and orientation of the inserts was determined by PCR (PFU enzyme 0.5 μ l + 5 μ l 10X PFU buffer + 0.4 μ l dNTPs (25mM) to give 250 μ M + 41.1 μ l dH₂O + 0.5 μ l DNA (100 ng/ μ l) + 0.5 μ l sense primer (100 ng/ μ l) + 0.5 μ l anti-sense primer (100 ng/ μ l) + PCR grade water to make up to 50 μ l / reaction)

2.3. Transformation using the Competent *E. coli* JM109 cells

50 μ l of the competent *E. coli* JM109 cells (Promega) were pipetted into pre-chilled 1.5ml eppendorf tubes on ice. 2 μ l of the DNA ligation mixture (0.1-50ng of DNA) (1 μ l 10x DNA ligase buffer (Promega) + 1/2 μ l T4 DNA ligase (Promega) + 6 μ l Vector + Insert/H₂O (1 Vector : 5 Inserts) + sterile water to make up to 10 μ l per reaction tube) and 1 μ g of control plasmid were added to the eppendorfs, each was mixed with 50 μ l competent cells, gently mixed and incubated on ice for 30 minutes which allowed the DNA to precipitate around the competent cells. The cells were then heat shocked by incubating at 42 $^{\circ}$ C for 45 seconds, enabling the uptake of the DNA into the competent *E. coli* cells. The cells were carefully transferred back to the ice for 2 minutes after the heat shock. 500 μ l of sterile LB medium (10g NaCl + 10g Bacto-Tryptone + 5g yeast extract + 1L dH₂O + autoclaved at once and then used at room temperature) without antibiotics was added drop by drop in the eppendorfs and were incubated at 37 $^{\circ}$ C for 1 hour with shaking at approximately 200-250 rpm.

After recovery, cells were pelleted by centrifuging at 100 rpm and resuspended in 100 μ l of LB medium without antibiotics. The recombinant cells resuspended in 100 μ l LB medium were then plated out onto the LB agar plates containing the appropriate antibiotics (Ampicillin [50mg/ml]) for selection of resistant recombinant bacterial colonies. The LB ampicillin agar plates were prepared in advance of the transformation as follow (1.5% / 7.5g Agar powder + 500ml LB medium was autoclaved, cooled to ~50 $^{\circ}$ C and 1ml of ampicillin 50mg/ml was added. The 10 cm Petri-dishes was poured with the LB agar half

way through under the blue/yellow flame and was left in room temperature to set). The LB agar plates were then incubated overnight at 37°C. Individual single colonies of the recombinant clones will grow on the ampicillin LB agar plates which were then streaked from the LB agar plate and was grown in a 10ml LB ampicillin liquid medium (1ml of ampicillin 50mg/ml + 500ml LB medium) in the universal tube for overnight at 37 °C on the shaker (~225-250 rpm).

2.4. Extraction of Plasmid DNA from the Recombinant *E. coli* cells

After incubating the recombinant *E. coli* cells overnight in 10ml LB medium, glycerol stocks of the recombinant *E. coli* clones were made by mixing 1ml of 50% glycerol + 50% sterile LB with 1ml of bacteria culture which can be stored in -70°C for further inoculation. The rest of the recombinant *E. coli* suspension (9ml) were then pelleted, resuspended in STE (10mM EDTA pH=8.0 + 0.1M NaCl + 0.1M Tris-HCl pH=8.0) and was transferred to the 1.5ml sterile eppendorf tube. The DNA plasmid from the individual clones was extracted using a commercial DNA extraction mini prep kit (Midiprep; Machery Nagel) according to the manufacturer's instruction. DNA restriction digest was performed to ensure the correct DNA fragment was being cloned into the plasmid using the appropriate restriction enzyme (1µl of the appropriate restriction enzyme + 1µl 10X of appropriate enzyme buffer + 1µg of plasmid DNA + sterile distill H₂O to make up to 10µl / reaction). Eppendorfs were incubated for 1 hour at 37°C. After incubation, 2µl of DNA loading dye (4g Ficoll + 4ml 0.5M EDTA + 16ml sterile H₂O + a pinch of bromophenol blue) was added to terminate the restriction digest. The reaction mixture was loaded on a 1% agarose electrophoresis gel (1g of electrophoresis agarose (Roche) + 100ml of 1X TBE was dissolved in the microwave in the conical flask). Gel was run at 120V to separate the linear DNA plasmid according to size.

The recombinant clones, containing the correct size DNA plasmid were then grown in large quantity which was later used for cell transient transfection. The glycerol stock of the recombinant clone (100µl) was added to the flask containing 100ml LB medium and was incubated overnight at 37°C on the shaker (~225-250 rpm). All plasmid DNA cell transfection was extracted using a commercial DNA extraction and isolation kit (Sigma-Aldrich). Plasmid DNA underwent a DNA restriction digest again to reassure the correct *Nramp1* promoter constructs were obtained.

2.5. Extraction of Sterile DNA for Cell Transfection

Following extractions of the large quantities of DNA plasmid and provided the DNA plasmid was the correct size, DNA plasmid was then concentrated at $1\mu\text{g}/\mu\text{l}$. The absorbance at 260nm of the DNA was measured using a spectrophotometer to calculate the concentration of the DNA present. DNA plasmid was then ethanol precipitated by adding 1/10 volume of sodium acetate 3M (pH 5.2), 1 volume of 100% ethanol, inverted the tube a few times and was spun for 10 minutes at 12,000 rpm. Following centrifugation, the alcohol supernatant was carefully discarded by inverting the tube carefully in one direction, leaving a white pellet of DNA. The pellet was then washed in $800\mu\text{l}$ of 80% ethanol and followed with another 10 minutes of centrifugation at 12,000 rpm. The alcohol was removed in a sterile hood by pouring the alcohol supernatant in one direction and excess liquid was pipetted off. The DNA pellet was then dried in the flow hood and resuspended in sterile dH_2O at a concentration of $1\mu\text{g}/\mu\text{l}$ using the following equation.

$$\text{Reading of Absorbance}_{260\text{nm}} \times 50 \times 200 \text{ (dilution factor)} = X \mu\text{g of DNA.}$$

Therefore $X \mu\text{l}$ of water was used to resuspend the $X \mu\text{g}$ of DNA to give a DNA = $[1\mu\text{g}/\mu\text{l}]$.

2.6. Extraction of Transcription Factor Expression Plasmids

The transcription factor expression vector received was dotted on the piece of watman paper. The area where the transcription factor expression vector dotted was excised and soaked in $50\mu\text{l}$ of sterile water in the sterile 1.5ml eppendorf tube. The DNA contained-water underwent transformation, amplification and extraction for cell transfection (see transformation using the competent *E. coli* JM109 cells, extraction of plasmid DNA from the recombinant *E. coli* cells and extraction of sterile DNA for cell transfection).

- pEF-c-Myc were kindly provided by Yongfeng Shang - Nutrition Department, Pennsylvania State University, University Park, Pennsylvania 16802, USA
- pCMV-Miz-1 expression plasmid was provided by Frank Hanel - Hans Knöll Institut für Naturstoff-Forschung, Beutenbergstrasse 11, 07745 Jena, Germany
- USF1 was kindly provided by Sawadogo - Department of Molecular Genetics, The University of Texas, MD Anderson Cancer Center, 1515 Holcombe Boulevard, Houston, TX 77030, USA

- YY1 was kindly provided by S.Roberts - Department of Cell Biology, University of Massachusetts Medical Center, Worcester 01655, USA
- TFII-I was kindly provided by A Roy - Program in Immunology, Tufts University School of Medicine, Boston Massachusetts, USA.
- Sp1 were kindly provided by Jackson and Tjian - Department of Molecular and Cell Biology, Howard Hughes Medical Institute, University of California, Berkeley, 401 Barker Hall, Berkeley, CA 94720, USA.
- (pGal4)5-LUC and PM-Sp1 were provided by Yoshihiro Sowa - Division of Cancer Biology, Dana-Farber Cancer Institute, Harvard Medical School, Boston, Massachusetts 02115, USA

2.7. Cell Transient Transfection

Mouse Raw264.7/Cos-1 cell lines were transfected by the liposomal protocol using Lipofectamine reagent (Invitrogen). Briefly, the day before transfection, Raw264.7 cells were harvested by scraping in the complete DMEM media contained in the flasks. For the Cos-1 cells, cells were washed in sterile PBS, 5ml of sterile Trypsin-EDTA (Sigma) was added and was incubated at 37°C for 5 minutes. The trypsinized Cos-1 cells were then placed in complete DMEM media + 10% FCS + 100 U/ml penicillin, 100 µg/ml streptomycin, 2 mM L-glutamine to terminate trypsin digestion.

Cos-1 / Raw 264.7 cells were then transferred to the 50ml falcon tube and were counted using a haemocytometer. Cells were homogenised by pipetting up and down and equal volume of cell was mixed with tryphan blue solution to count the number of viable cells. The following equation was the number of cells needed for transfection:

$$\text{No. of cells counted (16 squares)} \times 2 \text{ (dilution factor)} \times 10^4 = \text{the number of cells /ml}$$

Raw 264.7 cells were plated at a density of 5×10^5 cells/well in a 12 well tissue culture plate and the Cos-1 cells were plated at a density of 1.5×10^5 cells/well in a 6 well tissue culture plate the day before transfection.

For every 3 wells of Cos-1 cells to be transfected, 3µg of the appropriate *Nramp1* constructs ± the appropriate amount of other transcription factor expression vector were dissolved in 150µl of sterile serum and antibiotic free DMEM in a 1.5 ml sterile eppendorf

tubes. 150 μ l of the free addition DMEM together with 7.5 μ l of Lipofectamine were also added to the first 1.5 ml tube containing plasmid DNA, giving a total volume of 300 μ l.

For every 3 wells of Raw 264.7 cells that were to be transfected, 1.5 μ g of appropriate *Nramp1* promoter constructs were co-transfected with the appropriate amount of other protein expression vectors and 5 μ l of Lipofectamine in no addition DMEM, giving the total volume of 200 μ l.

Cells were incubated at room temperature for ~20 minutes for the formation of liposomes with the DNA ready for uptake by the cells. During the 20 minutes incubation time, cells were washed with no addition DMEM. After 20 minutes of incubation at room temperature, 60 μ l or 90 μ l of the Lipofectamine + plasmid DNA mixture were applied to the wells with Raw264.7/ Cos-1 cells containing 0.5ml /1ml of no addition DMEM respectively. After 5 hours of transfection, 0.5 ml /1ml of 20% FCS+DMEM were added to the 12 well plates of Raw264.7 and in the 6 well plates with Cos-1 cells respectively.

For experiments using LPS+IFN- γ or BSO, Raw264.7 cells were treated with LPS (100ng/ml) + IFN- γ (25U/ml) or BSO (indicated concentration) for 24 hours and reporter gene activity assay performed. For studies on L-Gln and transcriptional regulation we used L-Gln-deficient media (Sigma) and the FCS was dialysed overnight against distilled water to remove residual L-Gln. L-Gln was made in L-Gln -deficient media and was added back as indicated after transfection or when needed.

2.8. Firefly Luciferase Reporter Assay

Luciferase assays were performed using a dual luciferase kit (Promega) according to the manufacturer's instructions and was measured by the luminometer (Tuner Design TD20/20). Briefly, Raw264.7 cells were washed twice with PBS (200ml dH₂O + 1 PBS tablet (Sigma) and were lysed directly in the wells with 50 μ l of 1x reporter lysis buffer. The cells were scraped and cell debris was pelleted by centrifugation at 12,000 rpm for 5 minutes and the supernatant was transferred to a 96 well plates. Samples were stored at 4°C on ice.

For each sample, 5 μ l of cell protein extract was added to 50 μ l of the luciferase assay reagent / 2ml eppendorf tube (Luciferase assay reagents were prepared by mixing 1:1 of the luciferase assay substrate + luciferase assay buffer provided in kit. The 1.3ml aliquots stored in -70°C was then thawed at room temperature before use). Sample tube was immediately placed in the luminometer and light emission was measured 3 times per sample with 100% sensitivity.

Protein assay was determined using the BioRad (1X phosphoric acid) assay kit and was used to normalize the luciferase activity per amount of protein (Luciferase Unit/ μg of protein). $1\mu\text{l}$ of the protein sample was added with $250\mu\text{l}$ of the BioRad protein reagent, incubated at room temperature for 5 minutes and was measured with the plate reader (absorbance 570 nm).

2.9. CAT Reporter Gene Assay

To perform CAT assay, cells were harvested by freeze thawing. Transfected cells were washed once with PBS and harvested by scraping into 1ml of PBS. Cell pellets were resuspended in $100\mu\text{l}$ of 0.25M Tris-HCl (pH7.8) and subjected to three rounds of freeze-thaw ($-140\text{ }^{\circ}\text{C}$ and $37\text{ }^{\circ}\text{C}$) lysis. The cell protein extract in the supernatant were transferred into the 96 well microtitre plates and stored at 4°C for assaying. Equal amount of protein extracts used in CAT assay was adjusted by CAT protein assay (see below – CAT protein assay).

After determining the amount of protein for assaying (10-20 mg), a premix of CAT assay reagents ($17.5\mu\text{l}$ Tris-HCl (pH 7.8) + $200\mu\text{l}$ acetyl coenzyme A (0.2mg ml^{-1}) + $0.5\mu\text{l}$ ^{14}C Chloramphenicol (54 Ci mmol^{-1} , Amersham Biosciences) was prepared and added to the $88\mu\text{l}$ of cell protein extract plus deionised water sample per 1.5ml eppendorf. Sample tubes were then incubated at 37°C for $\frac{1}{2}$ -3 hours, depending on the amount of CAT protein present, reflected by the activity of the *Nramp1* promoter activity. The reaction was then stopped by adding 0.5ml of ethyl acetate (Sigma). The extracted Acetyl CoA substrate and the acetylated ^{14}C product were dissolved in ethyl acetate by vortexing the eppendorf tubes, vacuumed dried and was re-dissolved in $\sim 100\mu\text{l}$ ethyl acetate ready for spotting onto the TLC plates.

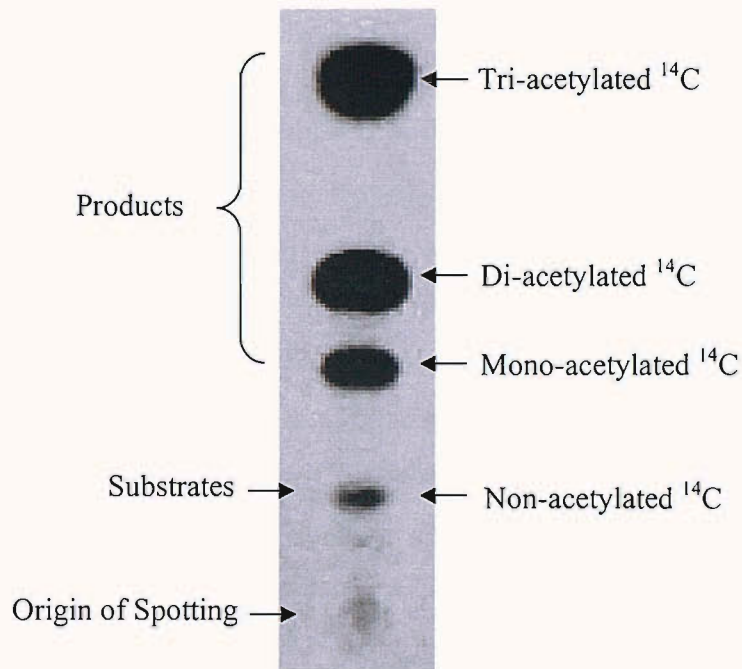
The spotted TLC plates were then placed into a tall glass tank containing CAT running solvent (95% v/v of chloroform (45ml) + 5% v/v of absolute methanol (5ml)). The solvent travelled to the top of the TLC plates to separate the acetylated chloramphenicol product. The TLC plate was then air dried, wrapped in cling film and was placed in the film case ready for quantification on the next day.

The film was then placed directly onto the phosphoimager system (Storm 860) where the radioactive product appeared as a black spot which was then quantified using an Image

Quant 5.0 programme. The CAT activities were described as CAT % conversion (Figure 2.1.).

2.9.1. CAT Protein Assay

The adjusted amount of protein extracts used in CAT assay was normalized by protein assay. 100 μ l of PBS + 0.1% SDS and 100 μ l of protein assay reagent (Pierce, Rockford, USA, made with the manufacturer's instructions) were added to 5 μ l of cell protein extract in the 96 well micro-titre plate. In addition to the samples, a protein standard curve was also produced by pipetting 0 to 11 μ l of BSA [2mg/ml] + 100 μ l of PBS +0.1% SDS and 100 μ l of protein assay reagent. Samples in the 96-well plate were then incubated at 37° C for 40 minutes. The 96-well plate was read at 570 nm and the amount of protein was then calculated.



$$\% \text{ CAT conversion} = \left[\frac{\text{Products}}{\text{Products+Substrates}} \right]$$

Figure 2.1 Calculation of % Chloramphenicol Acetyl Transferase (CAT) conversion. This is an autoradiograph of a CAT assay scanned by the phosphoimager. It indicates the origin and the different acetylated states of the [¹⁴C]-chloramphenicol. The equation shown above was used to calculate the % CAT conversion.

2.10. Stable Transfectant Macrophage Cell lines

Nramp1 stable transfectant cell lines R37 (*Nramp1* allele *G169*) and the control cell line R21 (*Nramp1* allele *D169*) were prepared as described previously⁷³ with *Nramp1* expression under the control of human b-actin promoter in the pHu-b-actin promoter-1-neo plasmid that was provided by P. Gunning (Children's Medical Research Institute, Australia). Anti-Nramp1 immunoblotting confirmed functional Nramp1 protein expression⁷³.

2.11. SDS – Polyacrylamide Gel Electrophoresis and Immunoblotting

2.11.1. Preparation for the Cell Nuclear Extracts

Nuclear extracts from the stable transfectants (R21 and R37) were prepared by resuspending the cell pellet (10^7 cells) with 100 μ l Dignam buffer A (see below) in the 2ml eppendorf. Then the eppendorf was spun at 13,000 rpm for 30 sec. Supernatant was pipetted into a fresh 2ml eppendorf and was mixed with 1 volume (100 μ l) of the Dignam buffer C (see below) which was obtained as cytoplasmic extract. The remaining cell pellet was resuspended in 50 μ l of Dignam buffer C, incubated on ice for 10 min, spun at 13,000 rpm for 30 sec where the supernatant was obtained as the cell nuclear extracts. The protein concentration of samples was determined using a Bradford DC assay kit (Bio-Rad) according to the manufacturer's instruction.

Dignam Buffer A	Dignam Buffer C
100 μ l 1M Hepes	200 μ l 1M Hepes
15 μ l 1M MgCl ₂	2.5ml Glycerol
100 μ l 1M KCl	842 μ l 5M NaCl
5 μ l 1M DTT (reducing agent)	15 μ l 1M MgCl ₂
200 μ l 1/10 NP40 (protease inhibitor)	5 μ l 1M DTT (reducing agent)
9.4ml dH ₂ O	4 μ l 0.5M EDTA
Total volume = 10ml	6.5ml dH ₂ O
	Total volume = 10ml

2.11.2. Preparation for Loading and Running the SDS - Polyacrylamide Gel

The nuclear extracts together with the protein dye was boiled to denature the secondary structure of protein for loading. Nuclear extracts (20 μ g) from the stable transfectant Raw264.7 cells (R21 and R37) and mouse Raw264.7 cells treated with BSO and L-Gln respectively were fractionated by electrophoresis through a 10% resolving gel (see below). ~1ml of Butanol was pipetted on top to straighten up the gel. When the 10 % resolving gel was set, butanol was discarded and was rinsed with dH₂O. Stacking gel was then prepared (see below), overlaid on the 10% resolving gel and the gel comb was inserted. Single SDS gel was run at ~100V in the 1X running buffer (see below) until the blue dye almost ran off the bottom and the gel was transferred into the transfer buffer (see below).

2.11.3. Transfer of Protein from the SDS-Polyacrylamide Gel onto Nitrocellulose Membrane by Semi-dry Electrophoresis

Nitrocellulose membrane (nitrocellulose membrane (Millipore PVDF with 45um filter pore size) and Watman paper was cut to size 6cm x 8cm. They were soaked in the transfer buffer (see below) prior to the transfer. Three Watman paper was laid on the electrophoresis plate of the semi-dry transfer machine (BioRad), then the nitrocellulose membrane, the polyacrylamide gel and finally the 3 pieces of Watman paper on top. After the transfer for 1 hour at 100V, the nitrocellulose membrane was blotted in the blocking solution (see below) for about 10 mins to prevent non-specific protein binding.

<p>10% Resolving Gel 4.2ml 4X resolving solution 5ml H₂O 3.3ml Acrylamide 30% 100µl of APS (100mg/1ml) 10µl TEMEM (last to mix in)</p>	<p>Stacking Gel 2.5ml stacking solution 2X 850µl Acrylamide 1.7ml H₂O 50µl APS 5µl TEMED (Last to mix in)</p>
<p>Resolving Solution 50ml of 1.5M Tris pH8.8 2ml of 10% SDS Distill H₂O to make 200ml in total</p>	<p>Stacking Solution 25ml 1M Tris pH6.8 2ml 10% SDS Distill H₂O to make up 200ml in total</p>
<p>Running Buffer 900ml dH₂O 100ml Running buffer solution 10X</p>	<p>Transfer Buffer 200ml Running buffer 1X 50ml Absolute Methanol</p>
<p>Blotting Solution 10g Marvel milk 100ml TBS-0.1% Tween (400ml TBS+0.4ml Tween 20)</p>	<p>TBS –Tween (pH7.4) 1.21g Tris 4g NaCl 500ml dH₂O 500µl Tween 20</p>

2.11.4. Immunoblots with Antibodies

The nitrocellulose blot was incubated for 1 hour with primary antibodies diluted in TBS-0.1%Tween 20 containing 5% Marvel. Rabbit polyclonal recognizing Nramp1

(1:1000) was raised to the amino-terminal cytosolic domain of Nramp1 using GSH-S-transferase (GST) fusion proteins⁸². After incubation with primary antibodies, blots were extensively washed (>3 times) in TBS-0.1% Tween 20 before incubation for 1 hour in the Goat anti-rabbit horseradish peroxidase conjugate immunoglobulin G (IgG) antibody at 1:15000 dilution in TBS-0.1% Tween 20 containing 5% Marvel. After extensive washing in TBS-0.1% Tween 20, the blots were soaked in distilled water for detection of protein using the chemiluminescence (Santa Cruz).

2.11.5. Visualisation of Protein on the Nitrocellulose Membrane

The amount of protein being transferred from the SDS-polyacrylamide gel to the nitrocellulose membrane can be visualised by staining the membrane with amido black (45% absolute methanol + 10% acetic acid + 0.1% naphthol blue black). Excess amido black on the membrane can be removed with some destain (45% absolute methanol + 5% glacial acetic acid + 50% distill H₂O).

2.12. Cell Proliferation Assay

Crystal violet was used to stain the cells and the density of the cells was measured with the plate reader at 570nm. Briefly, sparse number of cells (~1x10³) stable transfectant cells R21 and R37 were plated in 96-well micro titre plate. 100µM of FAS and the indicated amount of BSO were incubated with the cells which were left to grow from day 1-5 by incubating at 37°C. After incubation, medium in the wells were removed by flicking and blotted on the blue paper towel. On day 1, day 2, day 3, day 4 and day 5, one 96 well plate was then stained with ~500µl of crystal violet for ~1 min (20% absolute methanol (20ml) + 0.5% crystal violet (0.5g) + 79.5% dH₂O (79.5ml)). Post crystal violet staining, excess dye was removed by soaking the 96-well plate in tap water, blotted on the blue towel and then fixed in 100% methanol. The absorbance was then measured at 570nm.

3. Chapter 3

Role of the Initiator Binding Factors - USF1, YY1, c-Myc, Miz-1, TFII-I on the Regulation of *Nramp1* Promoter Activity

3.1. Introduction

3.1.1. c-Myc

c-Myc is the proto-oncoprotein that belongs to the bHLH/LZ transcription factor super family where its deregulation promotes tumour development and progression⁸³ (Figure. 3.1). The role of c-Myc in the regulation of *Nramp1* was initiated by the findings of Wu *et al.*,⁷⁸ which demonstrated that c-Myc positively regulates IRP2 and negatively regulates ferritin to enhance the cytosolic iron pool. The works suggested a fundamental role of c-Myc in the regulation of transcription for the control of genes that regulate iron homeostasis. c-Myc inhibits the *Nramp1* promoter by competing with the Inr-binding protein Miz-1 for the binding of co-activator p300^{56,57,84,85}. One interpretation of these data is that *Nramp1* reduces cytosolic iron in cells.

c-Myc expression promotes cell proliferation by inhibiting the expression of growth repressing genes such as *p21*⁸⁶, *p15*⁸⁷ and *p27*⁸⁸⁻⁹⁰ by binding indirectly to the Inrs in their promoters. Inr-binding factors through which c-Myc interacts include the Inr-binding proteins YY1^{91,92}, Miz-1⁸⁴, TFII-I⁹³ and Sp1⁹⁴.

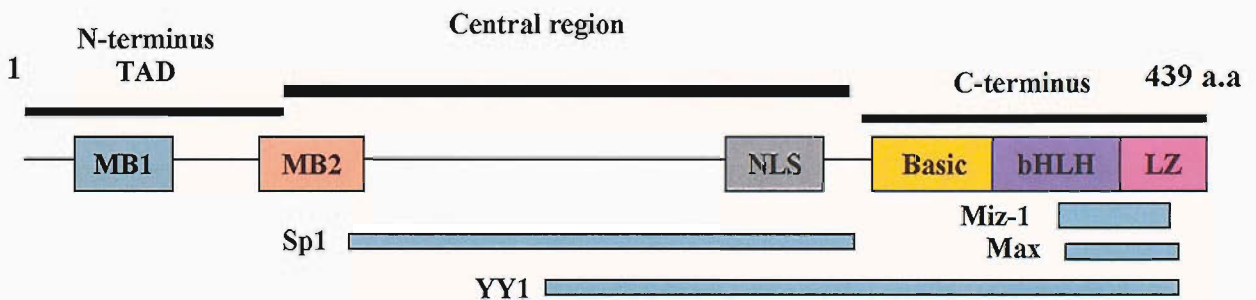


Figure. 3.1 A Schematic Diagram of the c-Myc Polypeptide Structure. c-Myc contains 3 domains: N-terminus, C-terminus and the central region consisting of 439 amino acid. The bHLH-LZ motifs promote protein-protein interaction. The basic region mediates sequence-specific DNA binding. The transcriptional activation domain (TAD) has been mapped to the amino terminus. Both the bHLH-LZ and TAD domains are essential for transcriptional transactivation, proliferation and trans-formation⁸³. Two highly conserved domains are found in the N-terminus of c-Myc – Myc box 1 (MB1) and MB2. Factors involved in Inr-dependent transcriptional repression such as Miz-1 binds to c-Myc at the C terminus HLH-LZ through the amino acid V394^{78,85}. Factors that are involved in Inr-dependent transcriptional repression such as Miz-1 and YY1 bind to the C-terminal of c-

3.1.2. USF1

USF1 is a member of the bHLH-LZ protein super family which includes Myc, Max and Mad (Figure 3.2) ⁹⁵. USF1 is ubiquitously expressed ⁹⁶ and is originally identified by its ability to bind to Inr or to the E-box site (CACGTG or CACATG) of the AdML promoter ^{53,60,97,98}.

USF interacts at the promoter by forming either homo (USF1/USF1 or USF2/USF2) or heterodimers (USF1/USF2) (the major form of USF present in most cell) ^{96,98}. In addition, USF1 physically interact with p300 ⁹⁹, Sp1 ¹⁰⁰, but not Miz-1 ⁸⁴. USF1 also interacts cooperatively with TFII-I at both Inr and E-box sites ⁶⁰.

c-Myc and USF1 differentially regulate cell proliferation, cellular transformation ¹⁰¹ and the promoter transcription ¹⁰². Interestingly, the opposing activity of USF and c-Myc on cellular transformation and proliferation resulted from their opposite effects on the expression of initiator-containing genes ¹⁰³.

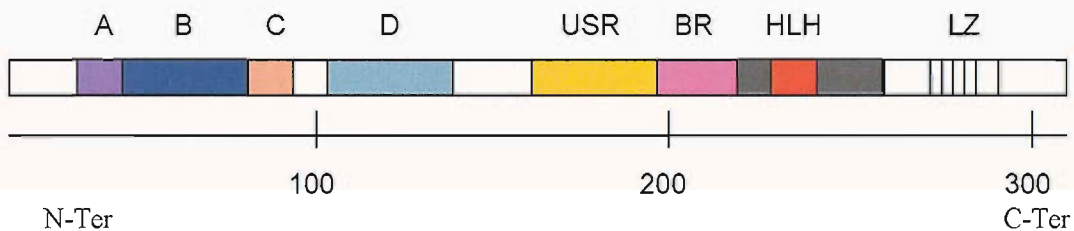


Figure. 3.2 The Schematic Diagram of USF1 Polypeptide Structure. USF1 domains include the basic region (BR), the helix-loop-helix region (HLH), the leucine zipper domain (LZ), USF specific region (USR) domain, the post-activation domain A (A), the negative regulatory domain B (B) and its counteracting activation domain A (C), and the spacer/activation domain D (D). The bar at the bottom indicates the positions within the 310 residue of USF1. USR is well conserved, located just upstream of the BR that is implicated both in nuclear localization and in the specific activation of promoters containing an initiator element ¹⁰¹.

3.1.3. Miz-1

Miz-1 was isolated as a novel c-Myc interacting transcription factor ^{84,104} which is made up of 803 amino acids with a predicted molecular weight of 87,970 Da ¹⁰⁵. It has 13 zinc fingers and 12 of which are immediately clustered in the central domain of the protein (Figure 3.3). Miz-1 forms a Miz-1/c-Myc/Max trimeric complex that specifically binds to the Inr elements and represses cell cycle inhibitor genes *p15*, *p21* and *p27* ^{84,106}. In

response to c-Myc down-regulation, these genes are activated in a Miz-1 dependent manner at the Inr.

Miz-1 positively regulates the *Nramp1* promoter and the repressive action of c-Myc requires the binding of Miz-1 at the Inr of *Nramp1*¹⁰⁷. Miz-1 also stabilizes c-Myc against ubiquitin-mediated proteolysis¹⁰⁸. Furthermore, Miz-1 binds c-Myc but not USF1⁸⁴.

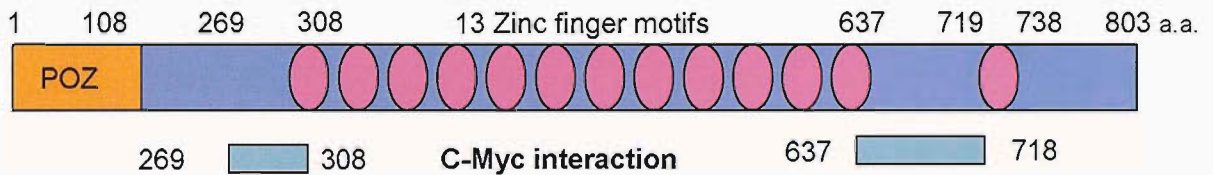


Figure. 3.3 A Schematic Diagram Representing the Miz-1 Protein Structural Domain. The N-terminal POZ domain is well conserved which is important for protein-protein interaction. The 13 zinc finger motifs are represented as ovals. Interacting region of c-Myc with Miz-1 is shown¹⁰⁵.

3.1.4. TFII-I

TFII-I is a transcription factor that binds to the Inr sites and stimulates transcription from the TATA and Inr containing AdML promoter with the consensus sequence 5'-YAYTCYYY-3'^{60,109} (Figure 3.4). TFII-I acts independently and synergistically with USF1 through E-box and Inr elements present in the AdML promoter^{53,60,109}. Studies have shown that simultaneous addition of USF1 and TFII-I generated a novel complex indicative of highly cooperative interactions⁵⁵. TFII-I physically and functionally interacts with transcription factors USF¹⁰⁹, c-Myc⁹³, and potentially YY1^{55,91}.



Figure. 3.4. Schematic Diagram of TFII-I. TFII-I has four alternatively spliced isoforms: α (977 amino acids), β (978 amino acids), γ (998 amino acids), and Δ (957 amino acids). TFII-I was characterized by the presence of six repeating 90-residue motifs that each possesses a potential helix-loop/span-helix homology (R1-6). Leucine zipper (LZ) motif occurs between amino acids 23 and 44 represented by the purple box. The functional nuclear localization sequence (a.a.278-284) and the basic region (a.a 301-306) are marked as nuclear localization signal (NLS) and (basic region) BR respectively⁶⁰.

3.1.5. YY1

YY1 is a ubiquitously expressed transcription factor that binds with its four C₂H₂ zinc fingers to the Inr of the AAV P5 promoter¹¹⁰ (Figure 3.5). YY1 plays a role to either activate or repress transcription through the interaction with HDACs or HATs^{58,111-113}. The role of YY1 implicates both Sp1^{114,115} or p300¹¹¹ factors and the general transcription machinery^{112,113}. YY1 associates with c-Myc^{91,53,92} and its increase DNA binding activities impaired the association of c-Myc with Max or Mad for regulation of transcription¹¹⁶.

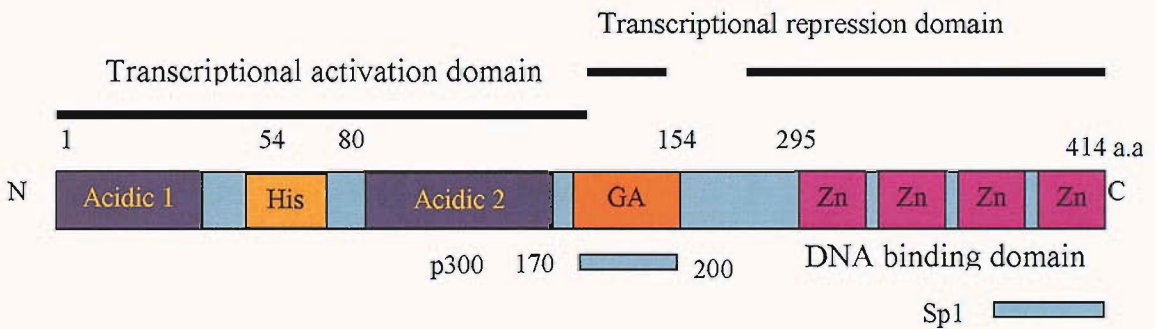


Figure 3.5 Schematic Diagram of the Human YY1 Primary Protein Structure. Acidic regions 1 and 2 are transactivation domain. ‘His’ represents a stretch of 11 consecutive Histidine residues. The acetylation of YY1 by p300 occurs at the GA which are glycine and alanine rich region; the spacer region contain no recognized structure but are required for optimal transactivation; The 4 Zn finger-DNA binding domains (Zn) are represented in pink. The first one and a half of the Zinc fingers of YY1 contain an element necessary for the interaction with Sp1^{114,115}.

3.2. Specific Aims

The aims of this chapter are to investigate:

1. Potential roles of the Inr-binding factors USF1, YY1, TFII-I, Miz-1 and c-Myc on the transcriptional regulation of *Nramp1* promoter.
 - a. In the context of AdML promoter, TFII-I and USF1 activated both at the Inr and at the E-box elements ^{60,109}. We investigate if TFII-I and USF1 has any consequence on the *Nramp1* promoter function.
 - b. As USF1 and Miz-1 do not interact functionally with each other ⁸⁴, yet both of the transcription factors functionally interact at the Inr of different promoters ^{2,56}, we investigate the role of USF1 and Miz-1 on the regulation of *Nramp1*.
 - c. c-Myc interacts with YY1 ^{91,92} where c-Myc alone negatively regulates the *Nramp1* promoter ⁸. Therefore, we investigate the role of YY1 and c-Myc on the regulation of *Nramp1* promoter.

3.3. Results

3.3.1. 5' Deletion Analysis of the *Nramp1* Promoter Activity

As the 5' *Nramp1* promoter sequence was deleted (Figure 3.6A), there was ~1.2-fold increase of *Nramp1* promoter activity when comparing *Nramp1* construct pHB4 with pHB20 (P=0.02). Furthermore, the deletion of the consensus Sp1 binding site (5'-GGGCG -3', -26/-21bp) caused a further ~6-fold activation of *Nramp1* construct pHB23 when compared with pHB20 (Figure 3.6A, P = 0.01).

3.3.2. USF1 Activated the *Nramp1* Promoter

Transfection of USF1 expression plasmid alone caused activation on different *Nramp1* promoter constructs, pHB4, pHB6, pHB20 and pHB23 when compared with the respective controls, which were without the addition of USF1 plasmid (Figure 3.6B ~3-, 3-, 11-, 16-fold activation respectively, P = 0.11, 0.05, 0.01 and 0.008). The highest fold of activation on pHB23 with USF1 suggested functional interaction of USF1 at the Inr.

3.3.3. Functional Redundancy of *Nramp1* promoter Inr Elements

Nramp1 construct pHB23 demonstrated ~100-fold activation when compared with pHB22 (Figure 3.7, P = 0.01), suggesting that the 2 Inr elements were necessary for the basal transcriptional activity of *Nramp1*.

To determine which Inr was necessary for the *Nramp1* promoter activity, Cos-1 cells were transfected with pHB23, pCAT24 (1st Inr sequence, CCACTCT mutated to CCACGGG) and pCAT25 (2nd Inr sequence, TCACTCG mutated to TCACGGG) (Figure 3.8). However, no significant reduction was observed in pCAT24 (P = 0.08) or in pCAT25 (P = 0.24) when compared with pHB23 indicating functional redundancy of Inr elements.

3.3.4. USF1 Activated the *Nramp1* Promoter was Dependent upon the Inr

The importance of the Inr elements for the positive regulation by USF1 in pHB23 was assessed (Figure 3.6B). Transfection of USF1 expression plasmid caused activation in pHB23 (Figure 3.9 – P = 0.004), but not in pHB22 when both the Inr elements were deleted (P = 0.45). This indicated that the activation of the *Nramp1* promoter by USF1 was dependent upon the 2 Inr elements.

3.3.5. YY1 Blocked the c-Myc Mediated Repression on the *Nramp1* Promoter

YY1 activated the *Nramp1* construct pHB23 (Figure 3.10, ~1.3- fold, P = 0.03) but not in pHB4 (P = 0.78). c-Myc repressed the activity of *Nramp1* constructs pHB4 and pHB23 (Figure 3.10, ~3 and 5- fold inhibition with P = 0.04 and 0.002 respectively) which was consistent with previous results ⁸.

Co-transfection of YY1 with c-Myc expression plasmids had no effect on pHB4 (Figure 3.10 – P = 0.38) and pHB23 (P = 0.07) when comparing with the plasmid controls. However, the combination of YY1 and c-Myc blocked the inhibition of c-Myc on both pHB4 and pHB23 *Nramp1* constructs (Figure 3.10, ~2- and 5- fold, P = 0.04 and 0.0008 respectively).

3.3.6. Synergistic Effect of TFII-I + USF1 on the *Nramp1* Promoter

Transfection of the TFII-I expression plasmid alone did not activate pHB6 (Figure 3.11, P = 0.3) or pHB20 (P = 0.35) when compared to the control. However, co-transfection of TFII-I and USF1 expression plasmids activated pHB20 in comparison with the control (Figure 3.11, ~19- fold activation, P = 0.01), but did not activate pHB6 (P = 0.12). In addition, synergistic activation was observed with USF1+TFII-I when compared to USF1 alone (Figure 3.11, ~2- fold activation, P = 0.04) in pHB20, but not in pHB6 (P = 0.6) that correlates with the loss of 2 putative E-box elements.

3.3.7. Miz-1 and USF1 did not Functionally Interact at the *Nramp1* Promoter

Co-transfection of Miz-1+USF1 caused 18- fold activation in construct pHB20 (Figure 3.12, P = 0.04) and pHB23 (P = 0.02, ~9-fold activation) when compared to the control. However, Miz-1+USF1 did not cause a synergistic increase of the *Nramp1* construct pHB20 or pHB23 when compared to USF1 alone (Figure 3.12 – P = 0.32 and 0.8 respectively). Transfection of USF1 alone activated the *Nramp1* construct pHB20 and pHB23 (Figure 3.12, 14- and 8.8- fold activation, P = 0.01 and 0.0001 respectively). Miz-1 alone caused activation on pHB20 but not in pHB23 (Figure 3.12, ~3-fold activation, P = 0.04 and 0.67 respectively), which was consistent with the results shown in the previous experiments ⁵⁷.

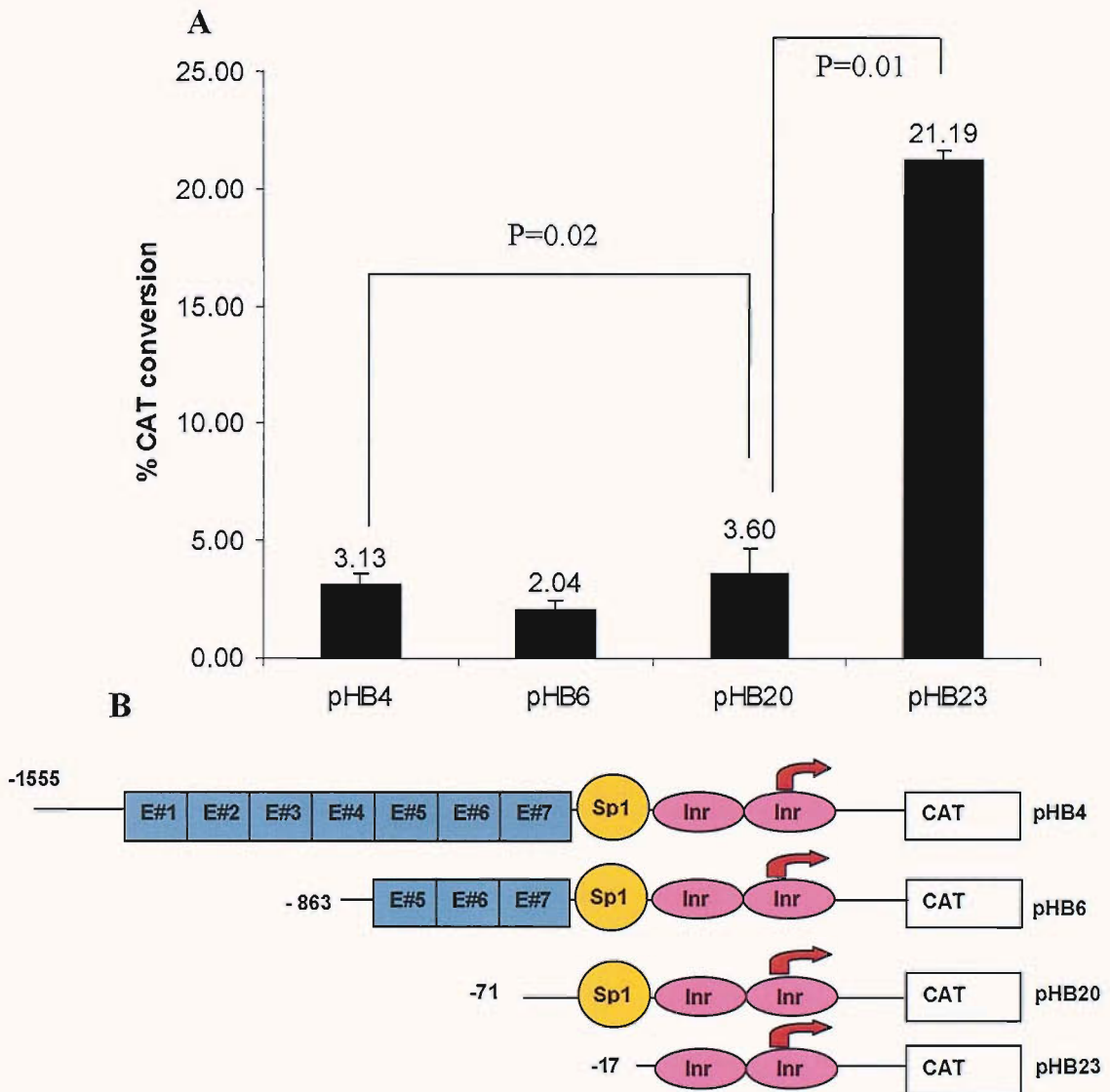


Figure 3.6A. 5' Deletion Analysis of *Nramp1* Promoter Activity. 1.5×10^5 Cos-1 cells were co-transfected with $1 \mu\text{g}$ of the deletion *Nramp1* CAT driven constructs pHB4, 6, 20 and 23. Results are presented as acetylated chloramphenicol product expressed as a percentage of substrate + product (CAT conversion, %). Five hours after transfection, 20% FCS no addition media was added for overnight. Cells were washed with PBS and lysed by freeze thawing. $20 \mu\text{g}$ of protein products were incubated for 4 hours at 37°C (see Material and Methods for CAT assay protocol).

B. Schematic diagram of the different *Nramp1* promoter 5' deletion constructs (pHB4, pHB6, pHB20, pHB23)

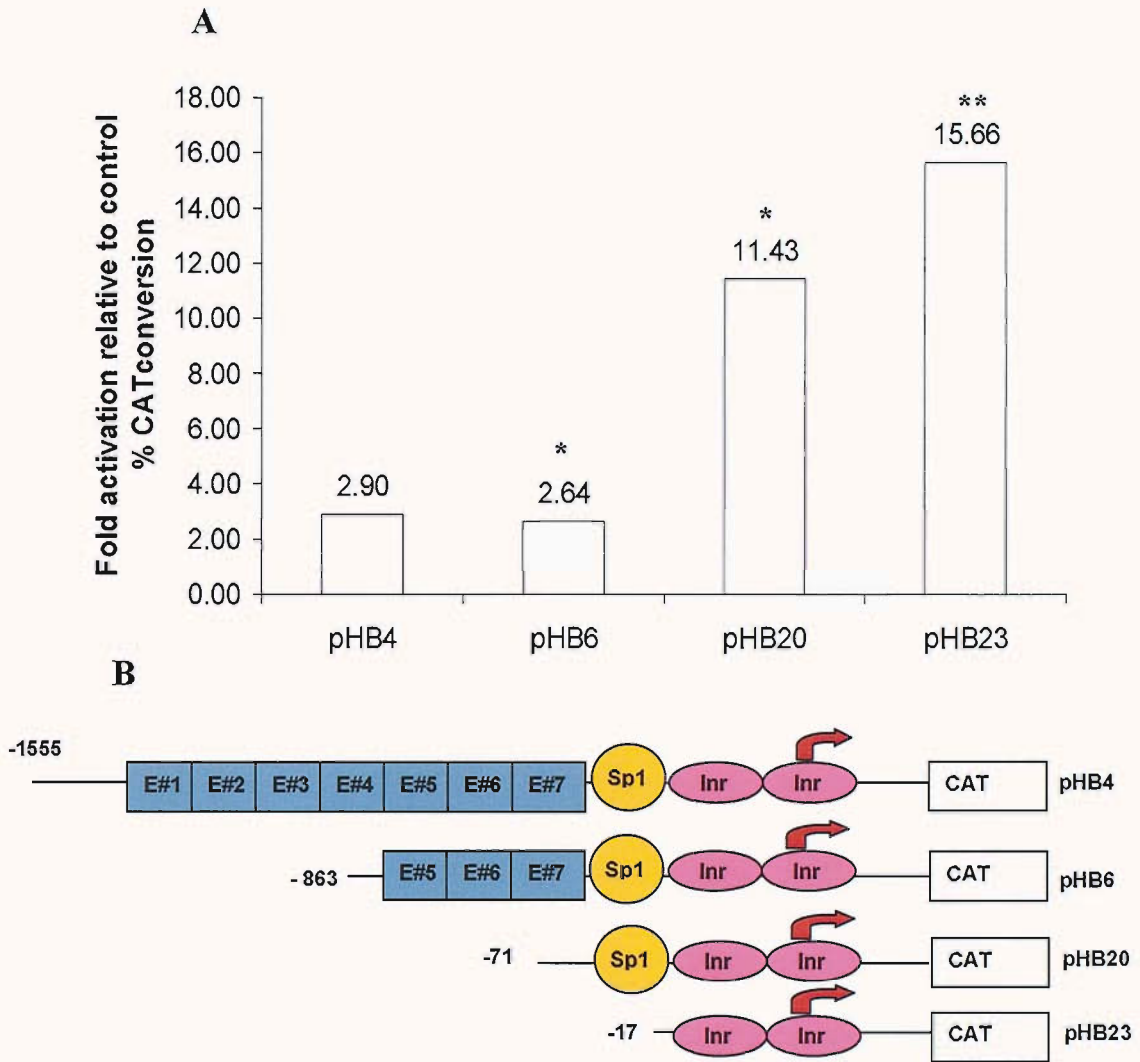


Figure 3.6B Activation of *Nrampl* Promoter Activity by Co-transfecting USF1 plasmids. 1.5×10^5 Cos-1 cells were co-transfected with $1 \mu\text{g}$ of *Nrampl* CAT driven constructs pHB4, 6, 20 and 23 with $0.1 \mu\text{g}$ of USF1 expression plasmid. Results were presented as fold activation by USF1 relative to their respective control (without the addition of $0.1 \mu\text{g}$ USF1), which was shown as an acetylated chloramphenicol product volume quantitation expressed as a percentage of substrate + product (% CAT conversion). The total amount of plasmid in the transfection experiments were normalized to $1.1 \mu\text{g}$ with the control plasmid. Five hours after transfection, 20% FCS with no addition DMEM- media was added. 24 hours later, cells were washed with PBS and lysed by freeze thawing. $20 \mu\text{g}$ of protein products were incubated for 4 hours at 37°C . Student T-test is represented as * = $P \leq 0.05$ ** = $P = 0.008$.

B. Schematic diagram of the different *Nrampl* promoter 5' deletion constructs (pHB4, pHB6, pHB20, pHB23)

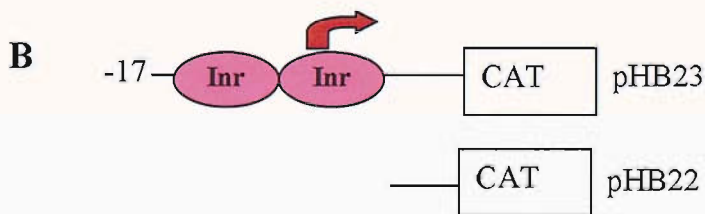
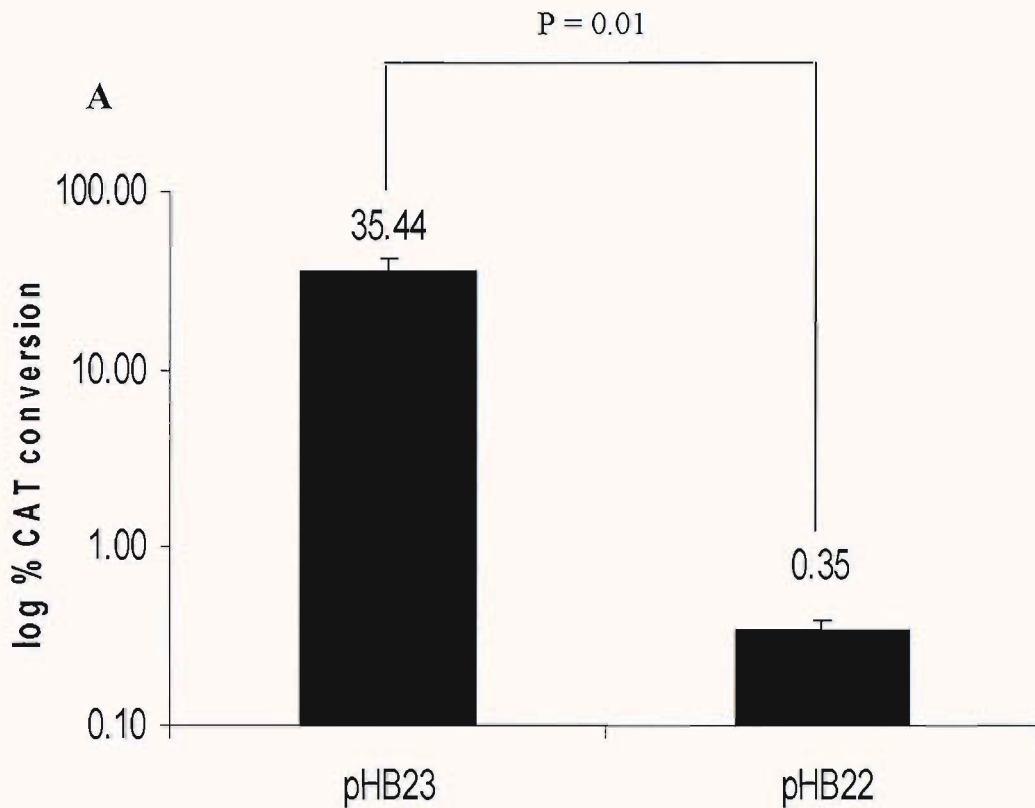


Figure 3.7 The Essential Function of the 2 Putative Inr Elements on *Nrampl* Promoter. A. 1.5×10^5 Cos-1 cells were co-transfected with $1 \mu\text{g}$ of *Nrampl* CAT driven construct pHB22 or pHB23. Five hours after transfection, 20% FCS no addition DMEM media was added for overnight. Cells were washed with PBS and lysed by freeze thawing. $20 \mu\text{g}$ of protein extract was incubated for $\frac{1}{2}$ hour at 37°C . Results were presented as log % CAT conversion.

B. Schematic diagram of the different *Nrampl* promoter 5' deletion constructs (pHB22, pHB23)

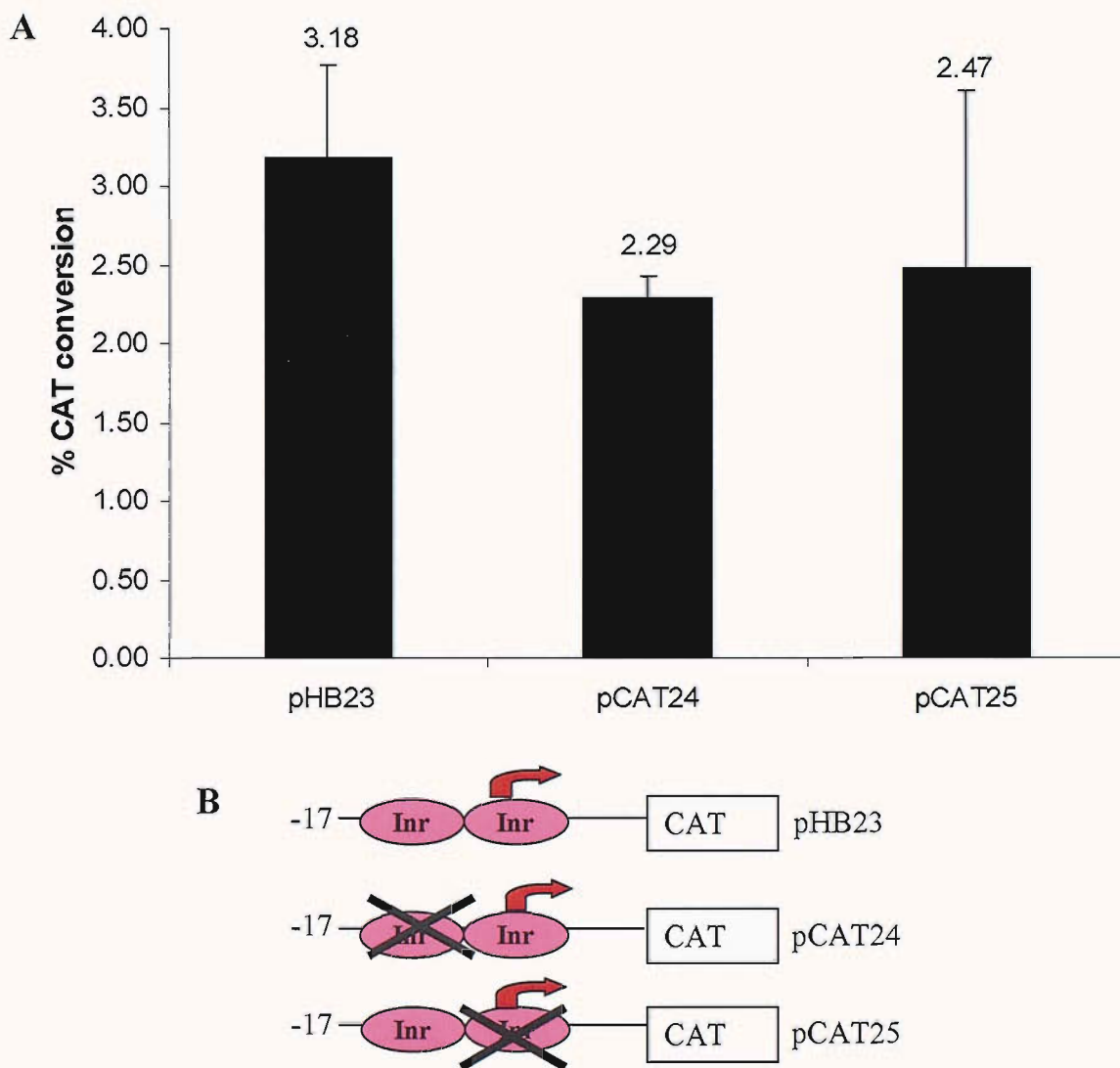


Figure 3.8 Functional Redundancy of the Inr Elements on *Nrampl* Promoter. A. 1.5×10^5 Cos-1 cells were co-transfected with $1 \mu\text{g}$ of the *Nrampl* CAT driven constructs pHB23, pCAT24 or pCAT25. Five hours after transfection, 20% FCS no addition DMEM media was added for overnight. Cells were washed with PBS and lysed by freeze thawing. $10 \mu\text{g}$ of protein extract was incubated for $\frac{1}{2}$ hour at 37°C . Data were presented as % CAT conversion.

B. Schematic diagram of the different *Nrampl* promoter 5' deletion constructs (pHB23, pCAT24, pCAT25)

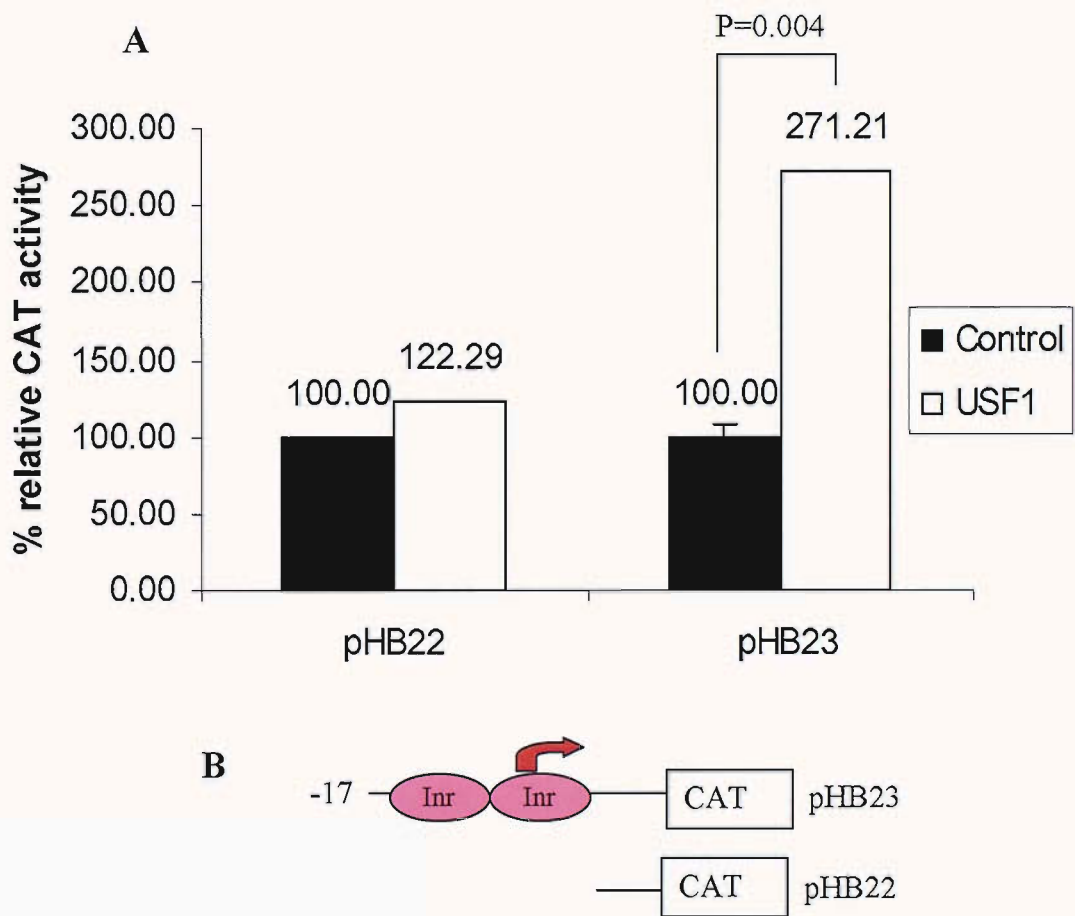


Figure 3.9 Functional Redundancy of Inr Elements on the Activation of *Nrampl* by USF1. A. 1.5×10^5 Cos-1 cells were co-transfected with $1 \mu\text{g}$ of *Nrampl* CAT driven construct pHB22 or pHB23 (black) with $0.1 \mu\text{g}$ of USF1 expression vector (clear). The total amount of plasmid in the transfection experiments were normalized to $1.1 \mu\text{g}$ with the control plasmid. Five hours after transfection, 20% FCS no addition DMEM media was added and incubated for overnight. Cells were then washed with PBS and lysed by freeze thawing. $20 \mu\text{g}$ of protein extract was incubated for $\frac{1}{2}$ hour at 37°C . Results were presented as % relative to the control plasmid of % CAT conversion.

B. Schematic diagram of the different *Nrampl* promoter 5' deletion constructs (pHB22, pHB23).

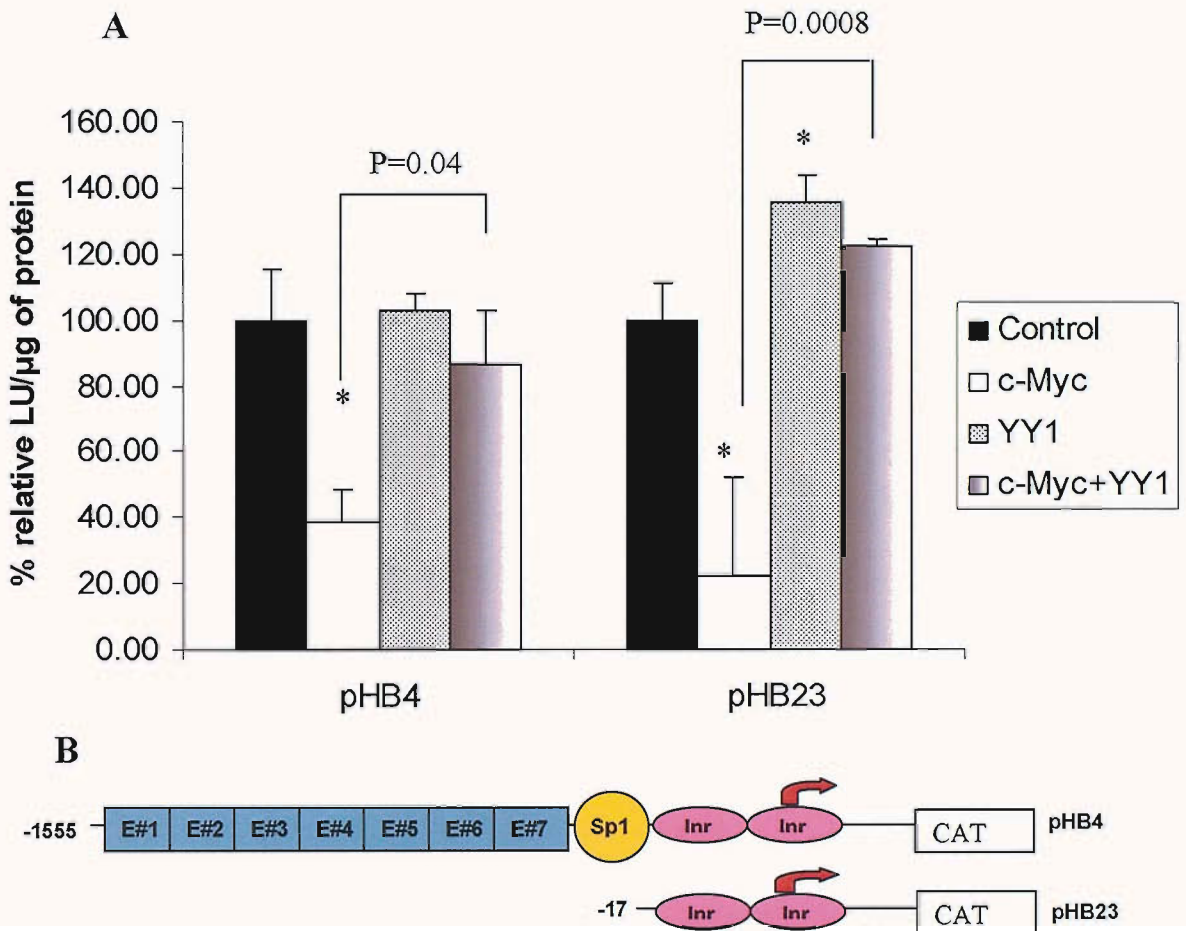


Figure 3.10. YY1 Prevented the Inhibitory Role of c-Myc on *Nrampl* Promoter. A. 1.5×10^5 of Cos-1 cells were co-transfected with $1 \mu\text{g}$ of *Nrampl* CAT driven construct pHB4 and pHB23 with $1 \mu\text{g}$ of c-Myc (clear), $1 \mu\text{g}$ of YY1 expression vector (spotted) or with both c-Myc and YY1 (shaded). The total amount of plasmid in the transfection experiments were normalized to $3 \mu\text{g}$ with the control plasmid. Five hours after transfection, 20% FCS media was added and incubated overnight. Cells were then washed with PBS and lysed by freeze thawing. $20 \mu\text{g}$ of protein extract was incubated for 3 hours at 37°C . Results were indicated as CAT conversion (%). Student t-tests are compared with respective control * = $P \leq 0.05$.

B. Schematic diagram of the different *Nrampl* promoter 5' deletion constructs (pHB4, pHB23)

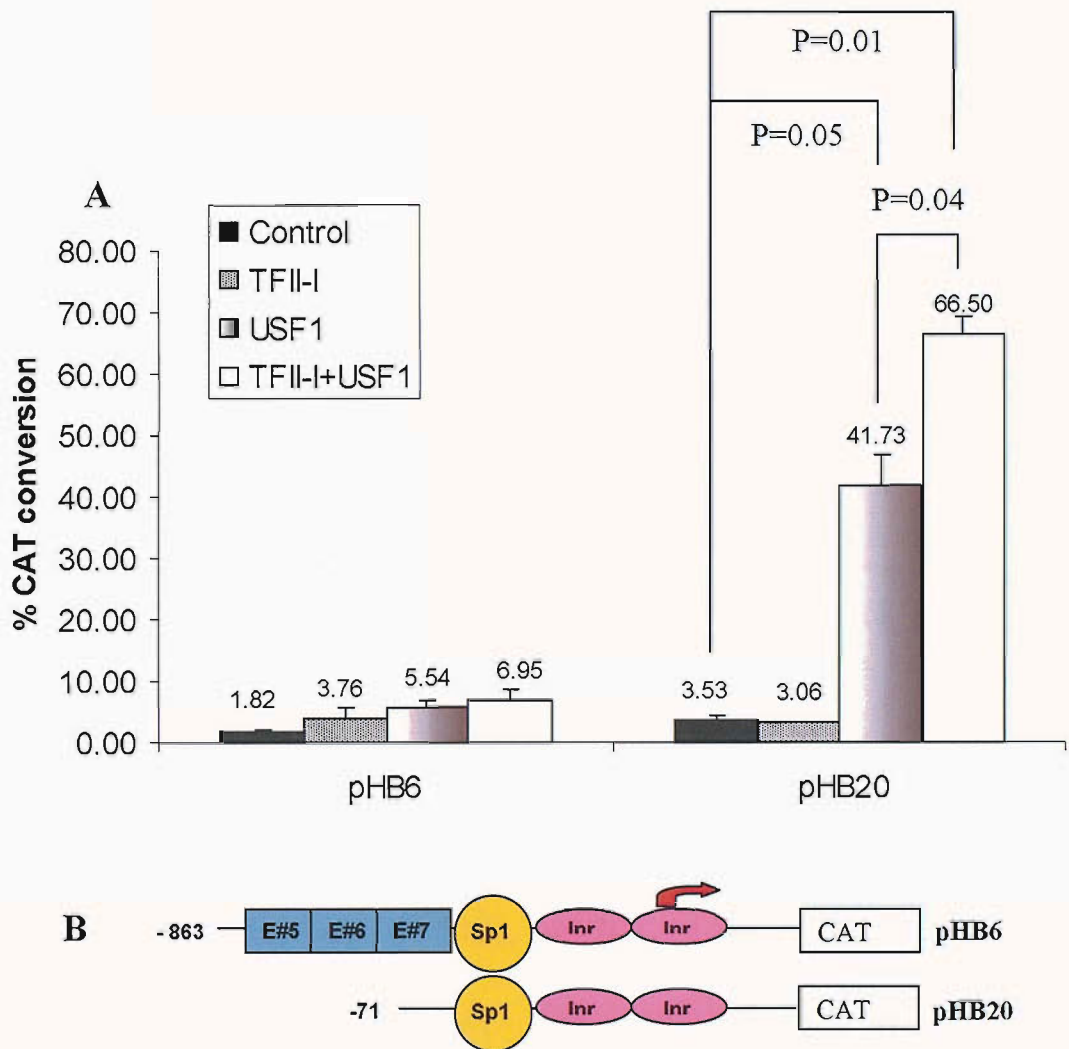


Figure 3.11. USF1 and TFII-I Activated *Nrampl* Promoter in a Synergistic Manner. A. 1.5×10^5 Cos-1 cells were co-transfected with $1 \mu\text{g}$ *Nrampl* CAT construct pHB6 or pHB20 with $1 \mu\text{g}$ of TFII-I (dotted), $0.1 \mu\text{g}$ of USF1 (Shaded) or in combination (clear). The total amount of plasmid in the transfection experiments were normalized to $2.1 \mu\text{g}$ with the control plasmid (black). Five hours after transfection, 20% FCS with no addition of media was added and incubated for overnight. Cells were then washed with PBS and lysed by freeze thawing. $20 \mu\text{g}$ of protein extract was incubated for 4 hour at 37°C . Results were indicated as % CAT conversion.

B. Schematic diagram of the different *Nrampl* promoter 5' deletion constructs (pHB6, pHB20)

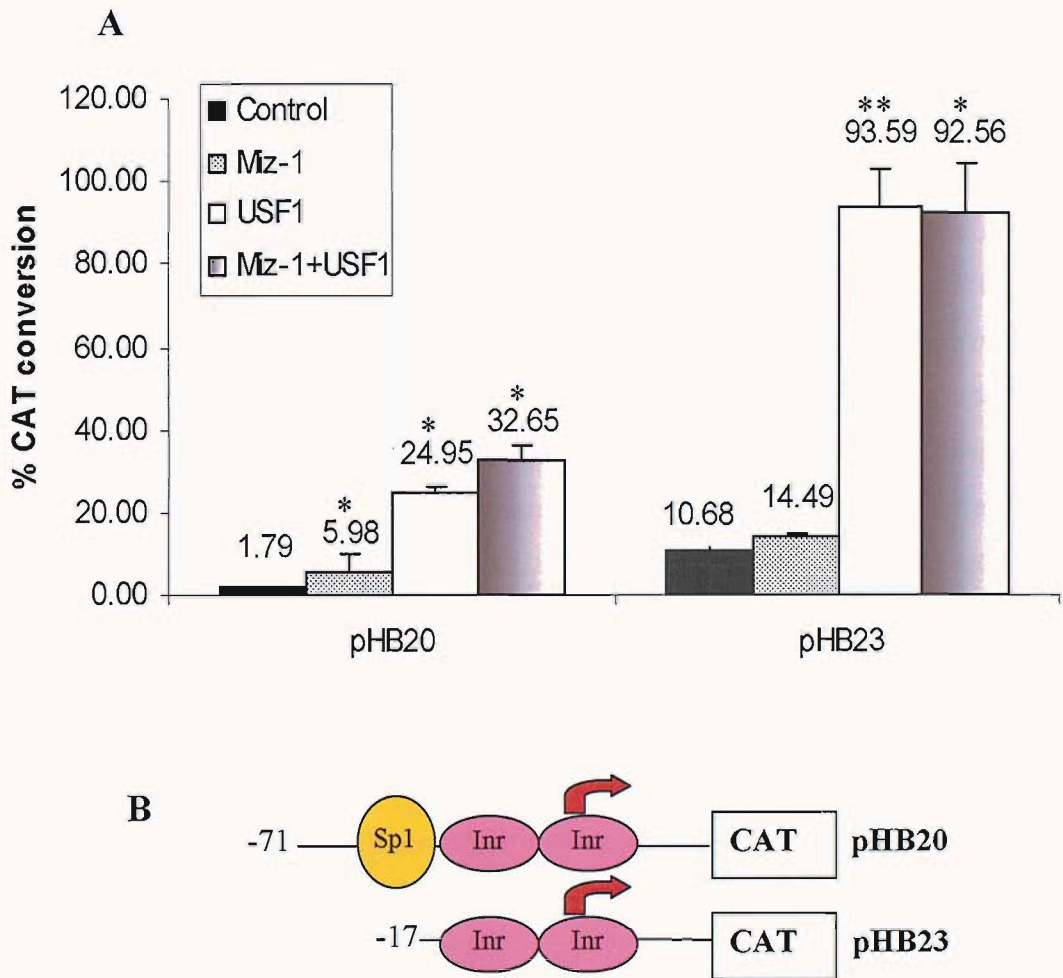


Figure 3.12. Miz-1 and USF1 Independently Activated *Nramp1* promoter but not in Synergy. A. 1.5×10^5 Cos-1 cells were co-transfected with $1 \mu\text{g}$ of pHB20 or pHB23 *Nramp1* CAT constructs with $1 \mu\text{g}$ of Miz-1 (dotted), $0.1 \mu\text{g}$ of USF1 (clear) or in combination (shaded). The total amount of plasmid in the transfection experiments were normalized to $2.1 \mu\text{g}$ with the control plasmid (black). Five hours after transfection, 20% FCS no addition DMEM media was added and incubated for overnight. Cells were then washed with PBS and lysed by freeze thawing. $20 \mu\text{g}$ protein extract was incubated for 4.5 hour at 37°C (for method, see chapter 2). Results were indicated as % CAT conversion. Student t-tests were compared with the control. * = $P \leq 0.05$, ** = $P = 0.0001$.

B. Schematic diagram of the different *Nramp1* promoter 5' deletion constructs (pHB20, pHB23)

3.4. Discussion + Future Experiments

This chapter demonstrated the role of Inr-binding transcription factors on the regulation of *Nramp1* promoter. The present study has focused on the following factors, USF1, TFII-I, Miz-1, c-Myc and YY1 which interact at the consensus Inr elements. Data supported the concept that USF1 transactivated the *Nramp1* promoter which was dependent upon the two Inr elements. The single Inr-deletion experiments supported the notion that the two Inrs are identical and functionally redundant. USF1 and TFII-I also activated the *Nramp1* promoter in a synergistic manner indicating functional interaction between USF1 and TFII-I on the *Nramp1* promoter. Interestingly, TFII-I or YY1 did not activate when transfected alone in a promoter construct that contained upstream promoter sequences. However, YY1 activated at the Inr, although significant, the fold induction was very low and the relevance was not clear. An interesting finding of YY1 function was that YY1 prevented the repressive activity of c-Myc on the *Nramp1* promoter. The present study also demonstrated that Miz-1 and USF1 individually activated *Nramp1*, but did not display synergy. This chapter has given insights to the role of the Inr-binding factors on the regulation of *Nramp1* transcription (Figure 3.13); however these functional data need to be validated by protein binding studies such as the use of the CHIP assay.

3.4.1. USF1 Positively Regulated the Murine *Nramp1* Promoter Transcription at the Inr

USF1 belongs to the same bHLH-LZ protein superfamily member as c-Myc⁹⁵ which binds at the E-box elements or at the Inr on AdML promoter^{60,98,109}. The result in Figure 3.6B demonstrated that USF1 caused the dramatic upregulation of the *Nramp1* construct pHB23 which indicated the role of USF1 in activating the *Nramp1* at the Inr.

c-Myc is shown to mediate the repression of Inr containing promoters such as HIV-1 and AdML while USF1 stimulates them^{52,53}. Other studies demonstrated the opposing activity of USF1 and c-Myc on transcription, where excess USF1 can overcome the inhibitory effect of c-Myc^{102,103}. c-Myc was previously shown to inhibit *Nramp1* promoter mediated by the interaction with Miz-1 at the Inr⁵⁶. Hence, the positive regulation of *Nramp1* by USF1 can be explained by the over expression of USF1 which may overcome the inhibitory effect of c-Myc on *Nramp1*. However, the exact mechanism requires further investigation.

The activation of *Nramp1* by USF1 may also be explained by the physical interactions between other transcription factors. It was found that USF1 upregulated promoter activity via interaction with Sp1¹⁰⁰, the co-activator p300⁹⁹ but not with Miz-1⁸⁴. As Sp1 and p300 were necessary for the upregulation of *Nramp1* promoter by Miz-1, it was possible for USF1 to interact physically with p300 and/or Sp1 for the positive regulation of *Nramp1* promoter. However, the deletion of the Sp1 binding site on pHB23 suggested that USF1 activated *Nramp1* promoter independently of the Sp1 binding site.

3.4.2. TFII-I and USF1 Synergistically Activated the *Nramp1* Promoter

The present studies showed that TFII-I alone has no role on *Nramp1* transcription alone but caused a synergistic activation in combination with USF1 (Figure 3.11). It is unclear why TFII-I alone caused no effect on *Nramp1* transcription. This may be explained by the possible interaction of TFII-I with the inhibitory effect of c-Myc at the *Nramp1* promoter, while c-Myc was suggested to prevent the further binding of TFII-I to the basal transcriptional machinery, thereby preventing transcriptional activation from the Inr¹¹⁷.

The synergistic activation of *Nramp1* by USF1+TFII-I was consistent to the previous experiment where TFII-I and USF1 activated transcription in synergy through both Inr and the E-box elements of the AdML^{60,109}. However, results showed a synergistic activation in *Nramp1* construct pHB20 but not in pHB6, suggesting a possible functional interaction at the core promoter region and not at the E-box elements (Figure 3.11). Alternatively, the possible interaction of c-Myc at the E-box elements on *Nramp1* prevents further interaction of TFII-I at the Inr/to the basal transcriptional machinery¹¹⁷, while c-Myc was suggested to functionally interact at E-box element and inhibit *Nramp1* transcription by looping over to prevent Miz-1 mediated activation at the Inr⁵⁶.

TFII-I is found to serve as a co-regulator that can integrate regulatory responses of USF to the basal machinery and enhance the binding of USF1 to Inr¹⁰⁹. This provided a possible mechanism for the initiation of transcription from TATA-less promoters¹¹⁸. A direct interaction between TFII-I and USF1 has never been reported, however, EMSA or CHIP assay could reveal the binding of USF and TFII-I at the Inr of *Nramp1* promoter.

An alternative hypothesis of the synergistic activation of *Nramp1* promoter could involve a co-activator that bridges the transcription factors to the basal transcriptional machinery and allows recruitment and/or stabilization of the pre-initiation complex. Although USF1 does not interact with p300 in the context of the TGF- β 2 promoter¹¹⁹, however, it has been shown that p300 mediates the transcriptional activation of the F1F0

ATP synthase promoter by USF2 through an Inr element ¹²⁰. In addition, co-activator p300 display intrinsic HAT activities. The acetylation of histone is thought to be involved in destabilization of nucleosomes, a crucial event for the access of transcription factors to their DNA templates ¹²¹. It may be hypothesized that a specific co-activator such as p300 that is common to TFII-I and USF, allows an enhancement of transcription through the binding of TFII-I and USF to the Inr element of *Nramp1* promoter.

3.4.3. USF1 and Miz-1 do not Functionally Interact with each other at the *Nramp1* Promoter

Miz-1 ⁵⁷ and USF1 (Figure 3.6B) individually upregulated the *Nramp1* promoter at the core promoter region but did not display synergy in combination (Figure 3.12) which suggested that they do not functionally interact with each other at the core promoter region. These results were consistent with the previous findings that Miz-1 and USF1 do not physically and functionally interact with each other ⁸⁴.

3.4.4. YY1 Blocked the c-Myc Mediated Negative Regulation of the *Nramp1* Promoter

As shown before that YY1 is an Inr binding factor that regulates Inr containing promoter ¹¹⁰. It is interesting to note that YY1 transactivated the *Nramp1* promoter through the Inr but not upstream of the *Nramp1* promoter (Figure 3.9, P = 0.03). Although the result was significant, the fold induction was very low and its relevance on *Nramp1* transcription was not clear.

Previous study showed that YY1 associated with c-Myc ^{91,92}. Interestingly, results suggested that co-transfection of YY1 with c-Myc prevented the c-Myc mediated repression on the *Nramp1* promoter at the Inr of *Nramp1* (Figure 3.10). Studies have shown that the impaired association between c-Myc, Max, and Mad resulted in an increased DNA binding activity of YY1, which is a repressor of the *CXCR4* promoter ¹¹⁶. Hence, the ability of YY1 to overcome the repression of c-Myc on *Nramp1* promoter may be explained by the interaction between YY1 and c-Myc, where YY1 mopped up c-Myc and prevented c-Myc mediated repression on *Nramp1* transcription. Alternatively, it may be explained by the interaction of YY1 with co-activators p300 ¹¹¹, which act as a repressor in preventing the p300 from activating *Nramp1* transcription.

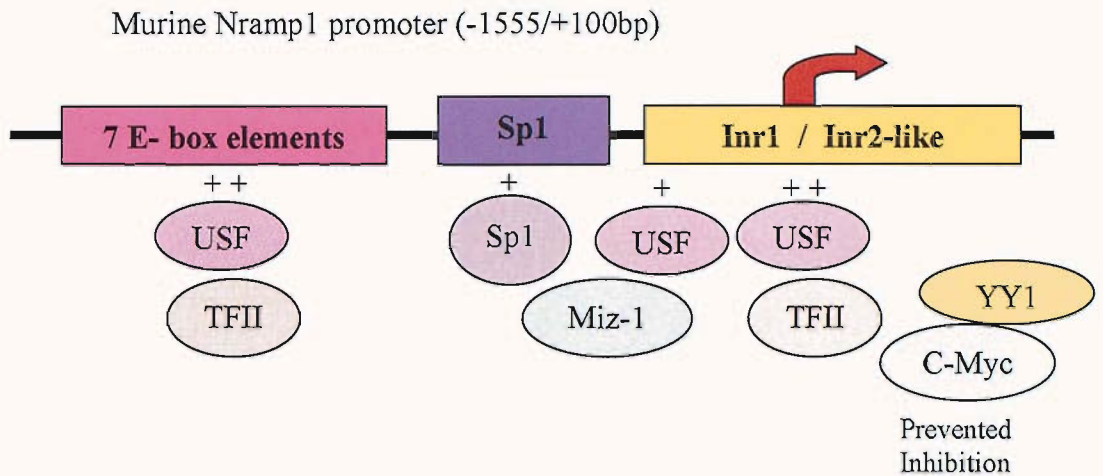


Fig. 3.13. The Proposed Model on the Regulation of Murine *Nramp1* Promoter by Different Inr-binding Factors. The schematic diagram showing the murine *Nramp1* promoter (-1555/+100bp) which contains the consensus transcription factor binding elements (represented by rectangle) ⁵⁰. Results showed that UFS1 and TFII-I causes a synergistic activation (+ +), both at the Inr and upstream of the *Nramp1* promoter. YY1 prevented the c-Myc mediated repressive activity at the Inr of the *Nramp1* promoter. USF1 and Miz-1 did not activate *Nramp1* promoter in a synergistic manner which indicated that they did not functionally interact with each other on *Nramp1* but individually activated *Nramp1* at the Inr (+). However, the direct binding region of the transcription factors is not known and awaits further investigations.

4. Chapter 4

**The Importance of the Sp1 Binding Site on the Regulation of
Nramp1 by LPS+IFN- γ , L-Glutamine and Oxidative Stress**

4.1. Introduction

4.1.1. The Transcription Factor Sp1

Sp1, the 778 amino acid DNA binding transcription factor, is ubiquitously expressed binds to and activates transcription from Sp1 binding sites or so-called GC-boxes (5'-GGGGCGGGG-3') within a few hundred base pairs of the transcriptional start site¹²²⁻¹²⁴. Many promoters which lack both the traditional TATA and CCAAT boxes rely on the presence of a single or multiple Sp1 consensus binding sites¹²⁵.

The Sp family of transcription factors is united by a combination of three conserved Cys₂His₂ zinc finger (containing two histidine and two cysteine residues which coordinate with a Zn²⁺ ion in each finger) that form the DNA-binding domain of Sp factors¹²⁶. It also contains the central activation domains that are often glutamine-rich or serine/threonine-rich which interact with TBP¹²⁷ and TAFII110¹²⁸ (Figure 4.1).

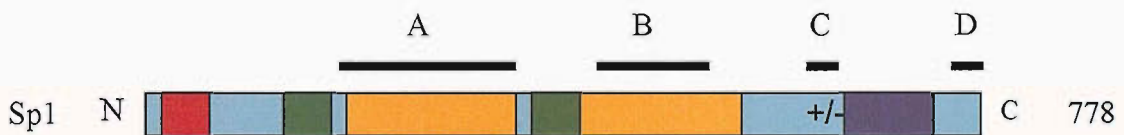


Figure 4.1. A Schematic Diagram Represents the Sp1 Polypeptide Structure. Sp1 consists of 778 amino acids and has three putative zinc fingers (blue) of the Cys₂ His₂ type which binds DNA. The Sp1 transactivation domain has been subdivided into two subdomains (A and B) with regions rich in glutamine residues (yellow), which are known activation domain. The red box indicated the known inhibitory domain. The green boxes indicated the regions of Sp protein that is rich in serine / theronine residues. A region close to the first zinc fingers largely composed of charged amino acids (+/-), which synergistically stimulate transcription. The region of Sp1 for YY1 interactions is located in domain D of Sp1¹²⁴.

4.1.2. Sp1 is Regulated and Function as a Regulator

Sp1 is a constitutive transcription factor, but increasing data suggest that Sp1 also has a regulatory role. Most of the regulation occurs through post-translational modification, which in turn regulates transcription.

There is evidence that O-glycosylation plays a role in controlling both the turnover and transactivation activities of Sp1¹²⁹. Jackson and Tjian showed that the ubiquitous

transcription factor Sp1 bears multiple O- glycosylation residues, containing ~ 8 molecule of O-glycosylation per protein molecule ¹³⁰. The recombinant Sp1 transactivation domain, which contains O-glycosylation, fails to bind to known Sp1 binding partners such as the TAFII110 in vitro, indicating that the regulated removal of O-glycosylation is necessary for Sp1 to bind to specific partners ¹³¹. O-glycosylation also protected the Sp1 transcription factor protein from proteasome degradation ^{132,133}.

In addition, *N*-acetylglucosamine in the NH₂-terminal transcriptional activation domain of Sp1 ^{130,134} and/or the phosphorylation modification to serine and threonine residues can also regulate the protein degradation, Sp1 protein abundance, protein-protein or protein-DNA interactions of Sp1 ¹³¹⁻¹³⁵.

4.1.3. Regulatory Role of Sp1 on the Promoter Regulation by L-Gln

Sp1 demonstrated a regulatory role on transcription through O-glycosylation which enhanced argininosuccinate synthetase promoter transcription via the hexosamine pathway in response to L-Gln ¹³⁶. This demonstrates a functional relationship between a regulating signal (L-Gln), a transcription factor Sp1, and transcription via O-glycosylation post translational modification.

4.1.4. Role of Sp1 on the Promoter Regulation with LPS

Several studies found that Sp1 sites conferred the responsiveness to bacteria LPS ^{79,80}, where Sp1 was a target in the signalling pathways involved with the activation of IL-10 gene with LPS in the macrophages ⁷⁹. In LPS-stimulated human macrophages, the p38MAPK pathway regulated the human IL-10 promoter via activation of Sp1 ⁷⁹. Furthermore, in human monocytic cells, Sp1 mediated the effect of LPS on the regulation of VEGF mRNA ⁸⁰. These results implied that the transcription factor Sp1 mediates gene regulation under LPS stimulation.

LPS+IFN- γ activates *Nramp1* transcription ^{8,50}, involving the transcription factor Miz-1 in synergy with ICSBP ⁶³ which requires the Sp1 binding site ⁵⁶. However, the role of the Sp1 binding site on the activation of *Nramp1* by LPS+IFN- γ is still unclear.

4.1.5. Regulatory Role of Sp1 under Oxidative Stress

Sp1 also senses OS to prevent apoptosis in the cortical neurons by activating a set of Sp1-regulated genes¹³⁷. Other studies have shown that the DNA-binding activity of Sp1 is affected directly by the redox status of the cell¹³⁸. In addition, Sp1 O-glycosylation is increased by OS in response to hyperglycaemia in PAI-1 promoter^{139,140}. These results indicated a regulatory role of Sp1 under OS.

OS can be caused by the excess accumulation of the ROS inside the cells and/or depletion of the key thiol antioxidants GSH to prevent scavenging of ROS. Excess labile iron pool contributes to the production of ROS through Fenton/Haber Weiss chemistry which results in the generation of excess highly reactive radicals and provokes OS (Figure 5.1). OS damages cell lipids, protein, DNA which leads ultimately to cell death¹⁴¹ (for more details about OS, see Chapter 5). Pharmacological reagent BSO is known to prevent the synthesis of antioxidant GSH by inhibiting the enzyme glutamylcysteine synthetase required for GSH synthesis to induce OS in cells (Iron and Infection by Bullen Griffiths, publisher Wiley) (Figure 5.2). Previous work had shown *Nramp1* responses to OS⁶² but it is unclear if the OS-responsive Sp1 plays a regulatory role on *Nramp1* transcription.

4.1.6. Reason for Studying the Transcriptional Regulation of the *Nramp1* Promoter via Sp1

Firstly, a single consensus Sp1 binding site was found in *Nramp1* promoter (5'-GGGCG-3') at position (-26/-21bp)⁵⁰ that has 100% conservation between human, mouse and rat suggesting the importance of the Sp1 binding site on *Nramp1* promoter (Figure 4.2). In addition, studies have shown that Sp1 activates *Nramp1* promoter in Raw264.7 cells⁵⁷. These results have indicated the importance of the Sp1 binding site on the *Nramp1* promoter.

Secondly, Sp1 has been shown to have a regulatory role on the TATA-less promoter transcription^{125,142}, in response to OS¹³⁷ and to L-Gln^{139,140}; therefore, we investigated whether the transcription factor Sp1 regulates *Nramp1* transcription in response to LPS+IFN- γ , L-Gln and OS. Hopefully, this may give insights to the role of Sp1 on the *Nramp1* promoter and the molecular mechanism of *Nramp1* transcription in response to LPS+IFN- γ , L-Gln and OS.

4.2. Specific Aims

The Sp1 binding site was found to be essential for the upregulation of *Nramp1* promoter by Miz-1⁵⁷ and a recent report suggested that Miz-1 was involved with the upregulation of *Nramp1* promoter by LPS+IFN- γ ⁶³. In addition, Sp1 was shown to be regulated by LPS to activate IL-10 genes in macrophage⁷⁹; therefore, we investigated if the consensus Sp1 binding site was necessary for the upregulation of the *Nramp1* promoter by LPS+IFN- γ .

Increasing data suggest that Sp1 plays a regulatory role under OS in response to hyperglycaemia which occur through the increase of the O-linked glycosylation by L-glutamine^{136,139,140}; therefore, we investigate if Sp1 plays a regulatory role on *Nramp1* promoter in response to L-Gln.

In addition, Sp1 has a regulatory role under the influence of OS¹³⁷. Previously, *Nramp1* promoter was shown to be upregulated by redox stress with H₂O₂ or iron loading itself⁶². The direct transport substrate of *Nramp1*, iron, can result in the generation of highly reactive radicals that provokes OS¹⁴¹; hence, we investigated whether Sp1 plays a regulatory role under OS which may provide insights to the role of Sp1 in the regulation of *Nramp1* promoter in response to the OS in macrophages.

1. Therefore, firstly, we investigate whether *Nramp1* promoter transcription and its protein expression are regulated by OS. BSO, a reagent which depletes the key anti-oxidant GSH was used for this purpose.
2. Secondly, we investigate whether OS regulates the Sp1-dependent promoter in the macrophage Raw264.7 cell line.

By studying the transcriptional regulation of the *Nramp1* promoter, it may help to determine the importance of Sp1 and the Sp1 binding site on the transcriptional regulation of the *Nramp1* promoter under LPS+IFN- γ , OS and L-Gln responses. In addition, this may give insights to the molecular mechanism of *Nramp1* promoter regulation in response to LPS+IFN- γ , L-Gln and OS.

4.3. Results

4.3.1. The Consensus Sp1 Binding Site was Necessary for the Upregulation of *Nramp1* Promoter Activity by LPS+IFN- γ

Nramp1 luciferase construct pL4 was activated by LPS+IFN- γ (Figure 4.3, P = 0.03, ~2- fold activation) with a 6-fold induction when co-transfected with Miz-1+LPS+IFN- γ (P = 0.01). Mutation of the Sp1 binding site abolished the basal *Nramp1* promoter activity (Figure 4.3, P = 0.03, ~9- fold inhibition), with LPS+IFN- γ (P = 0.03, ~25- fold reduction) plus Miz-1 (P = 0.01, 38- fold reduction). This result indicated that the single consensus Sp1 binding site was necessary for basal and activated *Nramp1* promoter activity with LPS+IFN- γ \pm Miz-1.

4.3.2. L-Gln Induced the *Nramp1* Promoter Activity

L-Gln (5 and 10mM) activated *Nramp1* construct pL4 (Figure 4.4A, P = 0.05 and 0.04 respectively, ~ 2 and 9 fold activation). The increased *Nramp1* promoter activity was also reflected by the increase of the *Nramp1* protein expression when N11 microglial cells were treated with 10mM of L-Gln (Figure 4.4B). This indicated that L-Gln increased the *Nramp1* transcription and protein expression.

4.3.3. Induction of the *Nramp1* Promoter Activity by L-Gln is Sp1 Dependent

Secondly, we determined if Sp1 is necessary for the upregulation of *Nramp1* promoter by L-Gln.

L-Gln (5mM) induced the *Nramp1* construct pL4Sp1MGal4 in the presence of pMSp1 (Figure 4.5, P = 0.005, ~26 fold activation) but not in the absence of pMSp1 (P = 0.4). This indicated that Sp1 played a role in the upregulation of *Nramp1* by L-Gln.

4.3.4. BSO Activated the *Nramp1* Promoter Activity

Nramp1 construct pL4 was induced with BSO (5mM) (Figure 4.6A, P = 0.047, ~ 3 fold activation). The induction of the *Nramp1* promoter activity by BSO was also reflected by an increase of the *Nramp1* protein expression (Figure 4.6B). This indicated that *Nramp1* promoter is OS-sensitive which resulted in the increase of *Nramp1* protein expression.

4.3.5. BSO-Induced OS Upregulated the Sp1-Dependent Promoter Transcription in Macrophage Cells

Next, we investigated whether Sp1 played a regulatory role in response to OS in the macrophage Raw264.7 cells.

BSO (1mM) activated the pG5-luc promoter activity in the presence of 1 μ g pM-Sp1 (Figure 4.7, P = 0.008 and ~2-fold activation) but not in the absence of pM-Sp1 (P = 0.15). This suggested that Sp1 played a regulatory role under OS-activated transcription in the macrophage Raw264.7 cell lines.

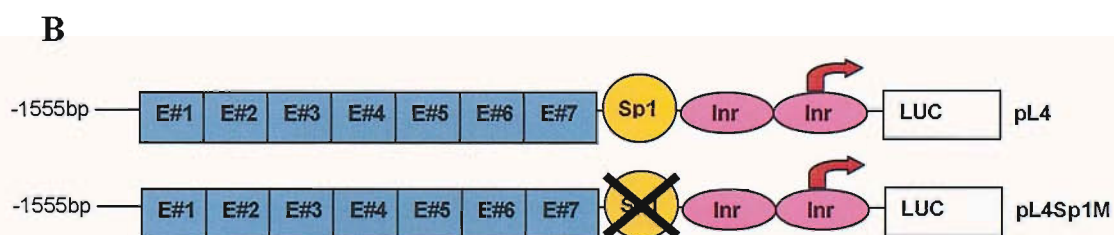
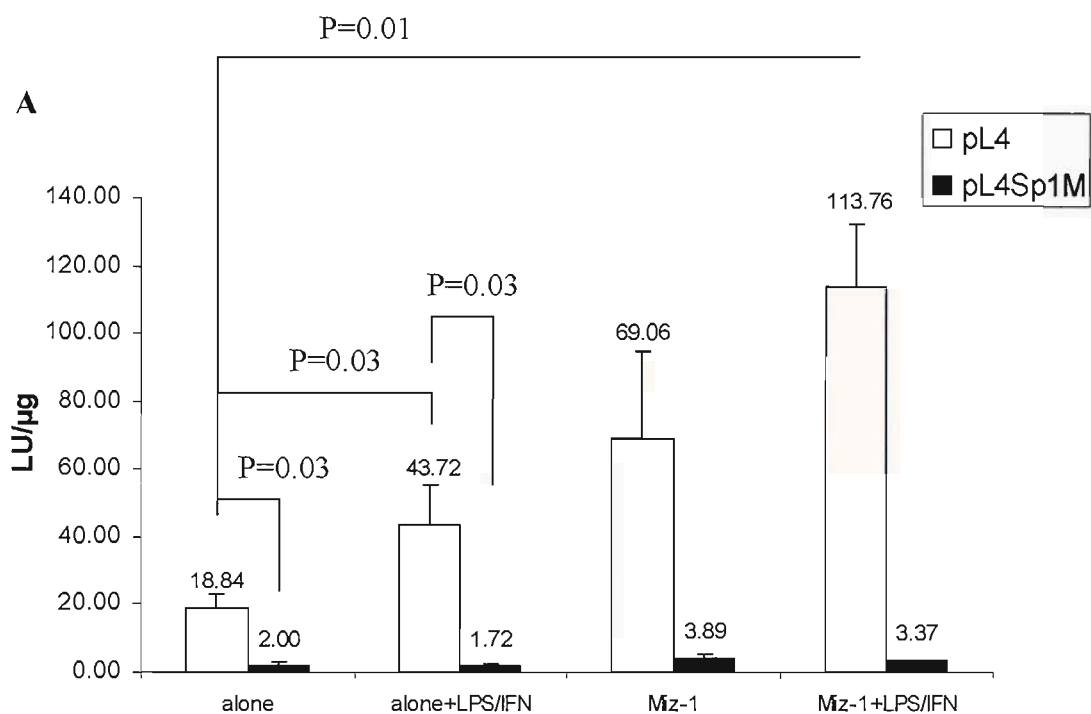


Figure 4.3 Sp1 Consensus Binding site was Necessary for the Basal and Activation of *Nrampl* Promoter by LPS+IFN- γ . A. 5×10^5 Raw 264.7 cells were transfected with 1.5 μ g wild-type *Nrampl* construct (pL4) or the mutant Sp1 construct (pL4Sp1M) \pm 1 μ g Miz-1 expression plasmid. Five hours after transfection, 20% FCS- no addition DMEM media \pm 25U/ml IFN- γ and 100ng/ml LPS were incubated overnight. Cells were washed with PBS and lysed with 1x lysis buffer (see chapter 2 Luciferase reporter assay). Cell lysates were analyzed for luciferase activity. Results were presented as luciferase unit per μ g of protein (LU/ μ g).

B. Schematic diagram represents the differences between *Nrampl* constructs pL4 and pL4Sp1M. (See chapter 2 – Construction of *Nrampl* promoter reporter plasmids.)

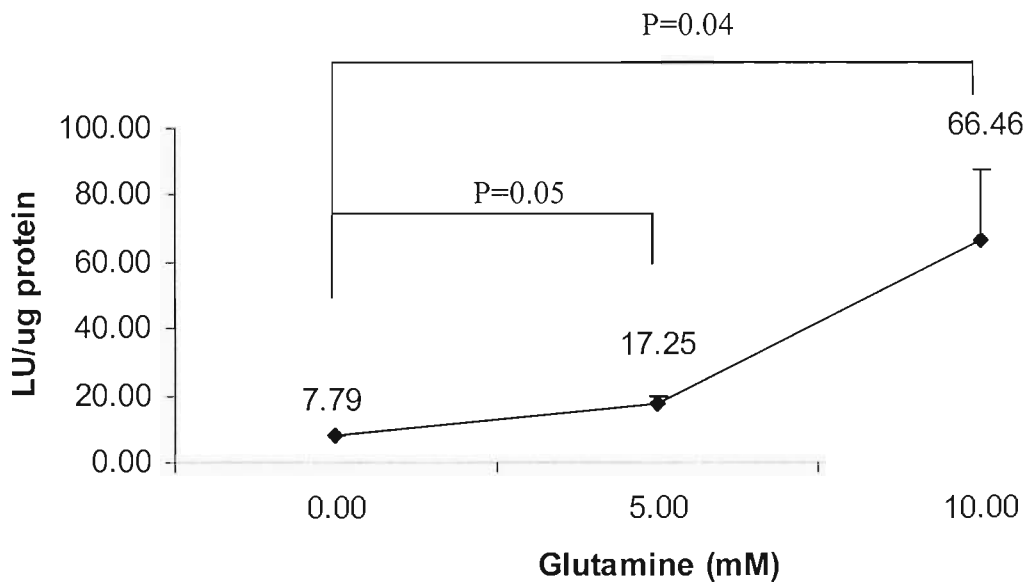


Figure 4.4A. Dose Dependent Increased of *Nrampl* Promoter by L-Gln. 5×10^5 Raw264.7 cells were transfected with $1.5 \mu\text{g}$ of *Nrampl* construct (pL4) in low L-glutamine no addition DMEM. After 5 hours of transfection, cells were treated with 5mM or 10mM L-glutamine overnight in low L-glutamine and dialysed 20% FCS-DMEM media. Data were represented as luciferase units per μg of protein relative to the control plasmid pcDNA3.1.

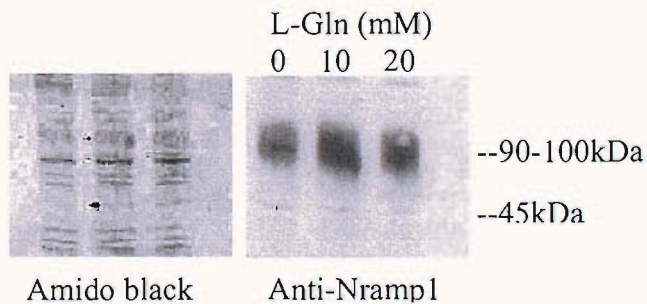


Figure 4.4B Western Immunoblotting Indicated the Increased Expression of *Nrampl* Protein with L-Glutamine. 70% confluence of N11 cells were plated out before the day of treatment in the 10cm petri dish and were then treated with 10mM or 20mM of L-glutamine for overnight. Cells were then harvested (See chapter 2 Western immunoblotting). Equal amount of the nuclear extract protein ($15 \mu\text{g}$) were loaded in each well on the SDS polyacrylamide gel. *Nrampl* antibody (1:1000 dilution) and the secondary antibody Goat anti Rabbit immunoglobulin G (IgG) (1:15000 dilution), conjugated to horseradish peroxidase were used for the immunodetection. Bands were visualized by chemiluminescence. Equal amount of the protein loading was visualized with the amido black staining on the nitrocellulose membrane.

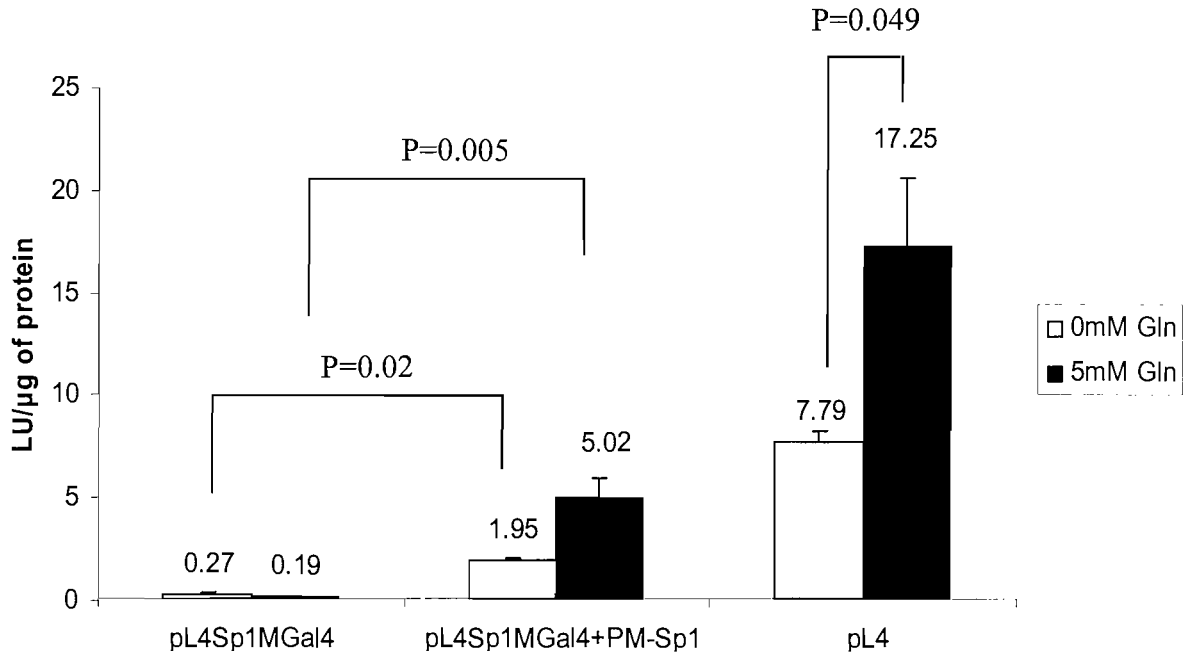


Figure. 4.5 The Sp1 Consensus Binding Site was Necessary for the Upregulation of *Nramp1* Promoter with L-Glutamine. 5×10^5 Raw264.7 cells were transfected with $1.5 \mu\text{g}$ of *Nramp1* luciferase construct (pL4) or with $1.5 \mu\text{g}$ pL4Sp1MGal4 (substitution of the Sp1 site with Gal4 DNA binding sequence) \pm pMSp1 expression plasmid. After 5 hours of transfection, cells were treated with 5mM of L-glutamine for overnight in low glutamine and dialysed 20% FCS-DMEM no addition media. See chapter 2 Luciferase reporter assay. Data were presented as luciferase units per μg of protein relative to the control plasmid pcDNA3.1.

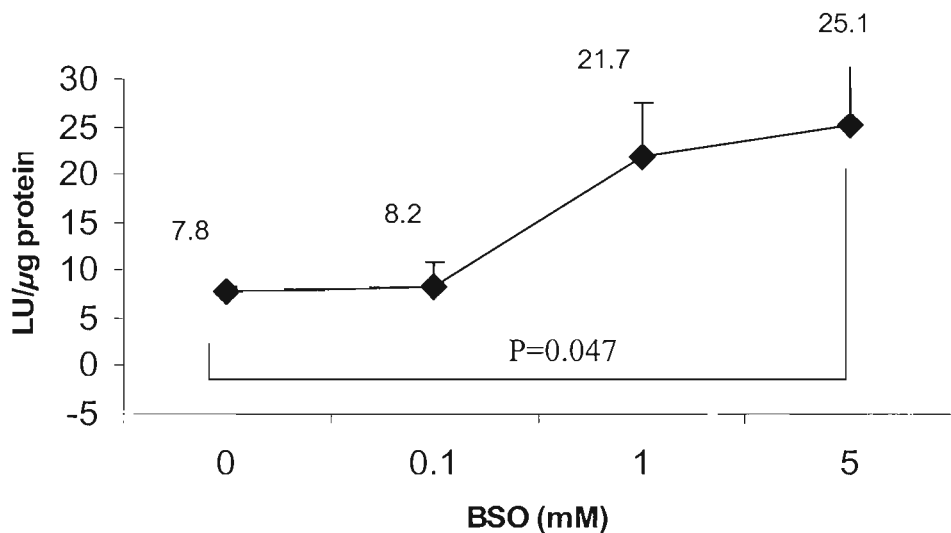


Figure 4.6A BSO-Induced Oxidative Stress Activated *Nramp1* Promoter. 5×10^5 Raw264.7 cells were transfected with *Nramp1* luciferase construct pL4 (-1555bp to +100bp). After 5 hours of transfection, cultures were treated with the indicated concentrations of BSO and incubated with 20% FCS-DMEM for overnight. Data were presented as luciferase units per μg of protein.

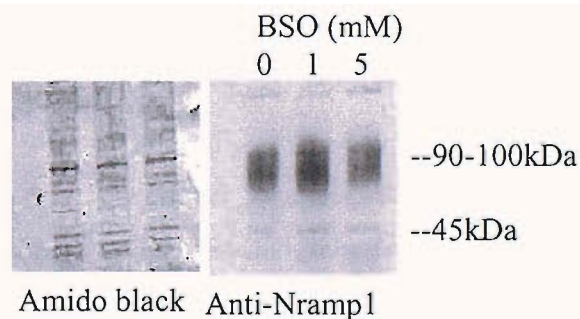


Figure 4.6B BSO-Induced Oxidative Stress Activated *Nramp1* Protein Expression. 70% confluence of N11 cells were plated out the day before BSO treatment on the 10cm petri dish and was either untreated or treated with BSO (1mM or 5mM) for overnight. Nuclear extract were obtained using buffer A and buffer C (see method Western immunoblotting). Equal amounts of protein lysate (15 μg) was loaded into each lane of the Polyacrylamide gel. *Nramp1* antibody (1:1000 dilution and goat anti rabbit immunoglobulin G (IgG) (1:15000 dilution), conjugated to horseradish peroxidase were used for the immunodetection. Bands were visualized by chemiluminescence. Equal amount of the protein loading is visualized with amido black staining on the nitrocellulose membrane.

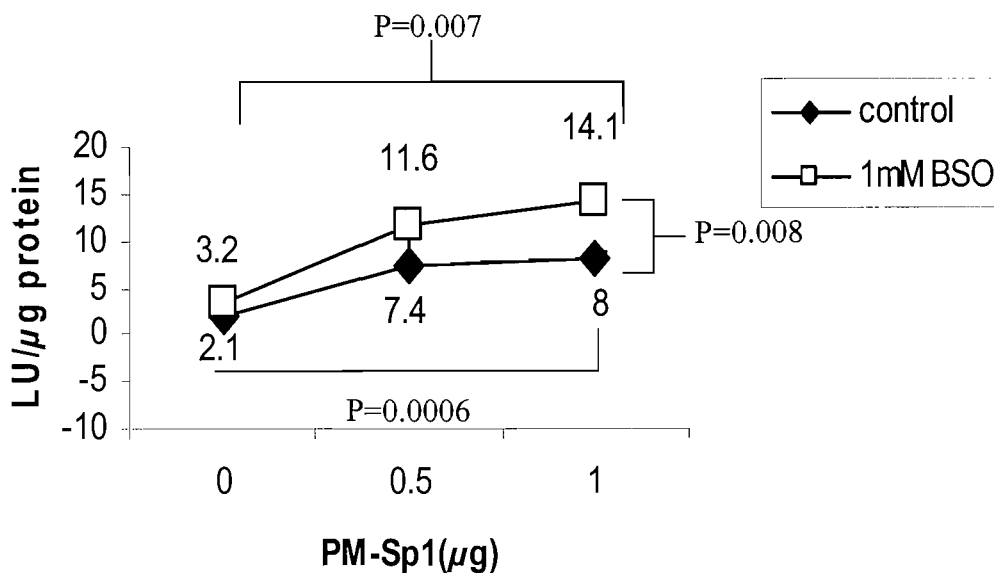


Figure 4.7 Sp1-dependent Promoter Transcription in Macrophage Cells was Responsive to OS. 5×10^5 Raw264.7 cells were co-transfected with 5xGal4 luciferase reporter construct (driven by a minimal promoter, pG5-luc) ($1.5 \mu\text{g}$) and the indicated amount of pM-Sp1 (a plasmid that directs the expression of an Sp1-Gal4 DNA-binding domain chimaeric protein). After 5 hours of transfection, cells were treated with the indicated amount of BSO for overnight. Data were presented as luciferase units per μg of protein.

4.4. Discussions + Future Experiments

The results in this present chapter highlighted the important role of Sp1 and the Sp1 consensus binding site for *Nramp1* transcription in response to LPS+IFN- γ , L-Gln and OS. The present results also demonstrated that both *Nramp1* promoter and the Sp1-dependent promoter were OS-sensitive with GSH depletion in macrophage Raw 264.7 cells which suggested the potential regulatory role of Sp1 on promoter transcription in response to OS.

4.4.1. Sp1 Binding Site was Necessary for the Basal Transcriptional Regulation of *Nramp1* Promoter

Results showed that the Sp1 consensus binding site was necessary for the basal *Nramp1* transcription (Figure 4.3, Figure 4.5). In addition, over expression of Sp1 activated the *Nramp1* promoter (Figure 4.5) which was consistent to the previous experiment⁵⁷.

Studies have shown that many genes that lack TATA boxes can employ the Sp1 binding site for basal transcription^{125,142}. In addition, Sp1 functions most effectively in the context of a core promoter containing an Inr element^{114,143}. Hence, it was not surprising that the interaction of Sp1 in its binding site was necessary for the basal transcriptional regulation of TATA-less *Nramp1* promoter. Therefore, *Nramp1* possesses a Sp1-dependent regulated promoter.

4.4.2. Sp1 Binding Site was Necessary for the Activation of *Nramp1* Promoter by LPS+IFN- γ

Results showed that the Sp1 binding site was necessary for the upregulation of *Nramp1* by LPS+IFN- γ as mutation of the Sp1 binding site abolished the upregulation of *Nramp1* with LPS+IFN- γ \pm Miz-1 (Figure 4.3). Previously, *Nramp1* promoter was induced by LPS+IFN- γ involving Miz-1⁶³. Furthermore, the Sp1 binding site was necessary for the upregulation of *Nramp1* promoter by Miz-1^{56,57} (Figure 4.3) which suggested the possible involvement of the Sp1 binding site on *Nramp1* promoter in response to LPS+IFN γ \pm Miz-1.

In addition, Sp1 was shown to be a signalling target which was responsive to LPS in macrophage cells on the activation of IL-10 and VEGF promoter^{79,80}, which suggested that the transcription factor Sp1 that was responsive to LPS, was important for promoter

activation in macrophages. Sp1 was necessary for *Nramp1* promoter activation⁵⁷, but the result in Figure 4.3 has not determined if Sp1 plays a regulatory role on the upregulation of *Nramp1* promoter under LPS+IFN- γ stimulation.

Therefore, further co-transfection experiments using the *Nramp1* promoter substituted with Gal4 DNA sequence at the Sp1 binding site (pL4Sp1MGal4) and pM-Sp1 could be done to investigate if the interaction of Sp1 at its consensus binding site is necessary for the upregulation of the *Nramp1* promoter with LPS+IFN- γ .

It will be of interest to determine how Sp1 plays a regulatory role on transcription as literature suggested that Sp1 can be regulated by post-translational modification such as phosphorylation or O-glycosylation^{131-133,135,136}. It has been suggested that O-glycosylation of the proteins display features that are essential for a role in signal transduction. Most signal induced modifications (phosphorylation and O-glycosylation) affect a protein's ability to associate with other proteins or affect its DNA binding activity, translocation into the nucleus, Sp1 protein expression, Sp1 degradation, interaction with other transcription factors¹⁴⁴. Hence, the molecular mechanism of *Nramp1* activation by LPS+IFN- γ via the Sp1 binding site required further investigation.

4.4.3. Sp1 was Necessary for the Upregulation of *Nramp1* Promoter by L-Gln

Results have shown that the Sp1 was necessary for the induction of *Nramp1* promoter with L-Gln (Figure 4.5).

It was well known that Sp1 is ubiquitously expressed and regulates the myeloid specific gene expression¹⁴². However, recent data suggested the regulatory role of Sp1 through O-glycosylation by L-Gln on argininosuccinate synthetase gene expression¹³⁶. At present, the results can not distinguish whether the effects of L-Gln on the *Nramp1* promoter can be explained by the direct O-glycosylation of Sp1. It is possible to hypothesis that the increase of *Nramp1* transcription by L-Gln is due to the alteration of O-glycosylation status on Sp1¹³⁰ or on other transcription factors such as YY1¹⁴⁵, c-Myc¹⁴⁶, which affects the protein-protein interaction properties, DNA binding activities and protein complexes at the *Nramp1* promoter. Interestingly, addition of pM-Sp1 with pL4Sp1Gal4 *Nramp1* construct did not give the same promoter response compared with the wild type pL4 *Nramp1* construct. This may indicate the involvement of other transcription factor such as Sp1 with YY1 and c-Myc, as Sp1 was shown to interact physically with YY1¹¹⁴ and c-Myc⁹⁴. However, further investigation on the post-translation modification of the

transcription factors needed to be undertaken before the regulatory role of Sp1 on the *Nramp1* promoter activity in response to L-Gln is understood. It may be possible to investigate the size of the Sp1 protein on SDS polyacrylamide gel. Alternatively, wheat germ agglutinin¹³⁰ can be used to determine the amount of O-glycosylation on Sp1 in response to L-Gln treatment.

4.4.4. Regulation of Promoter Transcription in Macrophages under OS is Sp1-Dependent

Results showed that Sp1 is under redox regulation in the macrophage Raw264.7 cell lines demonstrated by the activation of the Sp1-dependent promoter in the Raw264.7 cells with BSO-induced OS (Figure 4.7). In addition, results showed that the Sp1-dependent promoter, *Nramp1* was OS sensitive (Figure 4.6A and Figure 4.6B).

Previous results showed that *Nramp1*'s own transport substrate, iron and/or OS enhanced polypeptide and mRNA accumulation⁶². Hence, the *Nramp1* promoter activation and its increased protein expression by OS are consistent with the previous experiment.

The regulation of promoter activity via Sp1 under OS may be explained by the fact that Sp1 is a zinc finger protein and proteins containing zinc finger motifs is more susceptible to redox regulation¹⁴⁷. Sp1 is also shown to be a redox-regulated transcription factor and the DNA binding activity of Sp1 is redox regulated¹³⁸ which suggested that Sp1 can play a regulatory role in response to OS in the regulation of Sp1 dependent promoter in the macrophage cells (Figure 4.7). Interestingly, Sp1 was significantly induced by GSH depletion or H₂O₂ in the cortical neurons to prevent apoptosis caused by OS¹³⁷. Hence, the expression of genes controlled by Sp1 is likely to have beneficial consequences on cell viability to OS challenge. This suggested that Sp1 may play a regulatory role in response to OS on the activation of *Nramp1*.

Further investigation is required to determine the mechanism on the upregulation of *Nramp1* transcription under OS. It will be of interest to determine how Sp1 senses OS that regulates the Sp1-dependent promoter in the macrophage. As OS increased the Sp1 O-glycosylation in response to hyperglycaemia-induced OS^{139,140}, it is possible for the increase of Sp1 O-glycosylated in the regulation of *Nramp1* transcription for OS defences in the macrophages.

5. Chapter 5

The Role of *Nramp1*-mediated Iron Transport in the Regulation of Oxidative Stress Status and the *Nramp1* Promoter Responsiveness to LPS+IFN- γ Activation in Macrophages

5.1. Introduction

5.1.1. What is Oxidative Stress?

Under normal physiological conditions, up to 1% of the mitochondrial electron flow leads to the formation of O_2^\bullet , the primary oxygen free radical produced by mitochondria; and interference with electron transport can dramatically increase O_2^\bullet production^{141,148,149} (Figure 5.1). Apart from the mitochondria electron transport chain, ~40% of the O_2^\bullet are generated by the respiratory-burst NADPH oxidase by phagocytic cells^{141,148}. O_2^\bullet is rapidly converted to H_2O_2 by the antioxidant SOD within the cell. However, H_2O_2 can react with the reduced transition metals such as iron, via the Fenton reaction, to produce the highly reactive OH^\bullet/OH^- .

The generation of ROS such as O_2^\bullet , H_2O_2 and OH^\bullet/OH^- are in balance with antioxidant molecules, including GSH, Vitamin E, carotenoids, and Vitamin C which react with most oxidants. In addition, the antioxidant enzymes catalase and glutathione peroxidase (GP) detoxify H_2O_2 by converting it to O_2 and H_2O to maintain the tight homeostatic control¹⁴¹.

However, OS occurs when this critical balance is disrupted because of the depletion of antioxidants or with excess accumulation of ROS inside the cells which leads to the destruction of cellular components including lipids, protein, and DNA, and ultimately cell death via apoptosis or necrosis^{141,148,150}. There is a growing awareness that OS plays a role in malignant diseases, diabetes, atherosclerosis, chronic inflammation, HIV, infection, neurodegenerative diseases and aging^{141,148} (Figure 5.1).

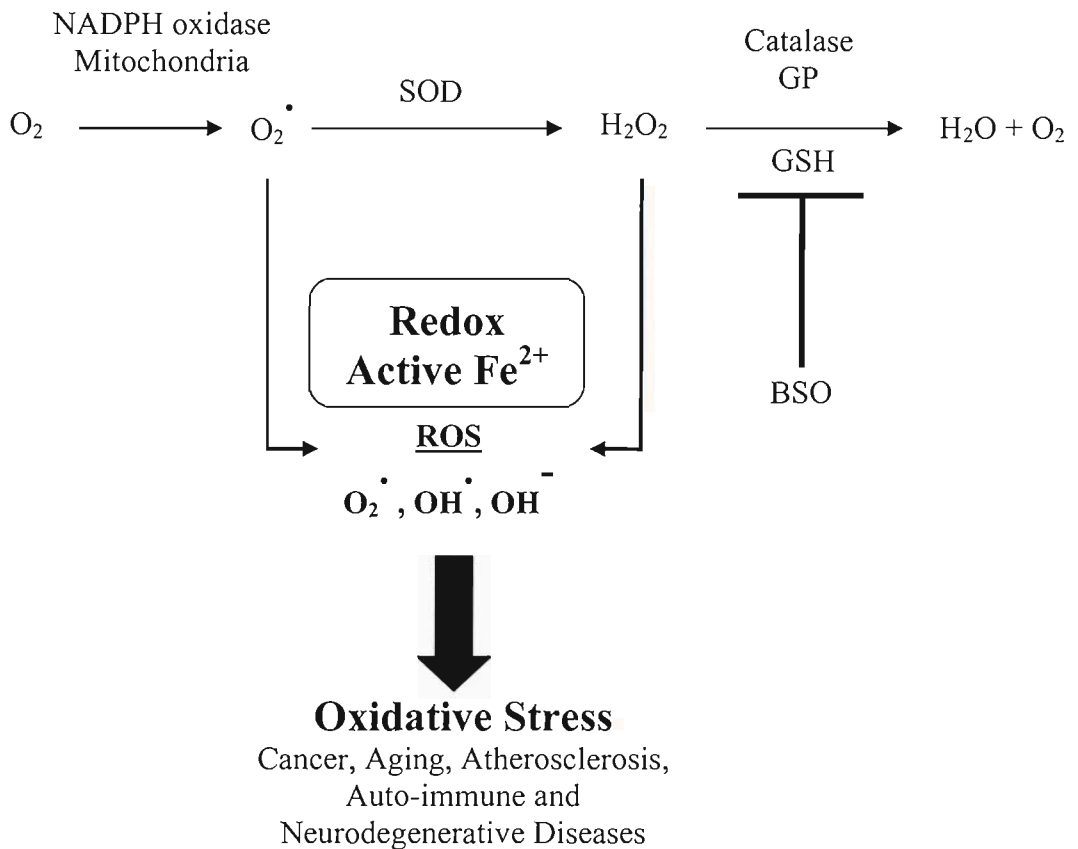


Figure 5.1. Metabolic Pathways of Reactive Oxygen Radicals Formation. Reactive oxygen species (ROS) such as hydrogen peroxide (H_2O_2), superoxide radicals (O_2^{\cdot}), hydroxyl radicals + anions ($OH^{\cdot} + OH^-$) are generated in cells by several pathways. O_2^{\cdot} is generated by NADPH oxidase and in the mitochondrion. Superoxide Dismutase (SOD) converts O_2^{\cdot} into H_2O_2 and then H_2O_2 is mostly degraded to H_2O by glutathione peroxidase (GP), catalase and glutathione (GSH). H_2O_2 produces a highly reactive radical $OH^{\cdot} + OH^-$ by Fenton or Haber-Weiss reactions through the redox active free iron (Fe^{2+}). Imbalance between ROS and anti-oxidant provokes OS which is known to be involved with diseases such as cancer, aging, atherosclerosis, auto-immune and neurodegenerative

5.1.2. Depletion of Glutathione Induce Oxidative Stress

The tripeptide glutathione (L- γ -glutamyl-L-cysteine-glycine, GSH) is the most important intracellular thiol antioxidant and a major determinant of the intracellular thiol/disulfide redox state ¹⁵¹. GSH works synergistically with other cellular anti-oxidants to scavenge free radical species to prevent or diminish OS. Almost one fifth of the intracellular GSH is located in the mitochondria and plays an important role in the protection against ROS which are constantly produced at the mitochondrial electron transport chain ¹⁵². GSH synthesis can be inhibited by BSO that induces OS (Iron and Infection by Bullen Griffiths, publisher Wiley) (Figure 5.2).

Evidence suggested that the intracellular redox state modulates the immunological functions of macrophages. Murata ¹⁵³ reported that macrophages vary strongly in their release of prostaglandins, IL-6, and IL-12, depending on the intracellular content of GSH. The balance between "reductive" and "oxidative" macrophages regulates the Th1/Th2 balance ¹⁵³. This is of significant interest given that functional *Nramp1* allelic variants correlate with a Th1 response to vaccination, whereas non-functional *Nramp1* variants a Th2 response ¹⁵⁴.

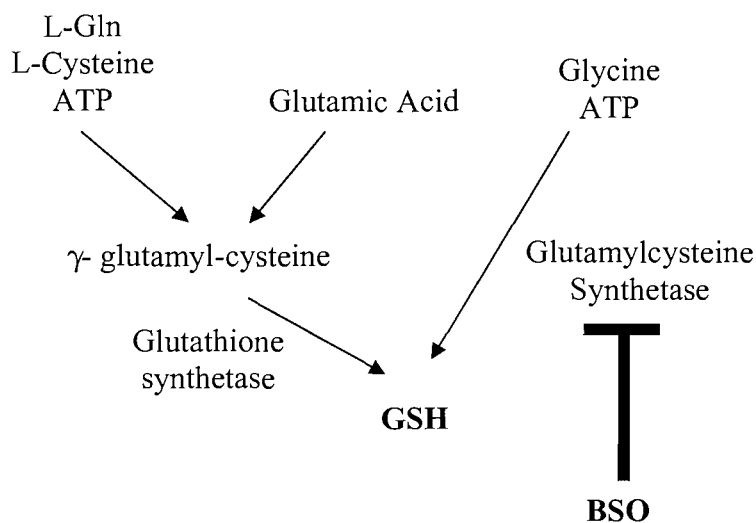


Figure 5.2 Mechanism of BSO Function. The glutathione (GSH) precursor, L-glutamine (L-Gln) is synthesised by 2 pathways shown above. Butathione Sulphoximine (BSO) inhibits glutamylcysteine Synthetase and prevents the synthesis of GSH (Iron and Infection by Bullen Griffiths, publisher Wiley).

5.1.3. Oxidative Stress is Provoked by Excess Redox Active Free Iron

Excess redox active free iron provoked OS in cells^{141,148}. Free radical inducer menadione and H₂O₂ is rapidly and specifically shown to down modulate the membrane transferrin receptor by blocking receptor recycling to prevent the influx of iron into the cells¹⁵⁵.

Previous data has shown *Nramp1* to be positively regulated by redox stress and iron loading⁶². When this is taken into consideration with data that demonstrated *Nramp1* depletes the cytosol of iron, a suggestion of an autoregulatory control pathway that was important for the maintenance of low cytoplasmic redox active iron levels in the macrophage was made⁶². In addition, the results in chapter 4 suggested that BSO-induced OS activated the *Nramp1* promoter and protein expression (Figure 4.6A and Figure 4.6B). This poses the possibility of *Nramp1*-mediated iron transport regulating *Nramp1* transcription and controlling the OS status in macrophage cells. This has implications for the effect of *Nramp1* genotype in modulating Th1/2 responses.

5.1.4. Role of Iron in the Regulation of Bacterial Infection, Immune Responses and the Pleiotropic Effect of *Nramp1*

Iron is necessary for cell growth and generates ROS via Fenton chemistry in an inflammatory environment which plays an important role as a first line of defence against pathogens⁷¹. Mice lacking the NADPH oxidase components gp91^{phox} or p47 exhibit reduced resistance to infection⁷⁶. However, NADPH oxidase is not necessary either for cytokine or *Nramp1*-mediated growth restriction of *M. avium* inside mouse bone marrow derived macrophages¹⁵⁶.

Iron needs to be tightly regulated in the macrophage, as too much iron increases bacterial cell growth^{67,71}. In addition, increased iron attenuates *iNos* transcription via effects on NF-IL6 and *Nramp1* function is needed for sustained *iNos* transcription via sustained activation of Stat-1^{75,77}. Studies by Weiss and colleagues have also shown that iron regulates post-transcriptional and post-translational events¹⁵⁷. Furthermore, Lafuse¹⁵⁸ has demonstrated that the oxidant-generated signalling pathway was essential for effects of *Nramp1* on mRNA stabilization regulated via p38 MAPK and PKC. This poses the possibility that *Nramp1*, by direct divalent cation transport, controls the pleiotropic effects such as the pro-inflammatory properties of the macrophage.

5.2. Specific Aims

1. To investigate if *Nramp1* genotype modulates basal *Nramp1* promoter activity using stable transfectant Raw264.7 cell lines (R21, allele *D169*; and R37, allele *G169*).
2. To investigate the effect of *Nramp1* genotype in responses to BSO and/or iron-induced OS.
3. To determine if *Nramp1* genotype regulates transcriptional responses to LPS+IFN- γ .

5.3. Results

5.3.1. Expression of *Nramp1* G169 Increased Cell Viability against BSO-Induced OS

Cell growth, a measure of cell viability was quantitated in the untreated or BSO treated cells expressing the functional allelic variant of *Nramp1* (R37) or the non-expressing *Nramp1* cells (R21) (Figure 5.3). Western blotting using antibodies against *Nramp1* showed that R21 do not express *Nramp1* protein and R37 expresses the *Nramp1* protein (Figure 5.3).

R21 cells grew 25% faster from day 2 to day 4 than R37 (Figure 5.3, $P = 0.028$). In contrast, higher relative cell growth (3 fold) was observed for R37 than R21 cells with BSO (5mM) treatment (Figure 5.3, $P = 0.01$).

5.3.2. Expression of *Nramp1* G169 Induced Cell Viability against BSO- and Iron- Induced OS

Next, to determine if *Nramp1*-mediated iron transport functions to protect cells against OS, cell viability was measured between the two stable cell lines with iron loading (100 μ M of FAS).

Addition of 100 μ M FAS reduced the relative growth in R21 cells (Figure 5.4, $P = 0.000002$, ~2 fold cell growth reduction), but enhanced the relative growth in R37 cells (Figure 5.4, $P = 0.003$). R37 cells did not reveal any additional growth suppression with 100 μ M FAS when treated with a low (0.5mM) dose of BSO when compared to 0.5mM BSO alone, (Figure 5.4, $P = 0.2$). However, a 44% decrease of the relative cell growth was observed in R21 cells with 100 μ M FAS+0.5mM BSO (Figure 5.4, $P = 0.002$).

These results indicate that the R21 cells which lack the functional *Nramp1* protein were more sensitive to OS, as shown by the decrease in relative cell growth as a consequence of BSO in the presence or absence of additional iron loading.

5.3.3. Basal *Nramp1* Transcription was Greater in Cells which Lacked the Functional *Nramp1*

Figure 5.5A shows that the normalised level of the *Nramp1* transcription was ~2 fold greater in R21 cells than in the R37 cells (Figure 5.5A, $P = 0.0016$). This indicates that the

absence of *Nramp1* function in macrophage cells activated signalling pathways that resulted in increased transcriptional responses including that of the *Nramp1* gene itself.

5.3.4. Iron Chelation Caused a Reduction of Basal *Nramp1* Transcription in Cells which Lacked the Functional *Nramp1*

The higher basal *Nramp1* transcription observed in the R21 cells (Figure 5.5A) might reflect the increase of iron induced OS due to the impaired iron transport. To determine whether iron present in R21 cells might be associated with the increased *Nramp1* promoter activity, cultures were treated with the iron chelator Def (100 μ M).

Iron chelation by Def (100 μ M) caused a 30% reduction of the *Nramp1* promoter activity in R21 cells (Figure 5.5B, P = 0.05), but no significant change in R37 cells (P = 0.49). This suggests that more chelatable iron was present in R21 cells that could be associated with the higher basal *Nramp1* transcriptional activity.

5.3.5. Function of *Nramp1* Was Necessary for the Activation of *Nramp1* Transcription in Response to LPS+IFN- γ Signalling

LPS+IFN- γ treatment activated *Nramp1* construct pL4 in R37 cells (Figure 5.6, P=0.0067, ~5- fold activation), but no activation response was observed in R21 cells (P = 0.3). This indicated that the expression of the functional *Nramp1* allele *G169* regulates the *Nramp1* activation in response to LPS+IFN- γ .

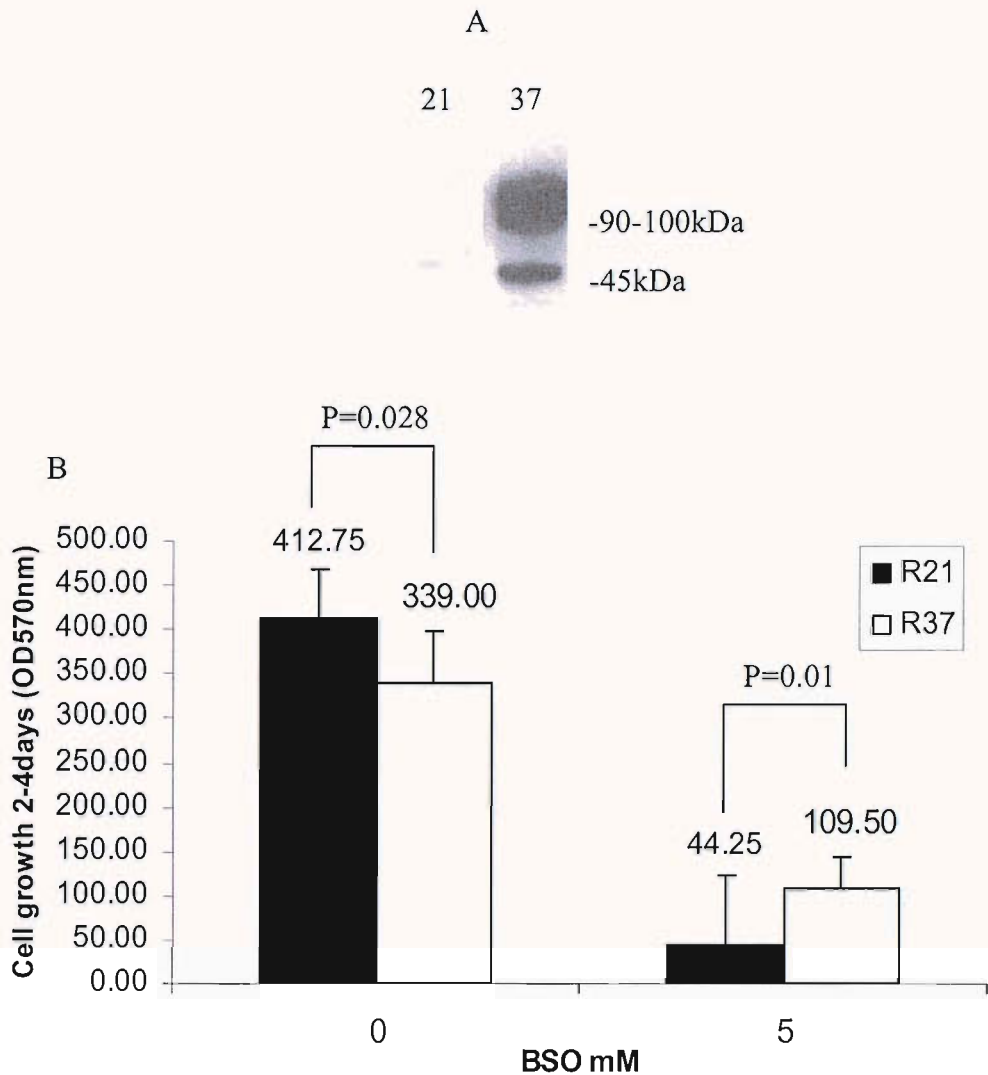


Figure 5.3 Increased Cell Viability with Nrampl Polypeptide Expression Under OS. A. Western immunoblotting (see chapter 2) demonstrated the Nrampl protein expression in *Nrampl* allele G169 stable transfectant Raw264.7 cells (R37) but not in control (R21). Molecular weight of the mature Nrampl proteins (~90-100kDa) were shown on the right.

B. Cell proliferation data for R21 (close bar) and *Nrampl* expressing R37 (open bar). 1×10^3 RAW264.7 cells were plated out in the 96 well micro titre plate from day 0 and treated with BSO (5mM). Each 96 well plates were collected from day 2 to day 4 and were stained with 0.5% crystal violet in 20% methanol and the cells were measured with an absorbance 570nm. Cell proliferation values were presented as a percentage growth of untreated cells for each respective line.

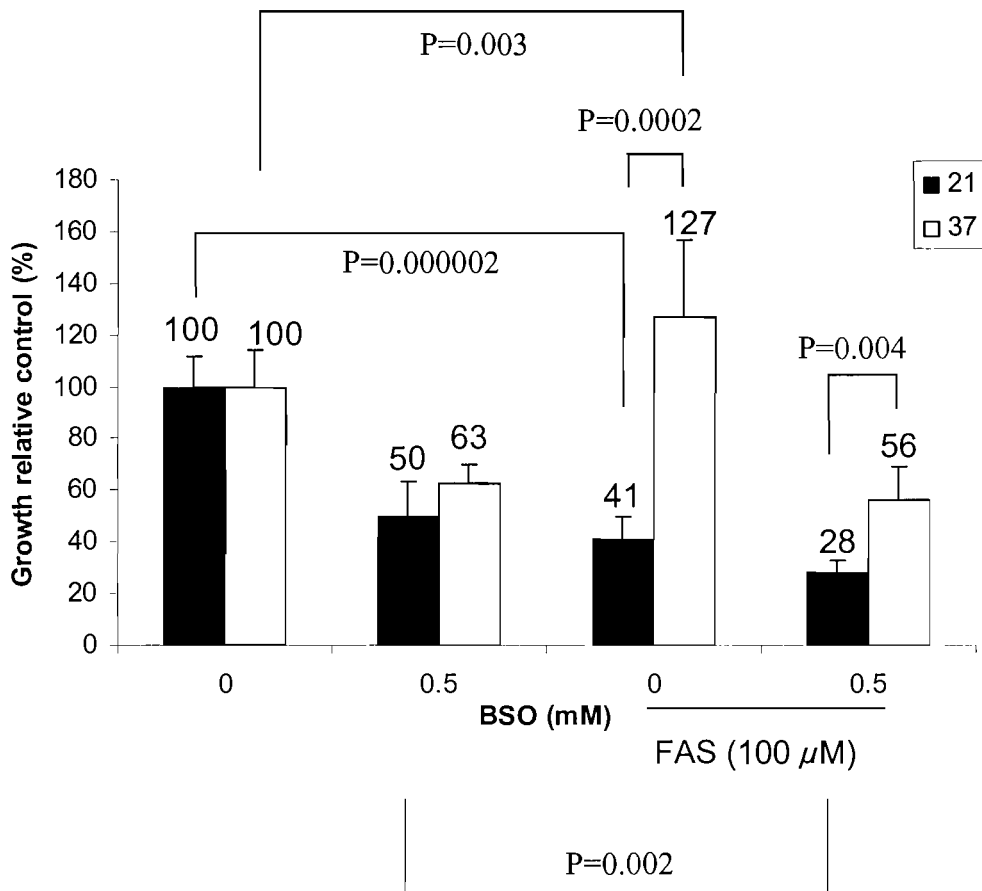


Figure 5.4 Increased Cell Viability with Nramp1 Expression Under BSO+FAS-Induced OS in the *Nramp1* Expressing Stable Transfectant Cells. 1×10^3 of control Raw 264.7 cell transfectants R21 (close bar) and *Nramp1* expressing Raw264.7 cell transfectants (open bar) were plated in 96 well plates and treated \pm Butathione Sulphoximine (BSO) (0.5mM) \pm Ferrous Ammonium Sulphate (FAS) (100 μ M). Each 96 well micro titre plate was collected from day 2 to day 5 which were stained with 0.5% crystal violet in 20% methanol and the cells were measured with an absorbance 570nm. Cell proliferation values are presented as a percentage growth of untreated cells for each respective line.

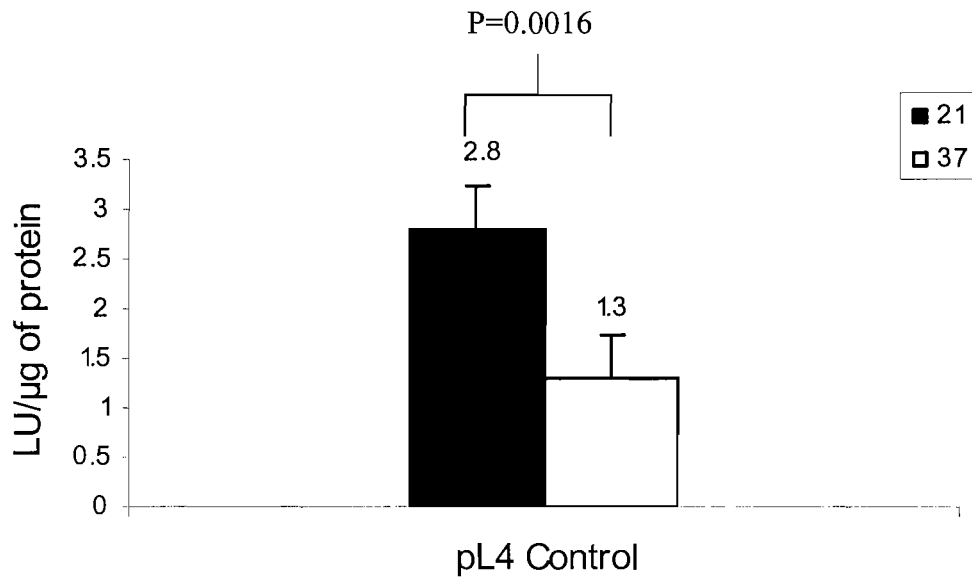


Figure 5.5A The Absence of the *Nramp-1* Allele *G169* in Stable Transfectant R21 Cells Caused a Higher Basal *Nramp1* Transcription. 5×10^5 of the *Nramp1* lacking Raw 264.7 cell stable transfectants R21 (close bar) and *Nramp1* expressing Raw264.7 cell stable transfectants R37 (open bars) were transfected with $1.5 \mu\text{g}$ *Nramp1* construct pL4 in parallel with the control plasmid pGL3. The transfection efficiency of pL4 was controlled by parallel transfection with pGL3 control. Results were presented as the mean LU/μg of protein for pL4 relative to LU/μg protein for pGL3 for each line.

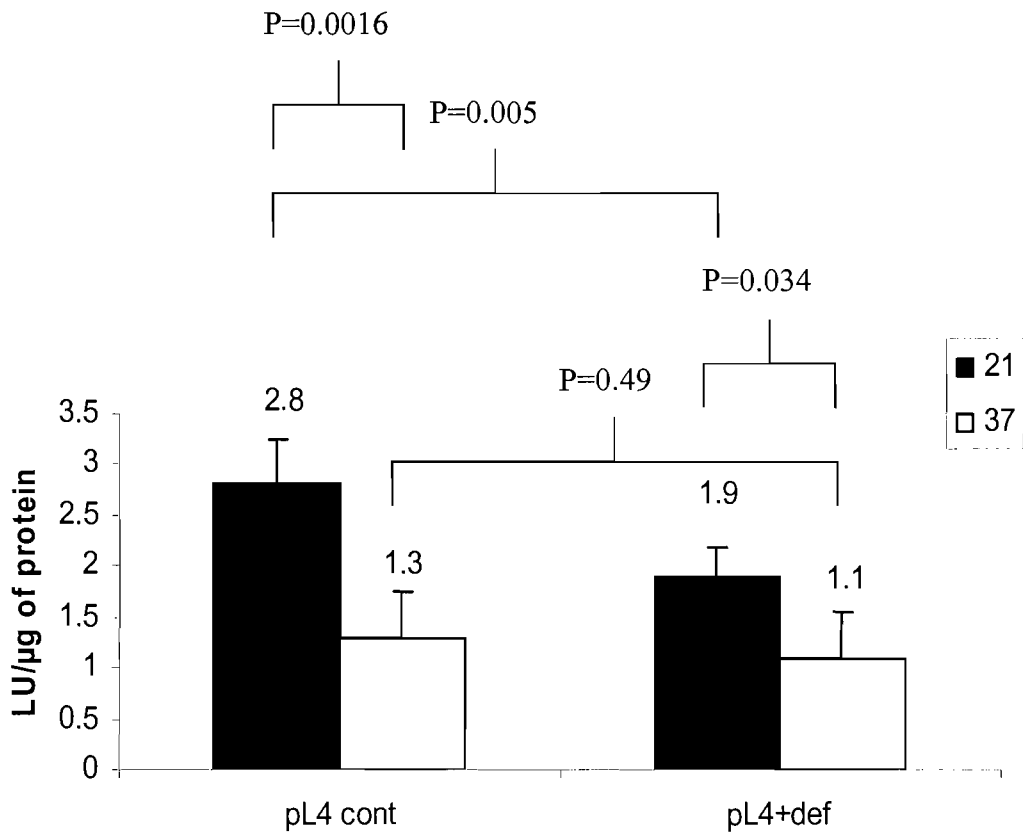


Figure 5.5B Role of Nramp-1 Regulated Iron transport which Affected *Nramp1* Transcription. 5×10^5 of the control Raw 264.7 cell transfectants R21 (close bar) and Nramp1 expressing Raw264.7 cell transfectants (open bars) were transfected with $1.5 \mu\text{g}$ *Nramp1* construct pL4 or with luciferase control reporter pGL3. After transfection, cultures were treated without Def ($100 \mu\text{M}$) (pL4cont) or with Def (pL4+def). The transfection efficiency of pL4 was controlled by parallel transfection with pGL3 control plasmids. Results were presented as the mean LU/ μg protein for pL4 relative to LU/ μg protein for pGL3 for each line and culture treatment.

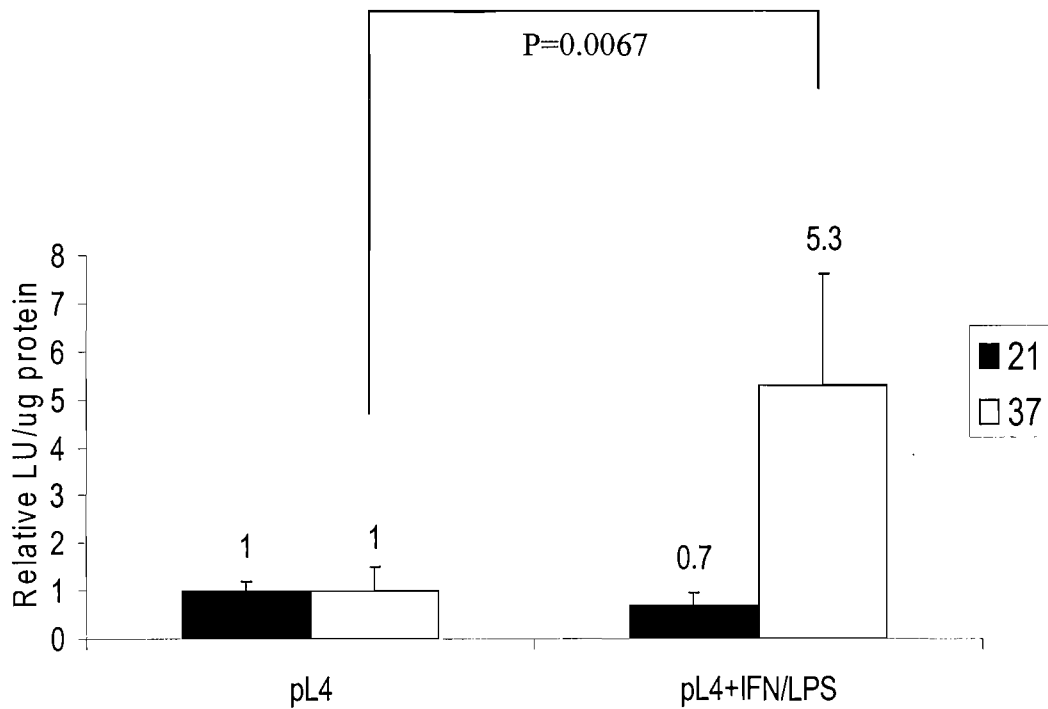


Figure 5.6 The Presence of *Nramp1* Allele *G169* in Stable Transfectant Cells R37 Cells Regulated the *Nramp1* activation in response to LPS+IFN- γ . 5×10^5 of the control Raw 264.7 stable cell transfectants R21 (close bar) and *Nramp1* expressing Raw264.7 cell transfectants (open bars) were co-transfected with $1.5 \mu\text{g}$ of *Nramp1* expression plasmid (pL4) in parallel with the luciferase control reporter pGL3. After 5 hours of transfection, cultures were treated \pm LPS (100 ng/ml) + IFN- γ (25 U/ml) as indicated. Results were presented as the mean LU/ μg protein for pL4 relative to LU/ μg protein for pGL3 for each line and culture treatment.

5.4. Discussions + Future Experiments

The results in this chapter have given insight to the possible role of *Nramp1* in increasing cell tolerance towards OS. In addition, *Nramp1* function was necessary for the upregulation of *Nramp1* transcription in response to LPS+IFN- γ . The results may also indicate that iron transport by *Nramp1* restricts Fenton chemistry in the cytosol and increases Fenton chemistry within the lumen of intracellular vesicles. The formation of ROS as described might explain how *Nramp1* plays a role in controlling OS status, pro-inflammatory responses and anti-microbial responses. Hence, these results may be interpreted in favour of the potential role of *Nramp1* in depleting iron from the cytoplasm of macrophage cells, however this notion was not universally accepted within the *Nramp1* field.

5.4.1. *Nramp1* Reduced the Iron Content in the cells

Previous results show that the basal cell growth rates were reduced in the macrophage cell lines expressing *Nramp1*, possibly via a decrease in iron availability, and iron loading does enhance the extent of cell growth in R37 cells⁶². Hence, one interpretation of the enhanced basal cell growth (Figure 5.3) and the increased basal *Nramp1* promoter activity described here (Figure 5.5A) in the non expressing *Nramp1* R21 cells was that a higher amount of iron was present relative to the cells with *Nramp1* function (allele *G169*). In addition, studies by Wu and colleagues revealed that c-Myc regulates genes, stimulatory and inhibitory effects, to increase the labile iron pool for cell proliferation. That *Nramp1* is inhibited by c-Myc is concordant with *Nramp1* iron transport depleting the labile iron pool.

5.4.2. *Nramp1* Protects the *Nramp1* Stable Transfectant Cells against OS caused by GSH Depletion

The decreased growth observed in both *Nramp1* functional (R37) and non-functional cells (R21), with GSH depletion, might indicate the depletion of GSH induced OS in the macrophage cells (Figure 5.4). Since GSH is an important intracellular antioxidant¹⁵¹, this was not surprising.

Interestingly, cell viability was increased in the *Nramp1* functional R37 cells with BSO treatment (5mM) when comparing with the R21 cells (Figure 5.4). One interpretation was

that in addition to the anti-oxidant GSH, Nramp1 function might also have a role in protecting cells against OS.

5.4.3. Potential Role of Nramp1 in the Protection of Cells from Oxidative Stress, via Iron Transport

Higher basal *Nramp1* promoter activity was observed in the *Nramp1* lacking R21 stable transfectant cell lines compared with the *Nramp1* functional R37 cells (Figure 5.3 and Figure 5.4). This result may suggest that the *Nramp1* functional R37 cells were iron limiting. These results may be interpreted that *Nramp1* functions by reducing the cytosolic redox active free iron, resulting in a lower OS which caused a lower basal *Nramp1* transcription. This assumption was supported by the experiment of iron chelation (Figure 5.5B). The basal *Nramp1* promoter activity in R21 cells was repressed by iron chelation. In contrast, the lower basal *Nramp1* promoter activity observed in R37 cells was not reduced by iron chelation. One could interpret this result as follows: that iron content was limited in the latter cells as a result of *Nramp1*-mediated iron transport.

It will be of interest to determine the underlying signalling mechanism that determines the *Nramp1* promoter transcription in the 2 stable transfectant cells. Lafuse has demonstrated that p38 MAPK is essential for effects of *Nramp1* on mRNA stabilization regulated by an oxidant-generated signalling pathway that requires PKC¹⁵⁸. PKCs contain a conserved Cys-SH residue within their active site domain that is not required for the activity but can be oxidised into Cys-SOH which altered the PKC activity¹⁵⁹. Inhibitors of p38MAPK (SB203580) or PKC (DN-PKC β or Calphostin) could be used to determine the signalling pathways involved in the *Nramp1* transcription. Not all studies have reported an increase of *Nramp1* expression that correlates with allele *G169*; however this may be related to the system for study. Here we have constitutive *Nramp1* expression, whereas others were dependent upon Nramp1 being activated. Since Nramp1 takes 24-48 hours for functional expression it is likely that Nramp1 phenotypic effects will manifest themselves later and correlate with a sustained inflammatory response.

The experiment showing a Sp1-dependent promoter was also regulated by OS (Figure 4.8) provided evidence for the role of Sp1 in the regulation of transcription under OS. Sp1 act as an effector to mediate the PKC-signalling pathway elicited by extracellular signals - PMA¹⁶⁰. It will be of interest to determine if Sp1 is involved in regulating the elevated *Nramp1* promoter activity by OS in the 2 stable transfectant cells.

5.4.4. Role of Nramp1 which determined the Stimulatory or Attenuated Effect of LPS+IFN- γ on Nramp1 Transcription

Results showed that *Nramp1* was necessary for increased activation of *Nramp1* promoter function in response to LPS+IFN- γ stimulation (Figure 5.6).

The mechanism responsible for the enhanced activation of *Nramp1* transcription with LPS+IFN- γ in the *Nramp1* functional cells has not been elucidated, but is probably related to *Nramp1*-mediated iron redistribution within the macrophage. The *Nramp1* genotype specific responses probably apply not only to *Nramp1* transcription itself, but have been reported from other IFN- γ inducible genes as *Nramp1* function is needed for sustained *iNos* transcription⁷⁷, I-A⁴⁴, MHCII¹⁶¹ and the arginine uptake transport⁴⁷. Hence, this suggested that *Nramp1* functionality is vital for IFN- γ transcriptional responses in macrophages.

Buschman stated that exclusion of iron from the phagosome by *Nramp1* can prevent bacterial growth and result in the pleiotropic effects of macrophage activation^{69,162}. However, other studies suggested that iron export from the phagosome into the cytosol by *Nramp1* might have an immunosuppressive activity on *iNos* expression^{75,77} as iron loading attenuates *iNos*.

It is unknown as to why the *Nramp1* transcription was enhanced in the functional *Nramp1* expressing cells in response to LPS+IFN- γ , but not in the *Nramp1* lacking cells. H_2O_2 has been shown to contribute to cellular signalling by activating the MAPK and inhibiting the PTPs such as SHP-1¹⁶³. H_2O_2 is particularly relevant here because Lee and co-workers recently concluded that the activation of a receptor tyrosine kinase following binding of the corresponding growth factor/cytokine, may not be sufficient to increase the steady state level of protein tyrosine phosphorylation in cells and that inhibition of protein-tyrosine phosphatases by H_2O_2 might also be required for sustained signalling¹⁶⁴. Thus maintaining high levels of H_2O_2 and minimizing hydroxyl radicals/anion might be central to a sustained pro-inflammatory response. *Nramp1*-mediated cytosolic iron depletion might be required to prevent the formation of OH^\bullet/OH^- via Fenton chemistry and enabling H_2O_2 generation. It was shown that the *Bcgs/Nramp1* resistant macrophages had a superior ability to phosphorylate p38 MAPK¹⁶⁵. This may indicate that the increased phosphorylation of p38MAPK or PKC through inhibition of PTPs by H_2O_2 contribute to the increased responsiveness of *Nramp1* promoter upon LPS+IFN- γ stimulation.

Hence, it is proposed here that *Nramp1*-mediated iron depletion participated in the process of Fenton chemistry or SOD activity producing H_2O_2 enhanced the pro-inflammatory reaction in response to LPS+IFN- γ . In addition, the proposed role of

Nramp1 in iron depletion may prevent OS in macrophage cells. There is also a possibility that the expression of the Nramp1 protein then regulates other pro-inflammatory responses.

6. Chapter 6

Final Conclusion

The purpose of this study was to investigate regulation of the *Nramp1* promoter, in order to gain insight into the molecular mechanisms underlying the regulation of *Nramp1* transcription by Inr element-binding transcription factors and to stimulation by LPS+IFN- γ , iron and OS.

In addition, knowledge of the transcriptional regulation of *Nramp1* is important because it is relevant to human autoimmune and infectious diseases. Secondly, many iron regulatory genes and transporters are regulated by iron in a manner related to their function. It is hoped that study of regulation is likely to provide further clues with regard to its function and this is the essence of microarray analysis.

6.1. *Nramp1* is a Classical Initiator Promoter

Nramp1, like many genes expressed within the differentiated macrophage, does not carry a TATA-box, but incorporates Inr and Inr-like elements⁵⁰. The molecular mechanisms directing transcription from such promoters are not well defined, but they are well represented within genes expressed by the macrophage. As many as 85% of genes contain initiator elements¹⁶⁶ suggesting that any mechanism of regulation of initiator promoters is likely to be widespread. A number of initiator binding factors including c-Myc/Max⁵², USF1⁵³, YY1⁵⁴, TFII-I⁵⁵ and Miz-1^{56,57} have been identified, although it is not clear what features of a promoter are important for a particular factor to function.

Experiments described in chapter 3 have given some insights to the transcriptional regulation of the *Nramp1* promoter by these factors. However, these functional data need to be validated by protein binding studies such as the use of CHIP/EMSA assay.

6.2. Consensus Sp1 Binding Site is Necessary for the Basal and Activated *Nramp1* Transcription

In the present study, a consensus Sp1 binding site was shown to be necessary for the basal and activated *Nramp1* transcription with LPS+IFN- γ and L-Gln. Results also showed that OS activated a Sp1-dependent promoter. Together these data could support the argument that Sp1 may be involved in the oxidant regulation of *Nramp1* transcription (Chapter 4), however direct oxidant activation of *Nramp1* by Sp1 still needs to be demonstrated. It is widely thought that Sp1 is a constitutive, but data suggest that it might have a regulatory role.

Studies in man have realized NRAMP1 polymorphisms are associated with resistance/susceptibility to infection ¹⁶⁷, and it is a candidate susceptibility locus for diseases such as type-1 diabetes ^{21,28,168}. Inappropriate Sp1 activation has also been linked with some of the associated pathological consequences in type-1 diabetes ¹⁶⁹. It is not known if these two events are linked, nor if the Sp1 site in human NRAMP1 is functional, although based on mouse studies it would be predicted to be essential. The Sp1 dependent regulation of NRAMP1 might be linked with the pathological consequences in type-1 diabetes and pro-inflammatory responses, although it is likely that the latter occur prior to the onset of the hyperglycaemic state.

Many other immune response genes are intimately linked with Sp1 activity ¹⁷⁰ and Sp1 is responsive to LPS and positively regulates many macrophage expressed genes ^{79,80}. In the context of *Nramp1*, the consensus Sp1 binding site is juxtaposed to the Miz-1-binding Inr within the core promoter ⁵⁷ and Miz-1 is implicated in the IFN- γ -mediated upregulation of *Nramp1* ⁶³. The precise role of Sp1 on *Nramp1* activation is not clear, but it might respond to LPS. It is difficult to study further given that the Sp1 binding site mutant promoter exhibits very low activity, furthermore, Sp1 and Miz-1 do not make direct contact with each other ⁸⁴, but are possibly bridged by factors such as p300.

6.3. Potential Role of Nramp1 to Protect Cells against Oxidative Stress via Iron Depletion

The current study has proposed a role of *Nramp1* in the protection of cells against OS. A possible link of *Nramp1* with OS is its ability to modulate the divalent cation/iron flux within macrophages. Redox active free iron can catalyze the formation of ROS via Fenton chemistry ^{141,148}. The protective effect of *Nramp1* towards OS, described here, could be direct, through sequestering iron. Alternatively, *Nramp1* could influence the activity of transcription factors that control the oxidant defences themselves, such that these defences were heightened. Ferritin is also believed to be protective against OS and, as proposed here, like *Nramp1* also depletes the cytosolic iron pool suggesting a possible direct effect.

Transport of cations into the cytosol, as proposed by Jabado ⁴ and Gomes ⁵, would result in an increase in OS unless the cations are buffered by iron-binding proteins. Mulero showed decreased ferritin expression in *Nramp1* G169 macrophages relative to the D169 allele cells, thereby lowering potential buffering capacity ⁷⁴.

Previous reports have suggested the concept of a negative auto-regulatory pathway, involving the *Nramp1*-dependent iron transport which auto-regulates *Nramp1* expression ⁶².

Iron administration enhanced the *Nramp1* expression and our data and those of others supported the concept that *Nramp1* functionality reduces the level of iron within the cytosol^{62,74}. If *Nramp1* transported iron or divalent cations from the lumen of an intracellular vesicle or phagosome and into the cytosol, then given the positive regulation of *Nramp1* by iron described previously⁶², *Nramp1*-mediated divalent cation/iron transport would be expected to increase its own expression, via a positive feed-forward loop. This is of course assuming that the cell senses the levels of iron in the cytosol as opposed to the lumen on an intracellular transport vesicle. However, results of the present study support the converse.

In conclusion, these results can be interpreted in favour of the role of *Nramp1* in depleting iron from the cytoplasm of macrophage cells and in the protection of cells against OS.

6.4. Role of *Nramp1* in the Regulation of the Pleiotropic Effects Associated with Iron / Iron generated Oxygen Radicals

Nramp1 controls the pro-inflammatory properties of macrophages and the growth of intra-macrophage pathogens by transporting divalent cations^{75,77,167}. The contribution of the *Nramp1*-mediated pathogen growth control by direct divalent cation transport at the level of the phagosome-cytosol interface is unclear, as *Nramp1* influences the macrophage transcriptome and wider inflammatory responses. The importance of this aspect of *Nramp1* is provided by its association with autoimmune diseases in man, where there is no evidence of an infectious aetiology. Other workers have suggested that the transcriptomes displayed by intracellular pathogens within the phagosomes in *Nramp1* null allele cells were in an iron rich environment^{171,172} supporting the iron efflux hypothesis^{67,68}. However, if the phagosome of the functional *Nramp1* macrophages was in an iron depleted state, then the iron transported by *Nramp1* would be unlikely to accumulate within the cytosol, as it might have an immunosuppressive activity like iron-loading does on the expression of *iNos*⁷⁵, whereas the functional *Nramp1* allele drives the enhanced *iNos* expression⁷⁷. Previous study demonstrated that the pleiotropic effects of allelic *Nramp1* can be reproduced in a Raw264.7 transfectant cell model and ROS were required for expression of the IFN- γ response⁴⁷. Carter¹⁷³ recently showed that TNF α gene expression is dependent on p38 MAPK and adequate steady state levels of H₂O₂ are required for p38 activation. Interestingly, Lafuse¹⁷⁴ demonstrated p38 MAPK was essential for effects of *Nramp1* on mRNA stabilization regulated by an oxidant-generated signalling pathway that

requires PKC. Given that both TNF α and mRNA stabilization are modulated by *Nramp1* genotype, it is possible that they are both influenced by *Nramp1* through the control of radical generation.

We propose that central to the inflammatory outcome is the choice between Fenton chemistry or superoxide dismutase activity producing H₂O₂ which takes place within the cytosol, and *Nramp1*-mediated iron transport regulates this process (Figure 6.1). Interestingly, Murata showed that GSH content influenced IL-6 or IL-12 production and proposed the concept of "reductive" and "oxidative" macrophages that regulate the ratio of Th1/Th2¹⁵³. In the context of *Nramp1* biology, allele *G169* has been linked with Th1 responsiveness. Our model indicated that expression of *Nramp1* plays a role to sequester divalent cations to potentiate IFN- γ signalling and pro-inflammatory responses. In addition, the sequestering of iron prevented the GSH depletion to compensate for the OS in cells. It is also suggested that the pro-inflammatory activities of *Nramp1* are important and cannot be separated from cation transport at the phagosome-cytosol interface.

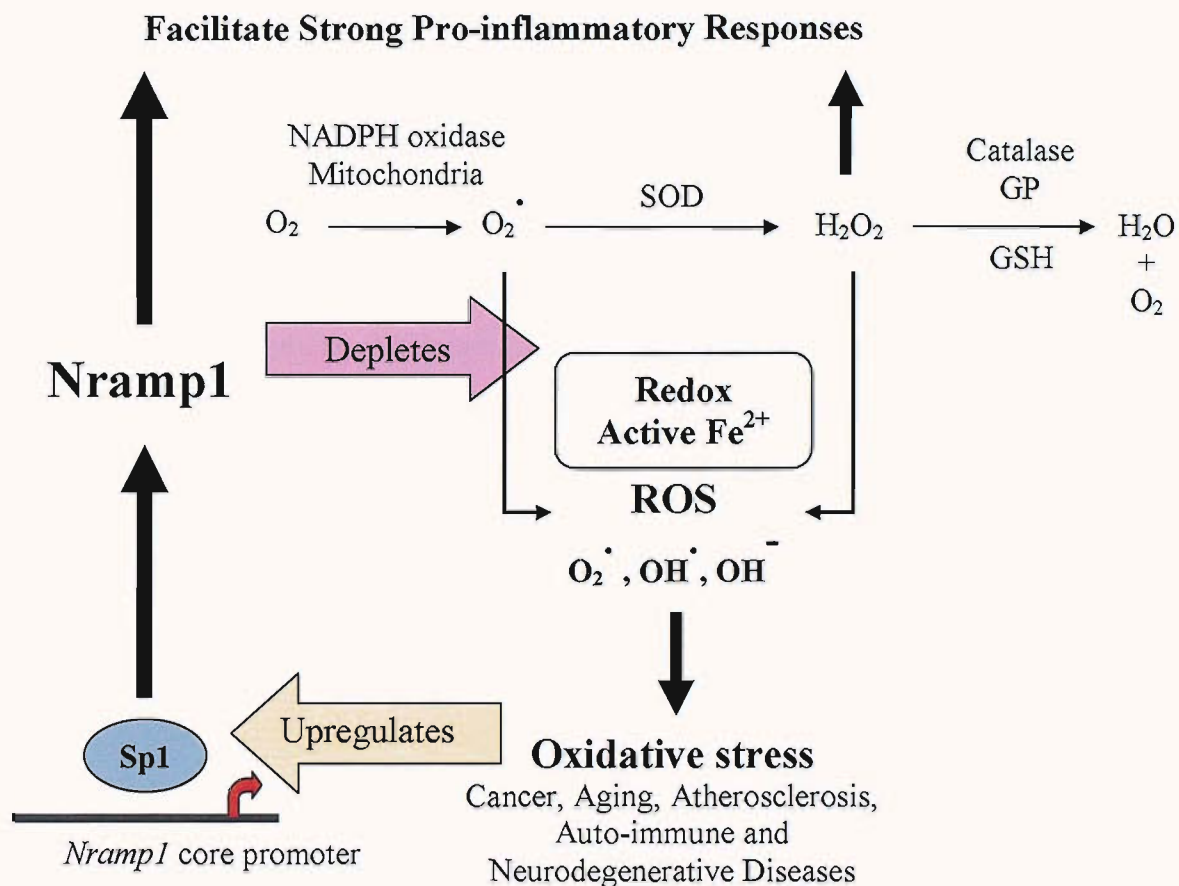


Figure. 6.1. Potential Role of the *Nramp1* – Mediated Bivalent Cation / Iron Transport. A model is proposed which suggests the expression of *Nramp1* in controlling the inflammatory response by Fenton chemistry in the generation of reactive oxygen species (ROS) mediated by iron transported by *Nramp1*. Excess redox active iron/ Fe^{2+} provoked oxidative stress (OS) which induced the Sp1-dependent promoter transcription. We propose that OS caused activation of *Nramp1* transcription, possibly via transcription factor Sp1, leading to increase *Nramp1* expression. The increased *Nramp1* expression is proposed to deplete the cytosolic iron and consequently reduced OS. In addition, the reduced iron in the cytosol via *Nramp1* transport led to the sustained inflammatory responses causing the robust LPS+IFN- γ signalling, by shifting the balance to increase the H_2O_2 production via superoxide dismutase (SOD). The present study favors the role of *Nramp1* in the depletion of cytosolic iron, which his consistent with the previous results shown.

References

1. Vidal, S. M., Malo, D., Vogan, K., Skamene, E. & Gros, P. Natural resistance to infection with intracellular parasites: isolation of a candidate for Bcg. *Cell* **73**, 469-85 (1993).
2. Bradley, D. J. Letter: Genetic control of natural resistance to *Leishmania donovani*. *Nature* **250**, 353-4 (1974).
3. Schurr, E., Skamene, E., Forget, A. & Gros, P. Linkage analysis of the Bcg gene on mouse chromosome 1. Identification of a tightly linked marker. *J Immunol* **142**, 4507-13 (1989).
4. O'Brien, A. D., Rosenstreich, D. L. & Taylor, B. A. Control of natural resistance to *Salmonella typhimurium* and *Leishmania donovani* in mice by closely linked but distinct genetic loci. *Nature* **287**, 440-2 (1980).
5. Plant, J. E., Blackwell, J. M., O'Brien, A. D., Bradley, D. J. & Glynn, A. A. Are the Lsh and Ity disease resistance genes at one locus on mouse chromosome 1? *Nature* **297**, 510-1 (1982).
6. Skamene, E., Gros, P., Forget, A., Kongshavn, P. A., St Charles, C., and Taylor, B. A. Genetic regulation of resistance to intracellular pathogens. *Nature* **297**, 506-9 (1982).
7. Malo, D., Vogan, K., Vidal, S., Hu, J., Cellier, M., Schurr, E., Fuks, A., Bumstead, N., Morgan, K., and Gros, P. Haplotype mapping and sequence analysis of the mouse *Nramp* gene predict susceptibility to infection with intracellular parasites. *Genomics* **23**, 51-61 (1994).
8. Vidal, S., Tremblay, M. L., Govoni, G., Gauthier, S., Sebastiani, G., Malo, D., Skamene, E., Olivier, M., Jothy, S., and Gros, P. The Ity/Lsh/Bcg locus: natural resistance to infection with intracellular parasites is abrogated by disruption of the *Nramp1* gene. *J Exp Med* **182**, 655-66 (1995).
9. Vidal, S., Gros, P. & Skamene, E. Natural resistance to infection with intracellular parasites: molecular genetics identifies *Nramp1* as the Bcg/Ity/Lsh locus. *J Leukoc Biol* **58**, 382-90 (1995).
10. Cellier, M., Govoni, G., Vidal, S., Kwan, T., Groulx, N., Liu, J., Sanchez, F., Skamene, E., Schurr, E., and Gros, P. Human natural resistance-associated macrophage protein: cDNA cloning, chromosomal mapping, genomic organization, and tissue-specific expression. *J Exp Med* **180**, 1741-52 (1994).

11. Blackwell, J. M., Barton, C. H., White, J. K., Searle, S., Baker, A. M., Williams, H., and Shaw, M. A. Genomic organization and sequence of the human NRAMP gene: identification and mapping of a promoter region polymorphism. *Mol Med* **1**, 194-205 (1995).
12. Shaw, M. A., Collins, A., Peacock, C. S., Miller, E. N., Black, G. F., Sibthorpe, D., Lins-Lainson, Z., Shaw, J. J., Ramos, F., Silveira, F., and Blackwell, J. M. Evidence that genetic susceptibility to Mycobacterium tuberculosis in a Brazilian population is under oligogenic control: linkage study of the candidate genes NRAMP1 and TNFA. *Tuber Lung Dis* **78**, 35-45 (1997).
13. Bellamy, R., Ruwende, C., Corrah, T., McAdam, K. P., Whittle, H. C., and Hill, A. V. Variations in the NRAMP1 gene and susceptibility to tuberculosis in West Africans. *N Engl J Med* **338**, 640-4 (1998).
14. Marquet, S., Sanchez, F. O., Arias, M., Rodriguez, J., Paris, S. C., Skamene, E., Schurr, E., and Garcia, L. F. Variants of the human NRAMP1 gene and altered human immunodeficiency virus infection susceptibility. *J Infect Dis* **180**, 1521-5 (1999).
15. Cervino, A. C., Lakiss, S., Sow, O. & Hill, A. V. Allelic association between the NRAMP1 gene and susceptibility to tuberculosis in Guinea-Conakry. *Ann Hum Genet* **64**, 507-12 (2000).
16. Gao, P. S., Fujishima, S., Mao, X. Q., Remus, N., Kanda, M., Enomoto, T., Dake, Y., Bottini, N., Tabuchi, M., Hasegawa, N., Yamaguchi, K., Tiemessen, C., Hopkin, J. M., Shirakawa, T., and Kishi, F. Genetic variants of NRAMP1 and active tuberculosis in Japanese populations. International Tuberculosis Genetics Team. *Clin Genet* **58**, 74-6 (2000).
17. Greenwood, C. M., Fujiwara, T. M., Boothroyd, L. J., Miller, M. A., Frappier, D., Fanning, E. A., Schurr, E., and Morgan, K. Linkage of tuberculosis to chromosome 2q35 loci, including NRAMP1, in a large aboriginal Canadian family. *Am J Hum Genet* **67**, 405-16 (2000).
18. Ryu, S., Park, Y. K., Bai, G. H., Kim, S. J., Park, S. N., and Kang, S. 3'UTR polymorphisms in the NRAMP1 gene are associated with susceptibility to tuberculosis in Koreans. *Int J Tuberc Lung Dis* **4**, 577-80 (2000).
19. Mohamed, H. S., Ibrahim, M. E., Miller, E. N., White, J. K., Cordell, H. J., Howson, J. M., Peacock, C. S., Khalil, E. A., El Hassan, A. M., and Blackwell, J. M.. SLC11A1 (formerly NRAMP1) and susceptibility to visceral leishmaniasis in The Sudan. *Eur J Hum Genet* **12**, 66-74 (2004).

20. Shaw, M. A., Clayton, D., Atkinson, S. E., Williams, H., Miller, N., Sibthorpe, D., and Blackwell, J. M.. Linkage of rheumatoid arthritis to the candidate gene NRAMP1 on 2q35. *J Med Genet* **33**, 672-7 (1996).
21. Esposito, L., Hill, N. J., Pritchard, L. E., Cucca, F., Muxworthy, C., Merriman, M. E., Wilson, A., Julier, C., Delepine, M., Tuomilehto, J., Tuomilehto-Wolf, E., Ionesco-Tirgoviste, C., Nistico, L., Buzzetti, R., Pozzilli, P., Ferrari, M., Bosi, E., Pociot, F., Nerup, J., Bain, S. C., and Todd, J. A. Genetic analysis of chromosome 2 in type 1 diabetes: analysis of putative loci IDDM7, IDDM12, and IDDM13 and candidate genes NRAMP1 and IA-2 and the interleukin-1 gene cluster. IMDIAB Group. *Diabetes* **47**, 1797-9 (1998).
22. Maliarik, M. J., Chen, K. M., Sheffer, R. G., Rybicki, B. A., Major, M. L., Popovich, J., Jr., and Iannuzzi, M. C. The natural resistance-associated macrophage protein gene in African Americans with sarcoidosis. *Am J Respir Cell Mol Biol* **22**, 672-5 (2000).
23. Sanjeevi, C. B., Miller, E. N., Dabadghao, P., Rumba, I., Shtauvere, A., Denisova, A., Clayton, D., and Blackwell, J. M. Polymorphism at NRAMP1 and D2S1471 loci associated with juvenile rheumatoid arthritis. *Arthritis Rheum* **43**, 1397-404 (2000).
24. Singal, D. P., Li, J., Zhu, Y. & Zhang, G. NRAMP1 gene polymorphisms in patients with rheumatoid arthritis. *Tissue Antigens* **55**, 44-7 (2000).
25. Yang, Y. S., Kim, S. J., Kim, J. W. & Koh, E. M. NRAMP1 gene polymorphisms in patients with rheumatoid arthritis in Koreans. *J Korean Med Sci* **15**, 83-7 (2000).
26. Searle, S. & Blackwell, J. M. Evidence for a functional repeat polymorphism in the promoter of the human NRAMP1 gene that correlates with autoimmune versus infectious disease susceptibility. *J Med Genet* **36**, 295-9 (1999).
27. Kojima, Y., Kinouchi, Y., Takahashi, S., Negoro, K., Hiwatashi, N., and Shimosegawa, T. Inflammatory bowel disease is associated with a novel promoter polymorphism of natural resistance-associated macrophage protein 1 (NRAMP1) gene. *Tissue Antigens* **58**, 379-84 (2001).
28. Takahashi, K., Satoh, J., Kojima, Y., Negoro, K., Hirai, M., Hinokio, Y., Kinouchi, Y., Suzuki, S., Matsuura, N., Shimosegawa, T., and Oka, Y. Promoter polymorphism of SLC11A1 (formerly NRAMP1) confers susceptibility to autoimmune type 1 diabetes mellitus in Japanese. *Tissue Antigens* **63**, 231-6 (2004).
29. Gruenheid, S., Cellier, M., Vidal, S. & Gros, P. Identification and characterization of a second mouse Nramp gene. *Genomics* **25**, 514-25 (1995).

30. Vidal, S., Belouchi, A. M., Cellier, M., Beatty, B. & Gros, P. Cloning and characterization of a second human NRAMP gene on chromosome 12q13. *Mamm Genome* **6**, 224-30 (1995).
31. Fleming, M. D., Trenor, C. C., 3rd, Su, M. A., Foernzler, D., Beier, D. R., Dietrich, W. F., and Andrews, N. C. Microcytic anaemia mice have a mutation in Nramp2, a candidate iron transporter gene. *Nat Genet* **16**, 383-6 (1997).
32. Barton, C. H., White, J. K., Roach, T. I. & Blackwell, J. M. NH₂-terminal sequence of macrophage-expressed natural resistance-associated macrophage protein (Nramp) encodes a proline/serine-rich putative Src homology 3-binding domain. *J Exp Med* **179**, 1683-7 (1994).
33. White, J. K., Stewart, A., Popoff, J. F., Wilson, S. & Blackwell, J. M. Incomplete glycosylation and defective intracellular targeting of mutant solute carrier family 11 member 1 (Slc11a1). *Biochem J* **382**, 811-9 (2004).
34. Vidal, S. M., Pinner, E., Lepage, P., Gauthier, S. & Gros, P. Natural resistance to intracellular infections: Nramp1 encodes a membrane phosphoglycoprotein absent in macrophages from susceptible (Nramp1 D169) mouse strains. *J Immunol* **157**, 3559-68 (1996).
35. Gruenheid, S., Pinner, E., Desjardins, M. & Gros, P. Natural resistance to infection with intracellular pathogens: the Nramp1 protein is recruited to the membrane of the phagosome. *J Exp Med* **185**, 717-30 (1997).
36. Goswami, T., Bhattacharjee, A., Babal, P., Searle, S., Moore, E., Li, M., and Blackwell, J. M. Natural-resistance-associated macrophage protein 1 is an H⁺/bivalent cation antiporter. *Biochem J* **354**, 511-9 (2001).
37. Gros, P., Skamene, E. & Forget, A. Cellular mechanisms of genetically controlled host resistance to *Mycobacterium bovis* (BCG). *J Immunol* **131**, 1966-72 (1983).
38. Gros, P., Skamene, E. & Forget, A. Genetic control of natural resistance to *Mycobacterium bovis* (BCG) in mice. *J Immunol* **127**, 2417-21 (1981).
39. Hackam, D. J., Rotstein, O. D., Zhang, W., Gruenheid, S., Gros, P., and Grinstein, S. Host resistance to intracellular infection: mutation of natural resistance-associated macrophage protein 1 (Nramp1) impairs phagosomal acidification. *J Exp Med* **188**, 351-64 (1998).
40. Frehel, C., Canonne-Hergaux, F., Gros, P. & De Chastellier, C. Effect of Nramp1 on bacterial replication and on maturation of *Mycobacterium avium*-containing phagosomes in bone marrow-derived mouse macrophages. *Cell Microbiol* **4**, 541-56 (2002).

41. Brown, D., Faris, M., Hilburger, M. & Zwilling, B. S. The induction of persistence of I-A expression by macrophages from Bcgr mice occurs via a protein kinase C-dependent pathway. *J Immunol* **152**, 1323-31 (1994).
42. Blackwell, J. M., Roach, T. I., Atkinson, S. E., Ajioka, J. W., Barton, C. H., and Shaw, M. A. Genetic regulation of macrophage priming/activation: the Lsh gene story. *Immunol Lett* **30**, 241-8 (1991).
43. Roach, T. I., Chatterjee, D. & Blackwell, J. M. Induction of early-response genes KC and JE by mycobacterial lipoarabinomannans: regulation of KC expression in murine macrophages by Lsh/Ity/Bcg (candidate Nramp). *Infect Immun* **62**, 1176-84 (1994).
44. Zwilling, B. S., Vespa, L. & Massie, M. Regulation of I-A expression by murine peritoneal macrophages: differences linked to the Bcg gene. *J Immunol* **138**, 1372-6 (1987).
45. Blackwell, J. M., Searle, S., Goswami, T. & Miller, E. N. Understanding the multiple functions of Nramp1. *Microbes Infect* **2**, 317-21 (2000).
46. Olivier, M., Cook, P., Desantctis, J., Hel, Z., Wojciechowski, W., Reiner, N. E., Skamene, E., and Radzioch, D. Phenotypic difference between Bcg(r) and Bcg(s) macrophages is related to differences in protein-kinase-C-dependent signalling. *Eur J Biochem* **251**, 734-43 (1998).
47. Barton, C. H., Whitehead, S. H. & Blackwell, J. M. Nramp transfection transfers Ity/Lsh/Bcg-related pleiotropic effects on macrophage activation: influence on oxidative burst and nitric oxide pathways. *Mol Med* **1**, 267-79 (1995).
48. Brown, D. H., Lafuse, W. P. & Zwilling, B. S. Stabilized expression of mRNA is associated with mycobacterial resistance controlled by Nramp1. *Infect Immun* **65**, 597-603 (1997).
49. Lang, T., Prina, E., Sibthorpe, D. & Blackwell, J. M. Nramp1 transfection transfers Ity/Lsh/Bcg-related pleiotropic effects on macrophage activation: influence on antigen processing and presentation. *Infect Immun* **65**, 380-6 (1997).
50. Govoni, G., Vidal, S., Cellier, M., Lepage, P., Malo, D., and Gros, P. Genomic structure, promoter sequence, and induction of expression of the mouse Nramp1 gene in macrophages. *Genomics* **27**, 9-19 (1995).
51. Javahery, R., Khachi, A., Lo, K., Zenzie-Gregory, B. & Smale, S. T. DNA sequence requirements for transcriptional initiator activity in mammalian cells. *Mol Cell Biol* **14**, 116-27 (1994).

52. Li, L. H., Nerlov, C., Prendergast, G., MacGregor, D. & Ziff, E. B. c-Myc represses transcription in vivo by a novel mechanism dependent on the initiator element and Myc box II. *Embo J* **13**, 4070-9 (1994).
53. Du, H., Roy, A. L. & Roeder, R. G. Human transcription factor USF stimulates transcription through the initiator elements of the HIV-1 and the Ad-ML promoters. *Embo J* **12**, 501-11 (1993).
54. Seto, E., Shi, Y. & Shenk, T. YY1 is an initiator sequence-binding protein that directs and activates transcription in vitro. *Nature* **354**, 241-5 (1991).
55. Roy, A. L., Malik, S., Meisterernst, M. & Roeder, R. G. An alternative pathway for transcription initiation involving TFII-I. *Nature* **365**, 355-9 (1993).
56. Bowen, H., Biggs, T. E., Phillips, E., Baker, S. T., Perry, V. H., Mann, D. A., and Barton, C. H. c-Myc represses and Miz-1 activates the murine natural resistance-associated protein 1 promoter. *J Biol Chem* **277**, 34997-5006 (2002).
57. Bowen, H., Lapham, A., Phillips, E., Yeung, I., Alter-Koltunoff, M., Levi, B. Z., Perry, V. H., Mann, D. A., and Barton, C. H. Characterization of the murine Nramp1 promoter: requirements for transactivation by Miz-1. *J Biol Chem* **278**, 36017-26 (2003).
58. Li, W. W., Hsiung, Y., Zhou, Y., Roy, B. & Lee, A. S. Induction of the mammalian GRP78/BiP gene by Ca²⁺ depletion and formation of aberrant proteins: activation of the conserved stress-inducible grp core promoter element by the human nuclear factor YY1. *Mol Cell Biol* **17**, 54-60 (1997).
59. Adrian, G. S., Seto, E., Fischbach, K. S., Rivera, E. V., Adrian, E. K., Herbert, D. C., Walter, C. A., Weaker, F. J., and Bowman, B. H. YY1 and Sp1 transcription factors bind the human transferrin gene in an age-related manner. *J Gerontol A Biol Sci Med Sci* **51**, B66-75 (1996).
60. Roy, A. L., Meisterernst, M., Pognonec, P. & Roeder, R. G. Cooperative interaction of an initiator-binding transcription initiation factor and the helix-loop-helix activator USF. *Nature* **354**, 245-8 (1991).
61. Barton, C. H., Biggs, T. E., Baker, S. T., Bowen, H. & Atkinson, P. G. Nramp1: a link between intracellular iron transport and innate resistance to intracellular pathogens. *J Leukoc Biol* **66**, 757-62 (1999).
62. Baker, S. T., Barton, C. H. & Biggs, T. E. A negative autoregulatory link between Nramp1 function and expression. *J Leukoc Biol* **67**, 501-7 (2000).
63. Alter-Koltunoff, M., Ehrlich, S., Dror, N., Azriel, A., Eilers, M., Hauser, H., Bowen, H., Barton, C. H., Tamura, T., Ozato, K., and Levi, B.-Z. Nramp1-

- mediated Innate Resistance to Intraphagosomal Pathogens Is Regulated by IRF-8, PU.1, and Miz-1. *J. Biol. Chem.* **278**, 44025-44032 (2003).
64. Biggs, T. E., Baker, S. T., Botham, M. S., Dhital, A., Barton, C. H., and Perry, V. H. Nramp1 modulates iron homeostasis in vivo and in vitro: evidence for a role in cellular iron release involving de-acidification of intracellular vesicles. *Eur J Immunol* **31**, 2060-70 (2001).
 65. Atkinson, P. G. & Barton, C. H. Ectopic expression of Nramp1 in COS-1 cells modulates iron accumulation. *FEBS Lett* **425**, 239-42 (1998).
 66. Dalton, T., Paria, B. C., Fernando, L. P., Huet-Hudson, Y. M., Dey, S. K., and Andrews, G. K. Activation of the chicken metallothionein promoter by metals and oxidative stress in cultured cells and transgenic mice. *Comp Biochem Physiol B Biochem Mol Biol* **116**, 75-86 (1997).
 67. Gomes, M. S. & Appelberg, R. Evidence for a link between iron metabolism and Nramp1 gene function in innate resistance against *Mycobacterium avium*. *Immunology* **95**, 165-8 (1998).
 68. Jabado, N., Jankowski, A., Dougaparsad, S., Picard, V., Grinstein, S., and Gros, P. Natural resistance to intracellular infections: natural resistance-associated macrophage protein 1 (Nramp1) functions as a pH-dependent manganese transporter at the phagosomal membrane. *J Exp Med* **192**, 1237-48 (2000).
 69. Buschman, E. & Skamene, E. From Bcg/Lsh/Ity to Nramp1: three decades of search and research. *Drug Metab Dispos* **29**, 471-3 (2001).
 70. Kuhn, D. E., Baker, B. D., Lafuse, W. P. & Zwillling, B. S. Differential iron transport into phagosomes isolated from the RAW264.7 macrophage cell lines transfected with Nramp1Gly169 or Nramp1Asp169. *J Leukoc Biol* **66**, 113-9 (1999).
 71. Zwillling, B. S., Kuhn, D. E., Wikoff, L., Brown, D. & Lafuse, W. Role of iron in Nramp1-mediated inhibition of mycobacterial growth. *Infect Immun* **67**, 1386-92 (1999).
 72. Wyllie, S., Seu, P. & Goss, J. A. The natural resistance-associated macrophage protein 1 Slc11a1 (formerly Nramp1) and iron metabolism in macrophages. *Microbes Infect* **4**, 351-9 (2002).
 73. Atkinson, P. G. & Barton, C. H. High level expression of Nramp1G169 in RAW264.7 cell transfectants: analysis of intracellular iron transport. *Immunology* **96**, 656-62 (1999).

74. Mulero, V., Searle, S., Blackwell, J. M. & Brock, J. H. Solute carrier 11a1 (Slc11a1; formerly Nramp1) regulates metabolism and release of iron acquired by phagocytic, but not transferrin-receptor-mediated, iron uptake. *Biochem J* **363**, 89-94 (2002).
75. Dlaska, M. & Weiss, G. Central role of transcription factor NF-IL6 for cytokine and iron-mediated regulation of murine inducible nitric oxide synthase expression. *J Immunol* **162**, 6171-7 (1999).
76. Shiloh, M. U., MacMicking, J. D., Nicholson, S., Brause, J. E., Potter, S., Marino, M., Fang, F., Dinauer, M., and Nathan, C. Phenotype of mice and macrophages deficient in both phagocyte oxidase and inducible nitric oxide synthase. *Immunity* **10**, 29-38 (1999).
77. Fritsche, G., Dlaska, M., Barton, H., Theurl, I., Garimorth, K., and Weiss, G. Nramp1 functionality increases inducible nitric oxide synthase transcription via stimulation of IFN regulatory factor 1 expression. *J Immunol* **171**, 1994-8 (2003).
78. Wu, K. J., Polack, A. & Dalla-Favera, R. Coordinated regulation of iron-controlling genes, H-ferritin and IRP2, by c-MYC. *Science* **283**, 676-9 (1999).
79. Brightbill, H. D., Plevy, S. E., Modlin, R. L. & Smale, S. T. A prominent role for Sp1 during lipopolysaccharide-mediated induction of the IL-10 promoter in macrophages. *J Immunol* **164**, 1940-51 (2000).
80. Sakuta, T., Matsushita, K., Yamaguchi, N., Oyama, T., Motani, R., Koga, T., Nagaoka, S., Abeyama, K., Maruyama, I., Takada, H., and Torii, M. Enhanced production of vascular endothelial growth factor by human monocytic cells stimulated with endotoxin through transcription factor SP-1. *J Med Microbiol* **50**, 233-7 (2001).
81. Yeung, I. Y., Phillips, E., Mann, D. A. & Barton, C. H. Oxidant regulation of the bivalent cation transporter Nramp1. *Biochem Soc Trans* **32**, 1008-10 (2004).
82. Searle, S., Bright, N. A., Roach, T. I., Atkinson, P. G., Barton, C. H., Meloen, R. H., and Blackwell, J. M. Localisation of Nramp1 in macrophages: modulation with activation and infection. *J Cell Sci* **111 (Pt 19)**, 2855-66 (1998).
83. Henriksson, M. & Luscher, B. Proteins of the Myc network: essential regulators of cell growth and differentiation. *Adv Cancer Res* **68**, 109-82 (1996).
84. Peukert, K., Staller, P., Schneider, A., Carmichael, G., Hanel, F., and Eilers, M. An alternative pathway for gene regulation by Myc. *Embo J* **16**, 5672-86 (1997).
85. Herold, S., Wanzel, M., Beuger, V., Frohme, C., Beul, D., Hillukkala, T., Syvaaja, J., Saluz, H. P., Haenel, F., and Eilers, M. Negative regulation of the mammalian UV response by Myc through association with Miz-1. *Mol Cell* **10**, 509-21 (2002).

86. Wu, S., Cetinkaya, C., Munoz-Alonso, M. J., von der Lehr, N., Bahram, F., Beuger, V., Eilers, M., Leon, J., and Larsson, L. G. Myc represses differentiation-induced p21CIP1 expression via Miz-1-dependent interaction with the p21 core promoter. *Oncogene* **22**, 351-60 (2003).
87. Feng, X. H., Liang, Y. Y., Liang, M., Zhai, W. & Lin, X. Direct interaction of c-Myc with Smad2 and Smad3 to inhibit TGF-beta-mediated induction of the CDK inhibitor p15(Ink4B). *Mol Cell* **9**, 133-43 (2002).
88. Nasi, S., Ciarapica, R., Jucker, R., Rosati, J. & Soucek, L. Making decisions through Myc. *FEBS Lett* **490**, 153-62 (2001).
89. Coller, H. A., Grandori, C., Tamayo, P., Colbert, T., Lander, E. S., Eisenman, R. N., and Golub, T. R. Expression analysis with oligonucleotide microarrays reveals that MYC regulates genes involved in growth, cell cycle, signaling, and adhesion. *Proc Natl Acad Sci U S A* **97**, 3260-5 (2000).
90. Dang, C. V. c-Myc target genes involved in cell growth, apoptosis, and metabolism. *Mol Cell Biol* **19**, 1-11 (1999).
91. Shrivastava, A., Saleque, S., Kalpana, G. V., Artandi, S., Goff, S. P., and Calame, K. Inhibition of transcriptional regulator Yin-Yang-1 by association with c-Myc. *Science* **262**, 1889-92 (1993).
92. Shrivastava, A., Yu, J., Artandi, S. & Calame, K. YY1 and c-Myc associate in vivo in a manner that depends on c-Myc levels. *Proc Natl Acad Sci U S A* **93**, 10638-41 (1996).
93. Roy, A. L., Carruthers, C., Gutjahr, T. & Roeder, R. G. Direct role for Myc in transcription initiation mediated by interactions with TFII-I. *Nature* **365**, 359-61 (1993).
94. Gartel, A. L. & Shchors, K. Mechanisms of c-myc-mediated transcriptional repression of growth arrest genes. *Exp Cell Res* **283**, 17-21 (2003).
95. Bendall, A. J. & Molloy, P. L. Base preferences for DNA binding by the bHLH-Zip protein USF: effects of MgCl₂ on specificity and comparison with binding of Myc family members. *Nucleic Acids Res* **22**, 2801-10 (1994).
96. Sirito, M., Lin, Q., Maity, T. & Sawadogo, M. Ubiquitous expression of the 43- and 44-kDa forms of transcription factor USF in mammalian cells. *Nucleic Acids Res* **22**, 427-33 (1994).
97. Gregor, P. D., Sawadogo, M. & Roeder, R. G. The adenovirus major late transcription factor USF is a member of the helix-loop-helix group of regulatory proteins and binds to DNA as a dimer. *Genes Dev* **4**, 1730-40 (1990).

98. Sirito, M., Walker, S., Lin, Q., Kozlowski, M. T., Klein, W. H., and Sawadogo, M. Members of the USF family of helix-loop-helix proteins bind DNA as homo- as well as heterodimers. *Gene Expr* **2**, 231-40 (1992).
99. Goueli, B. S. & Janknecht, R. Regulation of telomerase reverse transcriptase gene activity by upstream stimulatory factor. *Oncogene* **22**, 8042-7 (2003).
100. Ge, Y., Jensen, T. L., Matherly, L. H. & Taub, J. W. Physical and functional interactions between USF and Sp1 proteins regulate human deoxycytidine kinase promoter activity. *J Biol Chem* **278**, 49901-10 (2003).
101. Luo, X. & Sawadogo, M. Antiproliferative properties of the USF family of helix-loop-helix transcription factors. *Proc Natl Acad Sci U S A* **93**, 1308-13 (1996).
102. Bruno, M. E., West, R. B., Schneeman, T. A., Bresnick, E. H. & Kaetzel, C. S. Upstream stimulatory factor but not c-Myc enhances transcription of the human polymeric immunoglobulin receptor gene. *Mol Immunol* **40**, 695-708 (2004).
103. Choe, C., Chen, N. & Sawadogo, M. Decreased tumorigenicity of c-Myc-transformed fibroblasts expressing active USF2. *Exp Cell Res* **302**, 1-10 (2005).
104. Schneider, A., Peukert, K., Eilers, M. & Hanel, F. Association of Myc with the zinc-finger protein Miz-1 defines a novel pathway for gene regulation by Myc. *Curr Top Microbiol Immunol* **224**, 137-46 (1997).
105. Piluso, D., Bilan, P. & Capone, J. P. Host cell factor-1 interacts with and antagonizes transactivation by the cell cycle regulatory factor Miz-1. *J Biol Chem* **277**, 46799-808 (2002).
106. Staller, P., Peukert, K., Kiermaier, A., Seoane, J., Lukas, J., Karsunky, H., Moroy, T., Bartek, J., Massague, J., Hanel, F., and Eilers, M. Repression of p15INK4b expression by Myc through association with Miz-1. *Nat Cell Biol* **3**, 392-9 (2001).
107. Lapham, A. S., Phillips, E. S. & Barton, C. H. Transcriptional control of Nramp1: a paradigm for the repressive action of c-Myc. *Biochem Soc Trans* **32**, 1084-6 (2004).
108. Salghetti, S. E., Kim, S. Y. & Tansey, W. P. Destruction of Myc by ubiquitin-mediated proteolysis: cancer-associated and transforming mutations stabilize Myc. *Embo J* **18**, 717-26 (1999).
109. Roy, A. L., Du, H., Gregor, P. D., Novina, C. D., Martinez, E., and Roeder, R. G. Cloning of an inr- and E-box-binding protein, TFII-I, that interacts physically and functionally with USF1. *Embo J* **16**, 7091-104 (1997).
110. Houbaviy, H. B., Usheva, A., Shenk, T. & Burley, S. K. Cocystal structure of YY1 bound to the adeno-associated virus P5 initiator. *Proc Natl Acad Sci U S A* **93**, 13577-82 (1996).

111. Lee, J. S., Galvin, K. M., See, R. H., Eckner, R., Livingston, D., Moran, E., and Shi, Y. Relief of YY1 transcriptional repression by adenovirus E1A is mediated by E1A-associated protein p300. *Genes Dev* **9**, 1188-98 (1995).
112. Thomas, M. J. & Seto, E. Unlocking the mechanisms of transcription factor YY1: are chromatin modifying enzymes the key? *Gene* **236**, 197-208 (1999).
113. Galvin, K. M. & Shi, Y. Multiple mechanisms of transcriptional repression by YY1. *Mol Cell Biol* **17**, 3723-32 (1997).
114. Seto, E., Lewis, B. & Shenk, T. Interaction between transcription factors Sp1 and YY1. *Nature* **365**, 462-4 (1993).
115. Yao, Y. L., Dupont, B. R., Ghosh, S., Fang, Y., Leach, R. J., and Seto, E. Cloning, chromosomal localization and promoter analysis of the human transcription factor YY1. *Nucleic Acids Res* **26**, 3776-83 (1998).
116. Hasegawa, A., Yasukawa, M., Sakai, I. & Fujita, S. Transcriptional down-regulation of CXC chemokine receptor 4 induced by impaired association of transcription regulator YY1 with c-Myc in human herpesvirus 6-infected cells. *J Immunol* **166**, 1125-31 (2001).
117. Eisenman, R. N. Deconstructing myc. *Genes Dev* **15**, 2023-30 (2001).
118. Smale, S. T. Transcription initiation from TATA-less promoters within eukaryotic protein-coding genes. *Biochim Biophys Acta* **1351**, 73-88 (1997).
119. Kingsley-Kallesen, M. L., Kelly, D. & Rizzino, A. Transcriptional regulation of the transforming growth factor-beta2 promoter by cAMP-responsive element-binding protein (CREB) and activating transcription factor-1 (ATF-1) is modulated by protein kinases and the coactivators p300 and CREB-binding protein. *J Biol Chem* **274**, 34020-8 (1999).
120. Breen, G. A. & Jordan, E. M. Transcriptional activation of the F(1)F(0) ATP synthase alpha-subunit initiator element by USF2 is mediated by p300. *Biochim Biophys Acta* **1428**, 169-76 (1999).
121. Torchia, J., Glass, C. & Rosenfeld, M. G. Co-activators and co-repressors in the integration of transcriptional responses. *Curr Opin Cell Biol* **10**, 373-83 (1998).
122. Dynan, W. S., Saffer, J. D., Lee, W. S. & Tjian, R. Transcription factor Sp1 recognizes promoter sequences from the monkey genome that are simian virus 40 promoter. *Proc Natl Acad Sci U S A* **82**, 4915-9 (1985).
123. Dynan, W. S. & Tjian, R. The promoter-specific transcription factor Sp1 binds to upstream sequences in the SV40 early promoter. *Cell* **35**, 79-87 (1983).
124. Suske, G. The Sp-family of transcription factors. *Gene* **238**, 291-300 (1999).

125. Pugh, B. F. & Tjian, R. Mechanism of transcriptional activation by Sp1: evidence for coactivators. *Cell* **61**, 1187-97 (1990).
126. Philipsen, S. & Suske, G. A tale of three fingers: the family of mammalian Sp/XKLF transcription factors. *Nucleic Acids Res* **27**, 2991-3000 (1999).
127. Emili, A., Greenblatt, J. & Ingles, C. J. Species-specific interaction of the glutamine-rich activation domains of Sp1 with the TATA box-binding protein. *Mol Cell Biol* **14**, 1582-93 (1994).
128. Gill, G., Pascal, E., Tseng, Z. H. & Tjian, R. A glutamine-rich hydrophobic patch in transcription factor Sp1 contacts the dTAFIII10 component of the Drosophila TFIID complex and mediates transcriptional activation. *Proc Natl Acad Sci U S A* **91**, 192-6 (1994).
129. Comer, F. I. & Hart, G. W. O-GlcNAc and the control of gene expression. *Biochim Biophys Acta* **1473**, 161-71 (1999).
130. Jackson, S. P. & Tjian, R. O-glycosylation of eukaryotic transcription factors: implications for mechanisms of transcriptional regulation. *Cell* **55**, 125-33 (1988).
131. Roos, M. D., Su, K., Baker, J. R. & Kudlow, J. E. O glycosylation of an Sp1-derived peptide blocks known Sp1 protein interactions. *Mol Cell Biol* **17**, 6472-80 (1997).
132. Han, I. & Kudlow, J. E. Reduced O glycosylation of Sp1 is associated with increased proteasome susceptibility. *Mol Cell Biol* **17**, 2550-8 (1997).
133. Haurum, J. S., Hoier, I. B., Arsequell, G., Neisig, A., Valencia, G., Zeuthen, J., Neefjes, J., and Elliott, T. Presentation of cytosolic glycosylated peptides by human class I major histocompatibility complex molecules in vivo. *J Exp Med* **190**, 145-50 (1999).
134. Wells, L., Vosseller, K. & Hart, G. W. Glycosylation of nucleocytoplasmic proteins: signal transduction and O-GlcNAc. *Science* **291**, 2376-8 (2001).
135. Haltiwanger, R. S., Grove, K. & Philipsberg, G. A. Modulation of O-linked N-acetylglucosamine levels on nuclear and cytoplasmic proteins in vivo using the peptide O-GlcNAc-beta-N-acetylglucosaminidase inhibitor O-(2-acetamido-2-deoxy-D-glucopyranosylidene)amino-N-phenylcarbamate. *J Biol Chem* **273**, 3611-7 (1998).
136. Brasse-Lagnel, C., Fairand, A., Lavoinne, A. & Husson, A. Glutamine stimulates argininosuccinate synthetase gene expression through cytosolic O-glycosylation of Sp1 in Caco-2 cells. *J Biol Chem* **278**, 52504-10 (2003).

137. Ryu, H., Lee, J., Zaman, K., Kubilis, J., Ferrante, R. J., Ross, B. D., Neve, R., and Ratan, R. R. Sp1 and Sp3 are oxidative stress-inducible, antideath transcription factors in cortical neurons. *J Neurosci* **23**, 3597-606 (2003).
138. Ammendola, R., Mesuraca, M., Russo, T. & Cimino, F. The DNA-binding efficiency of Sp1 is affected by redox changes. *Eur J Biochem* **225**, 483-9 (1994).
139. Goldberg, H. J., Whiteside, C. I. & Fantus, I. G. The hexosamine pathway regulates the plasminogen activator inhibitor-1 gene promoter and Sp1 transcriptional activation through protein kinase C-beta I and -delta. *J Biol Chem* **277**, 33833-41 (2002).
140. Du, X. L., Edelstein, D., Rossetti, L., Fantus, I. G., Goldberg, H., Ziyadeh, F., Wu, J., and Brownlee, M. Hyperglycemia-induced mitochondrial superoxide overproduction activates the hexosamine pathway and induces plasminogen activator inhibitor-1 expression by increasing Sp1 glycosylation. *Proc Natl Acad Sci U S A* **97**, 12222-6 (2000).
141. Droge, W. Free radicals in the physiological control of cell function. *Physiol Rev* **82**, 47-95 (2002).
142. Clarke, S. & Gordon, S. Myeloid-specific gene expression. *J Leukoc Biol* **63**, 153-68 (1998).
143. Smale, S. T., Schmidt, M. C., Berk, A. J. & Baltimore, D. Transcriptional activation by Sp1 as directed through TATA or initiator: specific requirement for mammalian transcription factor IID. *Proc Natl Acad Sci U S A* **87**, 4509-13 (1990).
144. Kamemura, K. & Hart, G. W. Dynamic interplay between O-glycosylation and O-phosphorylation of nucleocytoplasmic proteins: a new paradigm for metabolic control of signal transduction and transcription. *Prog Nucleic Acid Res Mol Biol* **73**, 107-36 (2003).
145. Hiromura, M., Choi, C. H., Sabourin, N. A., Jones, H., Bachvarov, D., and Usheva, A. (YY1 is regulated by O-linked N-acetylglucosaminylation (O-glcNAcylation). *J Biol Chem* **278**, 14046-52 (2003).
146. Chou, T. Y., Dang, C. V. & Hart, G. W. Glycosylation of the c-Myc transactivation domain. *Proc Natl Acad Sci U S A* **92**, 4417-21 (1995).
147. Kadonaga, J. T., Carner, K. R., Masiarz, F. R. & Tjian, R. Isolation of cDNA encoding transcription factor Sp1 and functional analysis of the DNA binding domain. *Cell* **51**, 1079-90 (1987).
148. Finkel, T. Oxidant signals and oxidative stress. *Curr Opin Cell Biol* **15**, 247-54 (2003).

149. Droge, W. Oxidative stress and aging. *Adv Exp Med Biol* **543**, 191-200 (2003).
150. Kannan, K. & Jain, S. K. Oxidative stress and apoptosis. *Pathophysiology* **7**, 153-163 (2000).
151. Sies, H. Glutathione and its role in cellular functions. *Free Radic Biol Med* **27**, 916-21 (1999).
152. Meister, A. Mitochondrial changes associated with glutathione deficiency. *Biochim Biophys Acta* **1271**, 35-42 (1995).
153. Murata, Y., Shimamura, T. & Hamuro, J. The polarization of T(h)1/T(h)2 balance is dependent on the intracellular thiol redox status of macrophages due to the distinctive cytokine production. *Int Immunol* **14**, 201-12 (2002).
154. Soo, S. S., Villarreal-Ramos, B., Anjam Khan, C. M., Hormaeche, C. E. & Blackwell, J. M. Genetic control of immune response to recombinant antigens carried by an attenuated *Salmonella typhimurium* vaccine strain: Nramp1 influences T-helper subset responses and protection against leishmanial challenge. *Infect Immun* **66**, 1910-7 (1998).
155. Malorni, W., Testa, U., Rainaldi, G., Tritarelli, E. & Peschle, C. Oxidative stress leads to a rapid alteration of transferrin receptor intravesicular trafficking. *Exp Cell Res* **241**, 102-16 (1998).
156. Gomes, M. S. & Appelberg, R. NRAMP1- or cytokine-induced bacteriostasis of *Mycobacterium avium* by mouse macrophages is independent of the respiratory burst. *Microbiology* **148**, 3155-60 (2002).
157. Oexle, H., Kaser, A., Most, J., Bellmann-Weiler, R., Werner, E. R., Werner-Felmayer, G., and Weiss, G. Pathways for the regulation of interferon-gamma-inducible genes by iron in human monocytic cells. *J Leukoc Biol* **74**, 287-94 (2003).
158. Lafuse, W. P., Alvarez, G. R. & Zwilling, B. S. Role of MAP kinase activation in Nramp1 mRNA stability in RAW264.7 macrophages expressing Nramp1(Gly169). *Cell Immunol* **215**, 195-206 (2002).
159. Hanks, S. K. & Quinn, A. M. Protein kinase catalytic domain sequence database: identification of conserved features of primary structure and classification of family members. *Methods Enzymol* **200**, 38-62 (1991).
160. Tanaka, T., Kurabayashi, M., Aihara, Y., Ohyama, Y. & Nagai, R. Inducible expression of manganese superoxide dismutase by phorbol 12-myristate 13-acetate is mediated by Sp1 in endothelial cells. *Arterioscler Thromb Vasc Biol* **20**, 392-401 (2000).

161. Wojciechowski, W., DeSanctis, J., Skamene, E. & Radzioch, D. Attenuation of MHC class II expression in macrophages infected with *Mycobacterium bovis* bacillus Calmette-Guerin involves class II transactivator and depends on the *Nramp1* gene. *J Immunol* **163**, 2688-96 (1999).
162. Buschman, E., Vidal, S. & Skamene, E. Nonspecific resistance to Mycobacteria: the role of the *Nramp1* gene. *Behring Inst Mitt*, 51-7 (1997).
163. Lee, K. & Esselman, W. J. Inhibition of PTPs by H₂O₂ regulates the activation of distinct MAPK pathways. *Free Radic Biol Med* **33**, 1121-32 (2002).
164. Lee, S. R., Kwon, K. S., Kim, S. R. & Rhee, S. G. Reversible inactivation of protein-tyrosine phosphatase 1B in A431 cells stimulated with epidermal growth factor. *J Biol Chem* **273**, 15366-72 (1998).
165. Kovarova, H., Necasova, R., Porkertova, S., Radzioch, D. & Macela, A. Natural resistance to intracellular pathogens: modulation of macrophage signal transduction related to the expression of the *Bcg* locus. *Proteomics* **1**, 587-96 (2001).
166. Suzuki, Y., Tsunoda, T., Sese, J., Taira, H., Mizushima-Sugano, J., Hata, H., Ota, T., Isogai, T., Tanaka, T., Nakamura, Y., Suyama, A., Sakaki, Y., Morishita, S., Okubo, K., and Sugano, S. Identification and characterization of the potential promoter regions of 1031 kinds of human genes. *Genome Res* **11**, 677-84 (2001).
167. Blackwell, J. M., Searle, S., Mohamed, H. & White, J. K. Divalent cation transport and susceptibility to infectious and autoimmune disease: continuation of the *Ity/Lsh/Bcg/Nramp1/Slc11a1* gene story. *Immunol Lett* **85**, 197-203 (2003).
168. Bassuny, W. M., Ihara, K., Matsuura, N., Ahmed, S., Kohno, H., Kuromaru, R., Miyako, K., and Hara, T. Association study of the *NRAMP1* gene promoter polymorphism and early-onset type 1 diabetes. *Immunogenetics* **54**, 282-5 (2002).
169. Du, X. L., Edelstein, D., Dimmeler, S., Ju, Q., Sui, C., and Brownlee, M. Hyperglycemia inhibits endothelial nitric oxide synthase activity by posttranslational modification at the Akt site. *J Clin Invest* **108**, 1341-8 (2001).
170. Tenen, D. G., Hromas, R., Licht, J. D. & Zhang, D. E. Transcription factors, normal myeloid development, and leukemia. *Blood* **90**, 489-519 (1997).
171. Zaharik, M. L., Vallance, B. A., Puente, J. L., Gros, P. & Finlay, B. B. Host-pathogen interactions: Host resistance factor *Nramp1* up-regulates the expression of *Salmonella* pathogenicity island-2 virulence genes. *Proc Natl Acad Sci U S A* **99**, 15705-10 (2002).

172. Eriksson, S., Lucchini, S., Thompson, A., Rhen, M. & Hinton, J. C. Unravelling the biology of macrophage infection by gene expression profiling of intracellular *Salmonella enterica*. *Mol Microbiol* **47**, 103-18 (2003).
173. Carter, A. B., Tephly, L. A., Venkataraman, S., Oberley, L. W., Zhang, Y., Buettner, G. R., Spitz, D. R., and Hunninghake, G. W. High levels of catalase and glutathione peroxidase activity dampen H₂O₂ signaling in human alveolar macrophages. *Am J Respir Cell Mol Biol* **31**, 43-53 (2004).
174. Lafuse, W. P., Alvarez, G. R. & Zwilling, B. S. Regulation of Nramp1 mRNA stability by oxidants and protein kinase C in RAW264.7 macrophages expressing Nramp1(Gly169). *Biochem J* **351 Pt 3**, 687-96 (2000).

Book: Iron and Infection by Bullen Griffiths, publisher Wiley